Humboldt-Universität zu Berlin

DISSERTATION

Induction and regulation of antiviral defence mechanisms through intracytoplasmic sensors

Zur Erlangung des akademischen Grades doctor rerum naturalium (Dr. rer. nat.) im Fach Biologie

Mathematisch-Naturwissenschaftlichen Fakultät

Min-Hi Lee

Dekan: Prof. Dr. rer. nat. Lutz-Helmut Schön

Gutachter/in:
1. **Prof. Dr. Andreas Herrmann**
2. **Prof. Dr. Stefan Hippenstiel**
3. **Prof. Dr. Günther Schönrich**

Datum der Einreichung: 26.01.2009

Datum der Promotion: 16.06.2009

Zusammenfassung

Das Wechselspiel zwischen Viren und ihren Wirtszellen beginnt meist an *pattern recognition*-Rezeptoren (PRRs), die für die Erkennung unterschiedlichster Pathogene anhand bestimmter Strukturen, sogenannten *pathogen-associated molecular patterns* (PAMPs), zuständig sind. Nach Detektion lösen die PRRs über verschiedene Signalkaskaden eine antivirale Antwort aus, die zur Expression antiviraler Gene führt. RIG-I und MDA5 sind zytoplasmatisch lokalisierte PRRs und erkennen RNA-Strukturen, die insbesondere während der viralen Replikation und Transkription verfügbar sind.

Hantaviren sind humanpathogene RNA-Viren mit einem einzelsträngigen, segmentierten Genom. Die Konsequenzen hantaviraler Infektionen auf molekularer Ebene wurden bereits detailliert untersucht, aber die Mechanismen, die zur Induktion der Immunantwort führen, wie auch mögliche Immunevasionsstrategien, die wahrscheinlich in Zusammenhang mit der Pathogenität des jeweiligen Hantavirusstamms variieren, konnten bisher nicht identifiziert werden. Da Hantaviren im Cytoplasma ihrer Wirtszellen replizieren, stellen RIG-I und MDA5 potentielle Detektoren dar.

In dieser Doktorarbeit wird die Bedeutung von RIG-I und MDA5 für die Erkennung von Hantavirus-Infektionen untersucht. Wachstumskinetiken zeigten, daß RIG-I die Replikation von pathogenen wie auch apathogenen Hantaviren beeinträchtigt. Außerdem konnte die RNA hantaviraler Nukleocapsid- (N-) ORFs als eine virale Komponente identifiziert werden, die Typ I Interferon über RIG-I induziert. Das Ausmaß der Interferon-Aktivierung korrelierte hierbei tendenziell mit dem Virulenzgrad der Virusstämme und war für die nicht-pathogenen Hantaviren nicht nachweisbar. Unterschiede in der Aktivierungsstärke können anhand vorläufiger Daten wahrscheinlich auf noch nicht identifizierte Motive zurückgeführt werden, die am 3'-Ende der N ORFs liegen. Im Gegensatz dazu wurde keine Interferon-Aktivierung durch hantavirale Komponenten über MDA5 festgestellt.

Schlagwörter:

Hantavirus, angeborene Immunantwort, PRR, PAMP

Abstract

Host-virus interaction is usually initated by pattern recognition receptors (PRRs) which are responsible for the recognition of various pathogens based on so-called pathogen-associated molecular patterns (PAMPs). Upon detection, PRRs trigger an antiviral immune response through different signalling cascades that lead to the expression of antiviral genes including interferon genes. RIG-I and MDA5 are cytoplasmically localised PRRs and recognise RNA patterns that are particularly available during viral replication and transcription.

Hantaviruses are RNA viruses with single-stranded segmented genomes. The consequences of hantaviral infections have been analysed in detail, but the mechanisms that lead to the induction of the innate immune response as well as immune evasion strategies depending on the pathogenicity of the respective hantavirus strains have not been identified yet. Since hantaviruses replicate in the cytoplasm of their host cells, RIG-I and MDA5 represent potential PRRs for hantaviral detection.

This thesis investigates the impact of RIG-I and MDA5 on recognition of hantaviral infections. Growth kinetics show that RIG-I impairs the replication of pathogenic as well as non-pathogenic hantaviruses. Furthermore, the RNA of hantaviral nucleocapsid protein (N) ORF could be identified as a viral component responsible for the induction of RIG-I signalling. It is shown that the degree of interferon promotor activation correlates with the virulence of the hantavirus strain from which the N ORF was derived. Based on preliminary data, differences in activation strength may be attributed to not yet identified motifs at the 3' end of the ORF. In contrast, no interferon activation through MDA5 could be observed.

Keywords:

Hantavirus, innate immunity, PRR, PAMP

Abbreviations

aa	amino acid
APC	antigen presenting cell
APS	ammonium persulfate
Bcl-2	B-cell lymphocyte/leukemia-2 protein
BME	basal medium with Earls's salt
BSA	bovine serum albumin
BSL	biosafety level
$CaCl_2$	calcium chloride
CARD	caspase recruitment domain
CARDIF	CARD adaptor inducing IFN-β
CD	cluster of differentiation
CPE	cytopathic effect
cRNA	complementary RNA
DC	dendritic cell
DMEM	Dulbecco's modified Eagle medium
DMSO	Dimethylsulfoxide
DV	Dengue virus
DNA	deoxyribonucleic acid
EBOV	Ebola virus
EBV	Epstein-Barr virus
EDTA	ethylene-diamine-tetra-acetic acid
ELISA	enzyme-linked immunosorbent assay
EMCV	Encephalomyocarditis virus
ER	endoplasmic reticulum
FACS	fluorescence-activated cell sorting
FADD	Fas-associated protein with death domain
FCS	fetal calf serum
FFU	focus forming unit
FITC	fluorescein isothiocyanate
FLUAV	Influenza A virus
FLUBV	Influenza B virus
GM-CSF	granulocyte-macrophage colony-stimulating factor

HCl	hydrochloric acid
HCMV	human cytomegalovirus
HCPS	hantavirus cardiopulmonary syndrome
HCV	hepatitis C virus
HEPES	N-2-hydroxyethylpiperazine-N'-2-ethane-sulfonic acid
HFRS	hemorrhagic fever with renal syndrome
HLA	human leukocyte antigen
HMVEC-L	human pulmonary microvascular endothelial cells
HRP	horseradish peroxidase
HSV-1	herpes simplex virus type 1
HTNV	Hantaan hantavirus
HUVEC	human umbilical vein endothelial cells
ICAM-1	intercellular adhesion molecule-1
IF	immunofluorescence
IFN	interferon
IFNAR	IFN-α/β receptor
IKKi	IκB-binding kinase i
IL	Interleukin
IP-10	10 kDa IFN-inducible protein
IPS-1	IFN-β promoter stimulator protein
IRF	IFN regulatory factors
ISGF	IFN-stimulated gene factor
ISRE	IFN-stimulated response element
JAK	Janus protein tyrosine kinase
JEV	Japanese encephalitis virus
kb	kilobase
kbp	kilobasepairs
kDa	kiloDalton
KHF	Korean hemorrhagic fever
L	large genome segment
LASV	Lassa virus
LPS	lipopolysaccharide
M	medium genome segment

MAVS	mitochondrial antiviral signalling
MAP	mitogen-associated protein kinase
MDA5	melanoma differentiation-associated gene 5
MEM	minimum essential medium
MFI	mean fluorescence intensity
MOI	multiplicity of infection
MOPS	3-(N-morpholino)propanesulfonic acid
MV	Measles virus
N	nucleocapsid
NaCl	sodium chloride
NaN_3	sodium azide
NDV	New Castle disease virus
NE	nephropathia epidemica
NK cell	natural killer cell
NiV	Nipah virus
N protein	nucleocapsid protein
NS	non-structural
nt	nucleotides
OAS	2'-5'-oligoadenylate synthetase
OD	optical density
PAMP	pathogen-associated molecular pattern
PAGE	polyacrylamide gel electrophoresis
PBS	phosphate-buffered saline
PDGF	platelet-derived growth factor
PE	phycoerythrin
PFA	paraformaldehyde
PHV	Prospect Hill hantavirus
PKR	protein kinase R
PMBC	peripheral blood mononuclear cells
PMSF	phenylmethanesulphonylfluoride
polyI:C	polyinosinic-polycytidylic acid
PRD	positive regulatory domains
PUUV	Puumala hantavirus

RANTES	regulated in activation, normal T cells expressed and secreted
RIG-I	retinoic acid inducible gene I
RNA	ribonucleic acid
rpm	revolutions per minute
RPMI 1640	Roswell Park Memorial Institute medium (for cell culture)
RSV	respiratory syncytial virus
RT-PCR	reverse transcriptase-polymerase chain reaction
RV	Rabies virus
RVFV	Rift Valley fever virus
S	small genome segment
SDS-PAGE	sodiumdodecylsulphate-polyacrylamide gel electrophoresis
SeV	Sendai virus
STAT	signal transducer of activation and transcription
T7 pol	bacteriophage T7 RNA polymerase
TAP	transporter associated with antigen
TBK-1	Traf family member-associated NFκB activator-binding kinase 1
TBST	Tris-buffered saline Tween 20
TGF	transforming growth factor
TLR	Toll-like receptor
TNF	tumor necrosis factor
Treg	regulatory T cell
Tris-HCl	Tris-(hydroxymethyl)-aminomethan
TULV	Tula hantavirus
UV	ultraviolet
VEGF	vascular endothelial growth factor
VISA	virus-induced signalling adaptor
vRNA	viral genomic RNA
VSV	vesicular stomatitis virus
WB	Western blot
WNV	West Nile virus
wt	wild-type

Contents

1 Introduction

1.1 Hantaviruses

1.1.1 Overview

The earliest descriptions of diseases possibly caused by hantaviruses were recorded in the 10th century (Lee, 1982). During the Korean War (1950-1953), many UN soldiers were hospitalised with Korean hemorrhagic fever, resulting in mortality rates up to 7% (Jonsson and Schmaljohn, 2001; Smadel, 1953), but the causative agent still was not discovered until 1978 when the Hantaan virus (HTNV) was isolated from its reservoir host *Apodemus agrarius*, the striped field mouse (Lee et al., 2004).

In 1981, HTNV was the first hantavirus adapted successfully to cell lines for *in vitro* experiments. Taxonomic investigations showed that it belonged to the family of *Bunyaviridae* (White et al., 1982). The clinical feature of New World hantaviruses, called hantavirus cardiopulmonary syndrome (HCPS), was detected in 1993 (Peters and Khan, 2002). Until today other hantavirus species are being discovered in Europe, Asia, the Americas and Africa (Figure 1).

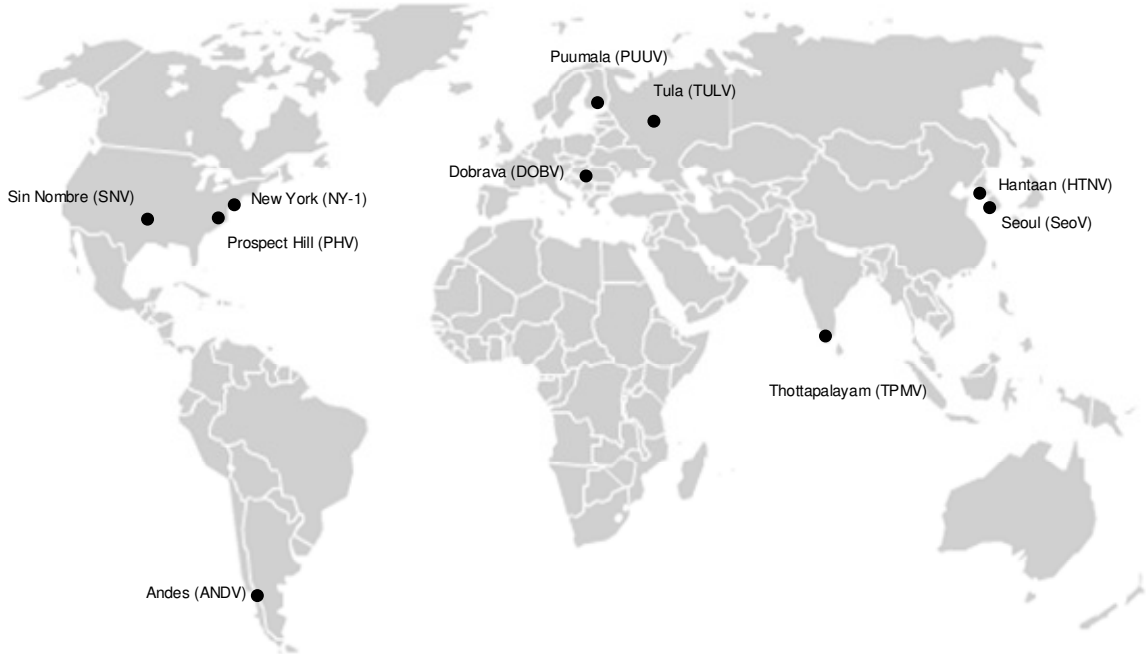

Figure 1. Global distribution of selected hantavirus strains (first isolation habitat)

Nowadays, hantaviruses are classified as emerging viruses, 20 of them being pathogenic for humans (Clement, 2003; Peters and Khan, 2002; Jones et al., 2008; Kruger et al., 2001). Although hantaviruses are categorised as potential biological warfare agent by the US Centers for Disease Control and Prevention (CDC) (Clement, 2003), few data exist about their interactions with the immune systems of their hosts.

Furthermore, there are no antiviral drugs for curing hantavirus infections, only symptoms can be controlled until convalescence. The guanoside-analog Ribavirin (1-β-D-ribofuranosyl-1,2,4-triazole-3-carboximide) initially showed promising results for antiviral therapy (Huggins et al., 1986; Huggins et al., 1991) which, unfortunately, could not be confirmed (Chapman et al., 1999; Chapman et al., 2002; Maes et al., 2004; Rusnak et al., 2008).

1.1.2 Taxonomy and morphology

Hantaviruses as well as four other virus genera form the family of *Bunyaviridae*. They are renowned for their negatively-orientated single-stranded RNA genome that is separated into three segments. The segments in turn differ in sequence and size; the longest segment (L) encodes the RNA-dependent RNA polymerase (RdRp), the intermediate segment M contains the coding sequences for both glycoproteins G1 and G2 or Gc and Gn, respectively, and the shortest segment S codes for the nucleocapsid protein (Figure 2) (Dunn et al., 1995; Elliott, 1990; Maes et al., 2004; Schmaljohn and Hjelle, 1997). *Arvicolinae*- and *Sigmodontinae*-associated hantaviruses possess an additional open reading frame (ORF) within the S segment, coding for a putative non-structural (NS) protein (Bowen et al., 1995; Plyusnin, 2002). Each segment is closed non-covalently due to complementary structures at its highly conserved 3' and 5' ends, thereby forming the typical so-called panhandle (Pardigon et al., 1982). Furthermore, the 5' termini of HTNV genome segments contain uridine monophosphates (UMP) (Garcin et al., 1995).

The enveloped virions have a diameter of approximately 120 nm and are spiked with the glycoproteins, G1 and G2, as heterodimers that mediate cell attachment and fusion (Arikawa et al., 1985; Lee and Cho, 1981; Martin et al., 1985; Obijeski et al., 1976; Okuno et al., 1986; Tsai, 1987). The virions contain the viral ribonucleoprotein complexes (vRNPs) consisting of the three genome segments (vRNA) attached to N protein trimers, thereby protecting the RNA from nuclease degradation (Alfadhli et al., 2001; Kaukinen et al., 2001). Furthermore, the

viral RdRp, that also functions as replicase, transcriptase and endonuclease, is associated with the vRNPs (Figure 2) (Elliott, 1990; Gott et al., 1993; Obijeski et al., 1976).

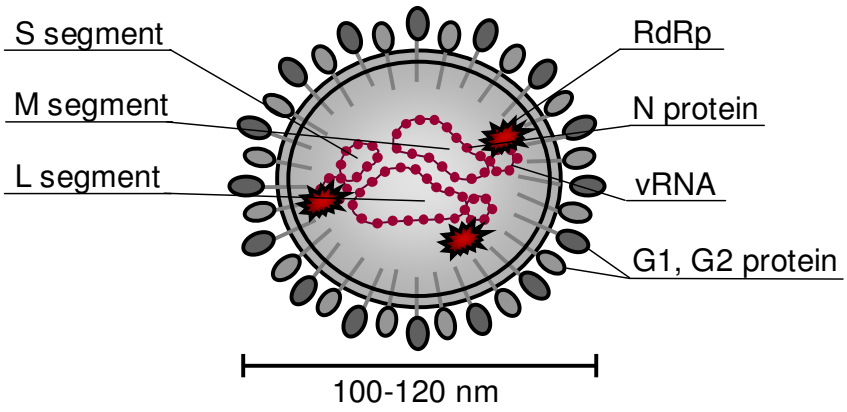

Figure 2. Hantavirus virion: Hantaviruses consist of a double-layer lipid membrane carrying the G protein heterodimers. The three vRNA segments coding for the four viral proteins are complexed with N protein, building the vRNPs, and viral RdRp.

1.1.3 Life cycle

Hantaviruses known to be pathogenic to humans enter the cells through β3 integrins (CD61) as receptors, found e.g. on endothelial cells, platelets and macrophages, whereas non-pathogenic hantaviruses use the ubiquitous β1 integrins (CD29) (Gavrilovskaya et al., 1998; Gavrilovskaya et al., 1999; Gavrilovskaya et al., 2002). Further receptors are supposed to be involved in hantavirus entry (Kim et al., 2002; Krautkramer and Zeier, 2008; Choi et al., 2008).

Entry takes place via clathrin-dependent endocytosis, mediated by the viral glycoproteins (Jin et al., 2002). After release of vRNPs into the cellular cytoplasm, cRNAs, full-length complementary strands of each segment, are synthesized, serving as templates for vRNA synthesis. mRNAs are also transcribed by the viral RdRp after accumulation of vRNA and matured by the so-called “cap-snatching” mechanism, i.e. the viral polymerase cleaves methylated 5’ caps from cellular mRNAs and attaches them to the viral mRNAs (Dunn et al., 1995; Garcin et al., 1995; Elliott et al., 1991).

At first, the N proteins as well as the RdRp are translated in the cytoplasm at free ribosomes and accumulate (Alfadhli et al., 2001; Kaukinen et al., 2001; Schmaljohn and Hjelle, 1997). After synthesis of the glycoprotein precursor at the endoplasmic reticulum, the precursor is cleaved into two glycoproteins G1 and G2 (Lober et al., 2001). These are in turn transported

to the Golgi apparatus for glycosylation and accumulate as heterodimers (Ruusala et al., 1992; Shi and Elliott, 2002), ready for building new virions with the vRNPs.

It has not been elucidated yet where the following assembly steps take place and how the virions leave the cells. The majority of the *Bunyaviridae* mature by budding into the Golgi cisternae (Ellis et al., 1988; Hobman, 1993; Jantti et al., 1997; Kuismanen et al., 1985; Rwambo et al., 1996), but some New World viruses also mature at the cell surface. For example, Sin Nombre virus (SNV) has been found to bud at the plasma membrane (Goldsmith et al., 1995; Ravkov et al., 1997; Ravkov et al., 1998). After maturation, the virions exocytose from the host cells through vesicles and are released into the cellular environment (Figure 3).

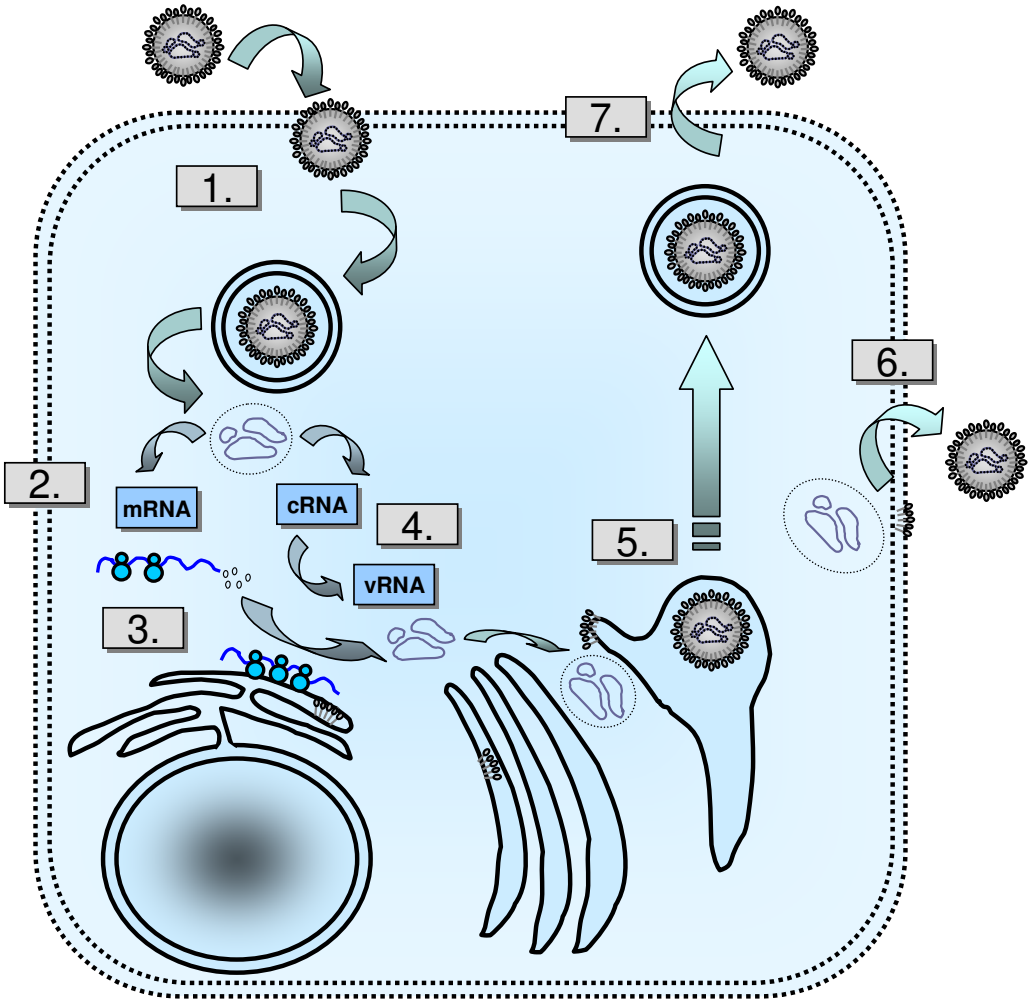

Figure 3. Replication cycle of *Bunyaviridae* (after Schmaljohn and Hooper 2001)**:** 1. Entry, 2. Transcription, 3. Translation, 4. Replication, 5. Assembly, 6. Alternative assembly, Egress, 7. Egress

1.1.4 Phylogeny and hosts

To date, more than 30 hantavirus species have been discovered (Hart and Bennett, 1999; Kanerva et al., 1998; Plyusnin, 2002). The strict reservoir host specificity of hantaviruses is remarkable, indicating a stringent co-evolution of virus and host (Hjelle and Yates, 2001; Plyusnin and Morzunov, 2001; Plyusnin, 2002). The Old World viruses from Asia and Europe like HTNV, Puumala virus (PUUV), Seoul virus (SEOV) and Dobrava virus (DOBV) are mainly *Murinae*- and *Arvicolinae*-associated, whereas New World viruses found in the Americas are often carried by *Sigmodontinae*. Furthermore, latest investigations revealed insectivores as additional reservoir hosts next to the known rodent classes (Table 1) (Carey et al., 1971; Yanagihara and Silverman, 1990; Song et al., 2007; Klempa et al., 2008; Rusnak et al., 2008).

Table 1: List of selected hantaviruses

Species	Abbreviation	Rodent host	Distribution	Disease	Case fatality
Murinae-associated					
Dobrava Belgrade virus	DOBV (Aa)	*Apodemus agrarius*	Central and East Europe	HFRS	0.9%
	DOBV (Af)	*Apodemus flavicollis*	South-East Europe	HFRS	9-12%
	DOBV (Ap)	*Apodemus ponticus*	South-East Europe	HFRS	6.5%
Hantaan virus	HTNV	*Apodemus agrarius*	Asia	HFRS	≤ 15%
Seoul virus	SEOV	*Rattus norvegicus*	Asia	HFRS	1-2%
Arvicolinae-associated					
Prospect Hill virus	PHV	*Microtus pennsylvanicus*	North America	-	-
Puumala virus	PUUV	*Clethrionomys glareolus* *Clethrionomys rufocanus*	Eastern and Southern Europe	HFRS (mild)	< 1%
Tula virus	TULV	*Microtus arvalis* *Microtus rossiaemeridionalis*	Central and East Europe	?	?
Sigmodontinae-associated					
Andes virus	ANDV	*Oligoryzomys longicaudatus*	Argentina	HCPS	43-56%
New York virus	NYV	*Peromyscus leucopus*	North America	HCPS	?
Sin Nombre virus	SNV	*Peromyscus maniculatus*	North America	HCPS	35%
Insectivore-associated					
Thottapalayam virus	TPMV	*Suncus murinus*	India	?	?

Nevertheless, phylogenetic analyses revealed inter- and intra-strain-dependent variabilities. Viruses in general have several possibilities to use genetic variations for increasing their "fitness", for example by genetic drift or genetic shift. For hantaviruses, one possibility of genetic variation is given by apparently impaired or absent proof reading activity of the viral RNA polymerase (Plyusnin et al., 1996; Choi et al., 2008; Ramsden et al., 2008). Furthermore, reassortment processes can be responsible for changes in the genetic background of hantaviruses (Li et al., 1995). Interestingly, the exchange of genomic segments is not distributed normally for all three segments; apparently, M seems to undergo reassortment with higher probability whereas S and L reassort primilary together (Rizvanov et al., 2004; Rodriguez et al., 1998; Klempa et al., 2005) (Kirsanovs, unpublished data).

1.1.5 Transmission, clinical features and epidemiology

Hantaviruses establish persistent infections in their reservoir hosts without any apparent disease (Botten et al., 2000; Hutchinson et al., 1998; Tkachenko and Lee, 1991; Yanagihara et al., 1985). They are transmitted to humans through aerosols containing viruses derived from rodent feces, urine, or saliva (Tsai, 1987). Thus the respiratory tract represents the primary replication site (McCaughey and Hart, 2000; Schonrich et al., 2008). However, virus transmission can also occur by rodent bites (Gonzalez et al., 1984; Hart and Bennett, 1999). Human-to-human transmissions usually do not occur and were only observed in individual cases for Andes virus (ANDV) (Padula et al., 1998; Wells et al., 1997).

Hantaviruses show similar tropisms in rodents and humans. The vascular endothelium is postulated as the main target tissue in hantavirus infections since viral antigen could be detected in endothelial cells derived from lung, kidney, heart and lymphoid organs (Green et al., 1998; Zaki et al., 1995). Typical human disease patterns after infection with Old and New World hantaviruses are hemorrhagic fever with renal syndrome (HFRS) and hantavirus cardiopulmonary syndrome (HCPS), respectively.

HFRS is characterised by fever, abdominal pain and drop in blood pressure and can even lead to vascular hemorrhage, kidney dysfunction, cardiogenic shock and renal failure which is mainly caused by HTNV, SEOV and DOBV (Cosgriff and Lewis, 1991; Kanerva et al., 1998; Tkachenko and Lee, 1991). The number of reported cases amounts to 100,000 per year with case fatality rates between 1 to 15% depending on the responsible hantavirus strain. In Europe, PUUV seems to be the major pathogenic hantavirus since it is responsible for ap-

proximately 6,000 annual cases of mild HFRS, also called nephropathia epidemica (NE), with fatality rates of 0.1% (Vapalahti et al., 2003).

HCPS is found in North and South America and caused by SNV and ANDV, respectively. The disease pattern is characterised by vascular hemorrhage, pulmonary edema and respiratory distress and can – in severe cases – lead to myocardial dysfunction; the case fatality rate reaches up to 50% (Khan and Young, 2001; Schmaljohn and Hjelle, 1997). However, clinical features of both disease patterns are not mutually exclusive and can also occur occasionally during infection with the respective other type of virus. Additionally, thrompocytopenia, proteinuria and leukocytosis may arise during both infection courses (Kanerva et al., 1998; Zaki et al., 1995). Some hantaviruses are constituted as non-pathogenic, but their pathogenic potential is not completely clear yet; for example, Tula virus (TULV) and Prospect Hill virus (PHV) seem to be non-pathogenic, but recently, a HFRS case after infection with TULV has been reported (Klempa et al., 2003).

1.2 Experimental systems for hantaviral studies in cell culture and animal models

All procedures involving pathogenic hantaviruses have to be carried out under biosafety level 3 (BSL3) conditions. Hantaviruses infect different cell types, for example A549 cells (human lung epithelial cells), VeroE6 cells (green monkey epithelial kidney cells), primary endothelial cells, monocytes, macrophages and megacaryocytes. However, inspite of strong dysregulation of endothelial cell function and an intense adaptive immune response in case of some pathogenic hantaviruses *in vivo*, neither pathogenic nor non-pathogenic hantaviruses seem to cause a cytopathic effect in permissive cells, and endothelial cell permeability is not increased *in vitro* (Hjelle and Yates, 2001; Kitamura et al., 1983; Nagai et al., 1985; Pensiero et al., 1992; Sundstrom et al., 2001; Yanagihara and Silverman, 1990).

Furthermore, the absence of appropriate animal models hampers *in vivo*-analyses of hantaviruses. Therefore, it is quite difficult to investigate how hantaviruses increase endothelial permeability and thereby cause disease (Kanerva et al., 1998), indicating cytokines or similar molecules released from infected cells as factors for hantavirus pathogenesis.

1.3 Immunology

1.3.1 Innate immunity

1.3.1.1 Pattern recognition receptors

The innate immune system provides a first line of defence against pathogens. In contrast to the specific adaptive immune system that comprises cellular (T cells) and humoral (B cells) mechanisms, the innate immune system senses broad spectra of pathogens with special characteristic structural features, so-called pathogen-associated molecular patterns (PAMPs).
The detection takes place through pattern recognition receptors (PRRs). There are two main receptor families involved in virus detection: Toll-like receptors (TLRs) and RIG-I-like receptors (RLRs). TLRs are membrane-spanning non-catalytic molecules which contain a subclass that recognises for example RNA and DNA patterns derived from pathogens including bacteria, viruses, parasites and fungi (Akira and Takeda, 2004; Janeway, Jr. and Medzhitov, 2002), whereas RLRs do not rely on membranes and are located in the cytoplasm of the cell. Both families induce signalling pathways after binding of PAMPs that for example merge in dimerisation of the transcription factor IRF3, followed by transport into the nucleus and transcription of type I interferons (IFN).

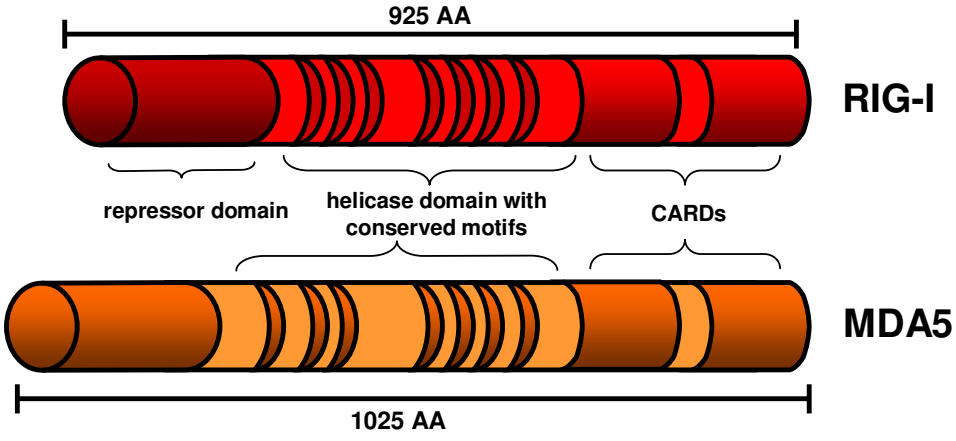

Figure 4. Domains of RIG-I and MDA5: Structure of the RLRs RIG-I and MDA5 with conserved motifs within the helicase domain depicted dark red or dark orange, respectively (Saito et al., 2007)

This study particularly focuses on RLRs and their influence on IFN-β activation by hantaviruses. Retinoic acid inducible gene (RIG-I, also known as DDX58) and melanoma differentiation-associated gene 5 (MDA5, also known as IFIH1) belong to the family of DexD/H box

helicases, both comprising two caspase recruitment domains (CARDs) located at the N-terminus (Figure 4). After binding of PAMPs with RIG-I, homodimerisation and a conformational shift occur. The CARDs are then free to interact with the adaptor molecule anchored in the outer mitochondrial membrane, IFN-β promotor stimulator (IPS-1) (also called mitochondrial antiviral signalling (MAVS; KIAA1271), virus-induced signalling adaptor (VISA), or CARD adaptor inducing IFN-β (CARDIF) thereby activating downstream signalling processes through Fas-associated protein with Death Domain (FADD) and other proteins like the Iκ-β kinase family members TBK-1, IKKi and IKKα/β that lead to activation of the transcription factors IRF3 and NFκB (Lin et al., 1998; Sato et al., 1998; Weaver et al., 1998; Li et al., 1999) (Figure 5).

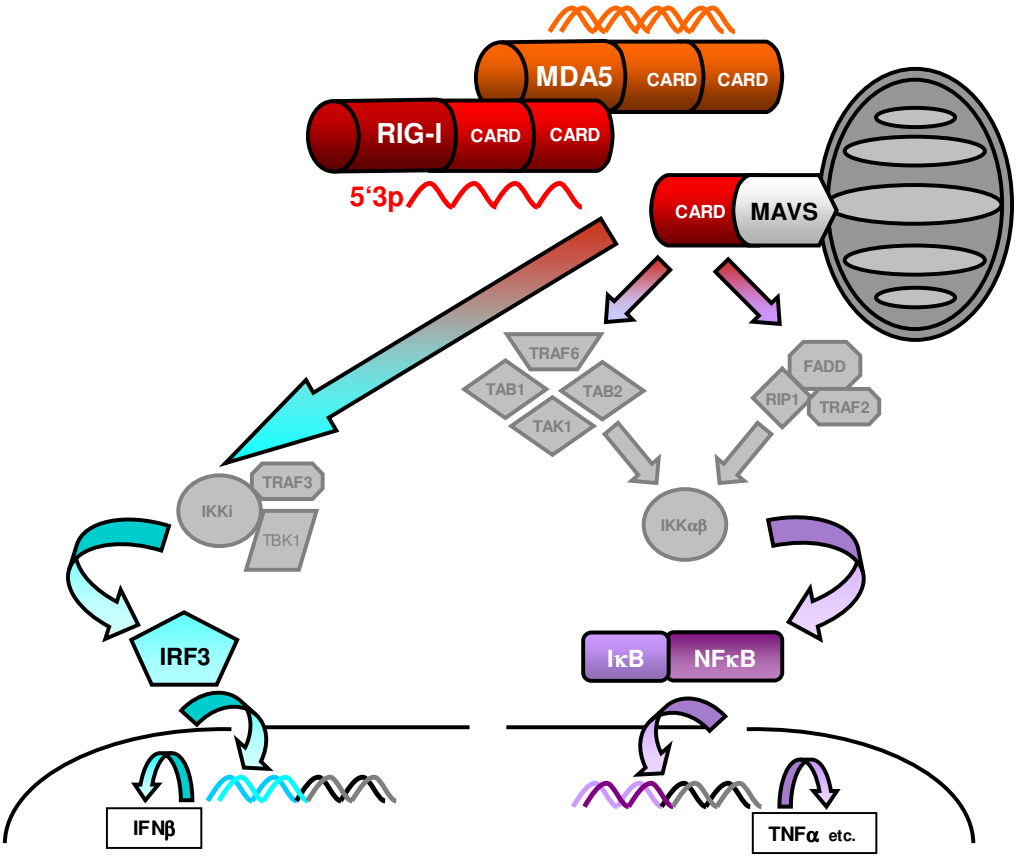

Figure 5. Signal transduction pathway of RIG-I and MDA5

IRF3 is phophorylated and then homodimerises for translocation into the nucleus (Akira and Takeda, 2004; Kawai et al., 2005; Meylan et al., 2005; Seth et al., 2005; Xu et al., 2005; Yoneyama et al., 2004). Coordinated binding of transcription factors leads to an induction of IFN-β expression, thus creating an antiviral status in the host. In addition, the RIG-I-associated signal transduction triggers the expression of other cytokines like tumor necrosis

factor α (TNF-α) through NFκB activation, thereby activating natural killer (NK) cells, dendritic cells (DCs) and macrophages (Balachandran and Barber, 2004; Du and Maniatis, 1992; Kato et al., 2005; Maniatis et al., 1998; Meylan et al., 2005; Seth et al., 2005; Xu et al., 2005; Yoneyama et al., 2004).

A third member of RLRs is LPG2, which is ubiquitously expressed like RIG-I and MDA5, but lacks the CARDs. It acts as a negative regulator of RIG-I when overexpressed in cells, but, on the other hand, features activating abilities when building heterodimers with RIG-I or MDA5 and their ligands (Komuro and Horvath, 2006; Saito and Gale, Jr., 2008b; Venkataraman et al., 2007; Yoneyama et al., 2005) (Figure 7).

1.3.1.2 Ligands of RLRs

The main PAMP recognised by RIG-I is single-stranded RNA (ssRNA) with a triphosphate at its 5' end, whereas MDA5 detects double-stranded RNA (dsRNA) (Alexopoulou et al., 2001; Hornung et al., 2006; Pichlmair et al., 2006). However, RIG-I is also able to bind RNA independent of 5'-triphosphates. MDA5 prefers longer dsRNAs of approximately 2 kbp whereas RIG-I shows only binding activity for short dsRNA of probably at least 70 bp to 1 kbp or short polyI:C (Kato et al., 2006; Kato et al., 2008). Furthermore, RIG-I has also been found to recognise homopolyuridine or homopolyadenine motifs for example within the 3' non-translated region of the hepatitis C virus (HCV) (Saito et al., 2008). For this kind of ligands, the 5'-triphosphate is necessary for triggering immune response, but not sufficient. In general, binding mainly relies on the ribonucleotide composition, length and structure (Saito and Gale, Jr., 2008a). In contrast, cellular RNAs, transcribed in the nucleus, are processed and modified, therefore not triggering innate immune mechanisms (Hornung et al., 2006; Kariko et al., 2005; Pichlmair et al., 2006).

1.3.1.3 Viruses and RLRs

Many viruses provide appropriate PAMPs to RIG-I during their life cycle. Most of them are RNA viruses as shown in Figure 6. However, activation of RIG-I signalling has also been shown for Epstein-Barr virus (EBV), a DNA virus (Samanta et al., 2006). For wide-spread DNA viruses like for example Herpes simplex virus (HSV), no interaction with RLRs could be detected yet, although they are known to generate dsRNA during replication (Weber et al., 2006).

MDA5 is known to be important for the detection of viruses belonging to the family of *Picornaviridae* (Gitlin et al., 2006). The specific structural component that is recognised by MDA5 has not been defined yet.

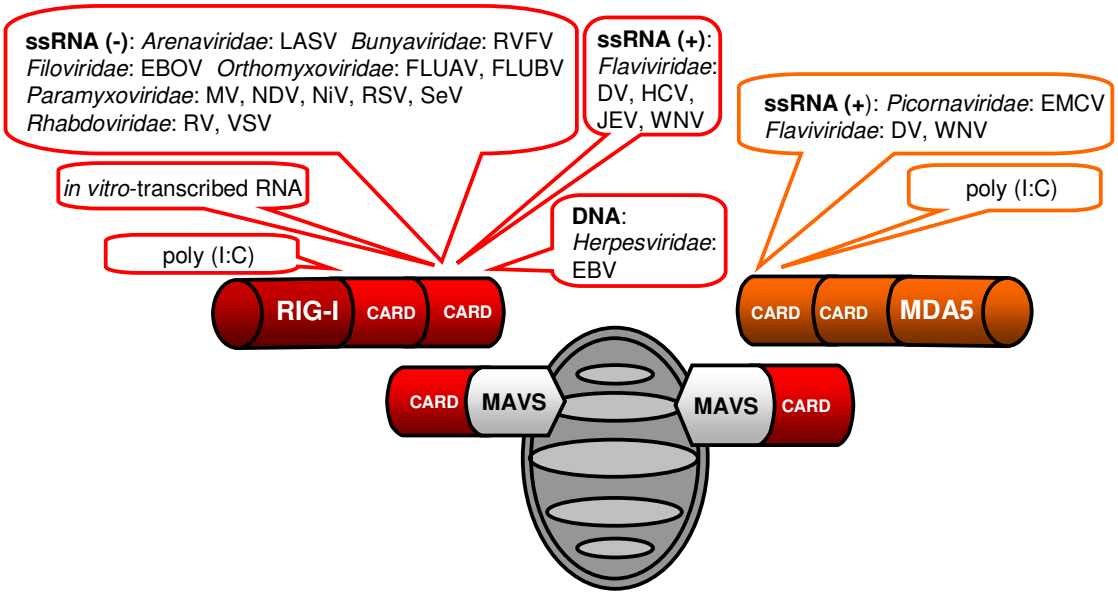

Figure 6. Ligands of RIG-I and MDA5: Artificial ligands and viruses inducing signalling cascades through RIG-I and MDA5, sorted by virus families and genome classifications (see list for abbreviations) (Loo et al., 2008).

Furthermore, some viral immune evasion mechanisms targeting cytoplasmic sensors have been detected. The V proteins of the familiy *Paramyxoviridae*, for example, have been shown to counteract MDA5, and NS3/4A protease of HCV disrupts RIG-I signalling by cleaving MAVS off the mitochondria (Kaukinen et al., 2006). Recently, different hantaviral G proteins were found to inhibit RIG-I signalling as well. More precisely, the G1 cytoplasmic tail of New York virus (NYV) – but not G1 derived from PHV - blocks RIG-I signalling upstream of IRF3 in human endothelial cells by interaction with the TBK1-TRAF3 complex, resulting in inhibited transcription from IFN-β promotors and ISREs (Figure 7) (Alff et al., 2006; Spiropoulou et al., 2007).

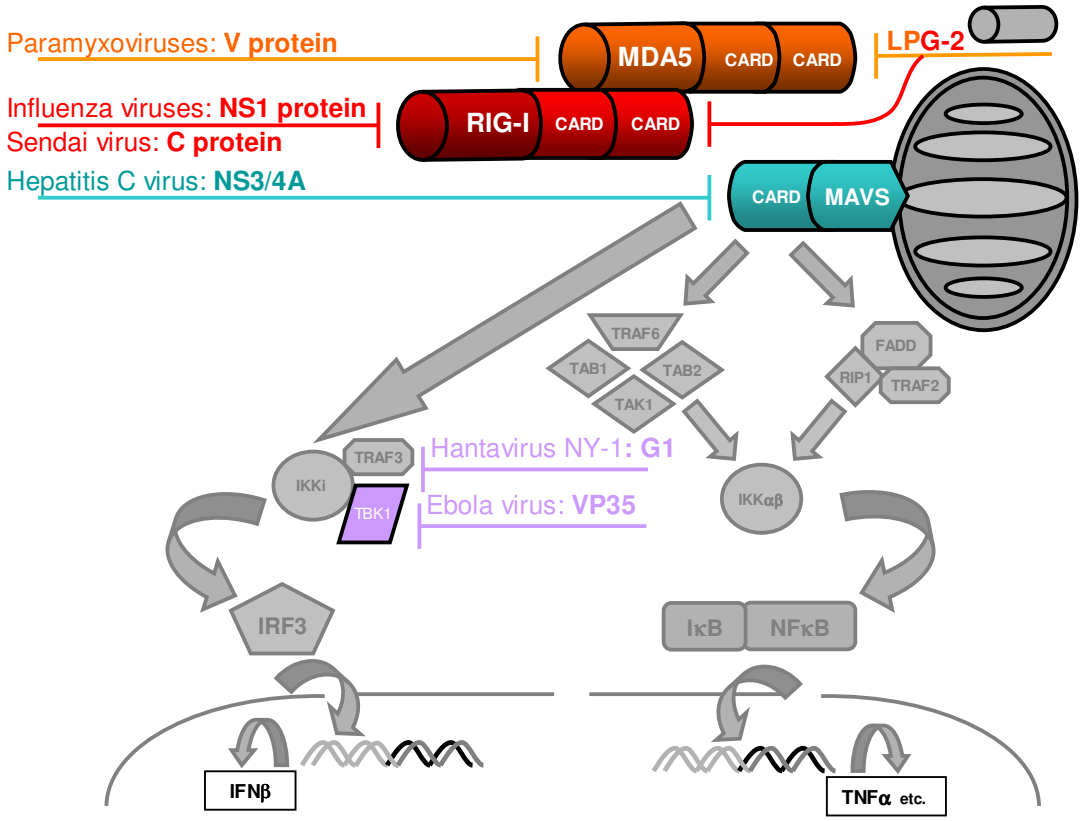

Figure 7. Viral evasion mechanisms counteracting signal transduction of RLRs: Viruses und their particular proteins interfering with RIG-I and MDA5 signalling are depicted in the same colour as the respective molecule of the the signaltransduction pathway.

1.3.2 Type I interferon

According to their amino acid sequence, interferons are grouped in three classes: Type I IFN, comprising IFN-α, IFN-β, IFN-ω, Type II represented by IFN-γ and Type III interferon with IFN-λ. IFN-α, belonging to a multi-gene family, is produced by monocytes and macrophages, lymphoblastoid cells, fibroblasts, and some other cell types, whereas IFN-β, encoded by only one gene, is mainly synthesised by fibroblasts, epithelial and endothelial cells (Roberts et al., 1998).

Type I IFNs are of crucial importance for the antiviral response, and they are produced constitutively in low amounts (Seth et al., 2006; Taniguchi and Takaoka, 2001). They link innate and adaptive immunity; for example, they modulate the differentiation of plasmacytoid (pDCs) and myeloid dendritic cells (mDCs), Th1/CD8+ T cell responses and cross priming and enhance the expression of costimulatory factors and major histocompatibility complex (MHC) class I molecules on antigen-presenting cells (APCs). Furthermore, they activate NK

cells and enhance primary antibody response (Le Bon et al., 2001; Le Bon et al., 2003; Montoya et al., 2002).

During the sensitisation phase, entering viruses can activate transcription factors, for example IRF3, NFκB and AP-1 through different signalling cascades that lead to production of IFN-β and other cytokines by coordinated binding to so-called positive regulatory domains (PRD) within the IFN-β promotor, thereby forming an "enhanceosome" (Yoneyama et al., 1998; Chu et al., 1999). In the late phase, secreted IFN-β binds to IFN-α/β receptors (IFNARs) in an autocrine and paracrine manner and initiates a positive feedback loop. IFNARs activate the Janus kinases JAK1 and Tyk-2 that in turn phosphorylate signal transducers and activators of transcription (STAT1 and STAT2), leading to a heterotrimeric complex with IRF9, called IFN-stimulated gene factor 3 (ISGF3) (Samuel, 2001). ISGFs bind to IFN-stimulated response elements (ISRE) within the genome, resulting in expression of more than 100 IFN-stimulated genes (ISGs). ISGs are for example 2'-5'-oligoadenylate synthetase (OAS) and dsRNA-dependent serin/threonin protein kinase R (PKR), causing degradation of viral RNAs and inhibition of viral protein synthesis (Williams, 2002) respectively, or Mx proteins. The latter are GTPases known to interfere with the replication of a broad range of RNA viruses by inhibition of viral replication (Frese et al., 1996).

1.3.3 Hantaviruses and immunity

Although hantaviruses do not necessarily induce strong type I IFN responses, IFNs inhibit hantavirus replication effectively (Kanerva et al., 1998; Nam et al., 2003; Temonen et al., 1995). Therefore, hantaviruses counteract innate immunity by blocking signalling pathways which lead to IFN expression. The effectiveness of influencing signalling cascades and therefore the success of replication and expansion differs between pathogenic and non-pathogenic hantaviruses.

Many ISGs are upregulated after infection of human endothelial as well as human lung epithelial cells with hantaviruses (Geimonen et al., 2002; Nam et al., 2003), but hantavirus strains differ in terms of impact on cellular gene expression patterns. Microarray studies showed high expressions of ISGs early after infection with non-pathogenic PHV, in contrast to pathogenic strains like HTNV and NYV that did not elicit immune response-related expressions earlier than 4 days post infection (d p.i.) (Geimonen et al., 2002). However, data about interactions of different hantavirus strains with innate immunity are incomplete.

Kraus *et al.* found that HTNV showed an induction of IFN-β in human umbilical vein endothelial cells (HUVECs) while this effect is only marginal for the less pathogenic TULV (Kraus et al., 2004). Furthermore, inefficient replication of TULV correlates with early MxA expression whereas strong replication of pathogenic HTNV goes along with retarded MxA expression.

Oelschlegel *et al.* conclude that MxA is not necessarily responsible for an inhibition of HTNV through class I IFN (Oelschlegel et al., 2007), whereas Frese *et al.* (Frese et al., 1996) showed an inhibition of several members of the *Bunyaviridae* including HTNV by stably transfected MxA expressed in Vero cells, congruently to Kanerva *et al.* who received similar results for PUUV and TULV (Kanerva et al., 1996). However, the latter group could not reproduce the inhibitory effect ascribed to transfected MxA in cell clones derived from a human leukemic monocyte lymphoma cell line (U-937).

Spiropoulou *et al.* observed high levels of IFN-β induced by PHV in human pulmonary microvascular endothelial cells (HMVEC-L), but no induction by ANDV early after infection, correlating with IRF3 activation, although both strains were able to downregulate IFN signalling (Spiropoulou et al., 2007). The study by Alff *et al.* detected strong IFN-β responses early after infection of human endothelial cells with PHV, but not with HTNV and NYV (Alff et al., 2006).

Furthermore, several groups have investigated whether single hantaviral components interact with cellular immune signalling components. As already mentioned above, the cytoplasmic tail of the G1 protein of pathogenic NYV but not non-pathogenic PHV blocks RIG-I signalling by disrupting the TBK1-TRAF3 complex and thereby inhibiting transcription from IFN-β promotors and ISREs (Alff et al., 2006; Alff et al., 2008; Spiropoulou et al., 2007).

G proteins from ANDV and PHV were able to downregulate IFN signalling by blocking the phosphorylation of STAT1 and STAT2 (Spiropoulou et al., 2007). Additionally, in G1 tails of HCPS-inducing hantaviruses, immunoreceptor tyrosine-based activation motifs were found that are able to interact with cellular kinases (Geimonen et al., 2003).

TULV- and HTNV-derived N proteins interact with ubiquitin-like modifier-1 (SUMO-1) (Kaukinen et al., 2003; Lee et al., 2003), whereas for PUUV N protein, interaction with an apoptosis enhancer, Daxx, has been observed (Li et al., 2002). Another recent finding indicates that the NS proteins of TULV (which, until recently, were undefined) and PUUV could be involved in IFN inhibition (Jaaskelainen et al., 2007).

1.3.4 Pathogenesis of hantaviruses

The immune response plays a crucial role for the pathogenesis of hantaviruses, although the exact mechanisms correlating with the severity of clinical symptoms caused by different hantaviral strains have not been elucidated yet. Cells involved in virus detection are immune cells, but also endothelial cells that function as main target cells after virus infection. Hantaviruses are also able to infect and to activate immature dendritic cells (DCs) thereby inducing cytokine secretion, for example TNF-α and Type I IFN, and upregulating MHC class I as well as adhesion molecules (Raftery et al., 2002).

Expression of vascular endothelial growth factor (VEGF), regulated in activation, normal T cells expressed and secreted (RANTES, CCL5) and the 10 kDa IFN-inducible protein (IP-10, CXCL10) is increased after infection of HMVEC-Ls with HTNV and SNV (Sundstrom et al., 2001). RANTES and IP-10 are known attract leucocytes, and IP-10 additionally plays an important role in the development of a Th1 response, whereas VEGF is a specific enhancer for microvascular permeability and can recruit monocytes (Khaiboullina and St Jeor, 2002; Sundstrom et al., 2001; Gavrilovskaya et al., 2008).

Activation of macrophages and monocytes triggers cytokine release. Many cytokines can be detected in significantly increased levels in human plasma such as IFN-β, IFN-γ, TNF-α, interleukin 2 (IL-2) and IL-6 during the acute phase of infection (Geimonen et al., 2002; Khaiboullina and St Jeor, 2002; Linderholm et al., 1996; Makela et al., 2004; Peters and Khan, 2002; Zaki et al., 1995). Furthermore, other biochemically active substances like nitrogen oxide and reactive oxygen are induced that may lead to local tissue damage, increased permeability of endothelial cells and possibly disturbed hemostasis (Kanerva et al., 1998).

In HFRS patients, the early cellular immune response is mainly directed against the N proteins, although epitopes against all structural proteins could be found. Hantaviral N protein is highly immunogenic and contains several B-cell as well as T-cell epitopes (Lundkvist et al., 1995; Van Epps et al., 1999; Van Epps et al., 2002; Vapalahti et al., 1995). During the humoral response against hantaviruses, all Ig subclasses are involved (Gott et al., 1997; Vapalahti et al., 1995). In later phases, the amount of IgM declines. Meanwhile, levels of IgG directed against both hantaviral glycoproteins overbalance (Groen et al., 1992; Kanerva et al., 1998; Lundkvist et al., 1993). Antibodies cross-react for many hantavirus species.

Nevertheless, the relation between adaptive immune response and pathogenesis has not been clarified yet. It has been suggested that the hantavirus-induced immunity plays a major role leading to microvascular leakage due to virus-specific CTL responses (Van Epps et al., 2002;

Schonrich et al., 2008). T lymphocyte activation is mainly triggered by dendritic cells in which hantaviruses are also able to replicate. After hantaviral infection, MHC I molecules are upregulated in both endothelial cells and DCs (Kraus et al., 2004; Raftery et al., 2002). The increased permeability of capillaries is in turn supposed to be the main cause of hantaviral symptoms, possibly caused by pathogenic hantaviruses in response to VEGF-directed regulation processes (Vapalahti et al., 2003; Gavrilovskaya et al., 2008).

It has been shown that in those reservoir hosts in which hantaviral infections remain asymptomatic, the induction of regulatory T cells (Tregs) takes place. Tregs normally function as suppressor of immune response thereby contributing to the maintainance of immune homoeostasis. By interfering with the proinflammatory immune response, Tregs possibly limit pathology in the reservoir hosts, but avoid virus cleareance (Easterbrook et al., 2007; Schountz et al., 2007), whereas in humans, the opposite could be assumed due to lacking Treg activation.

1.4 Aims and scope of this thesis

The aim of this thesis is to clarify the early steps of hantavirus-directed innate immunity. To analyse the influence of RIG-I for hantavirus replication, growth kinetics with pathogenic and non-pathogenic hantavirus strains are carried out on wild-type, control and ΔRIG-I cells. Furthermore, a respective hantaviral PAMP should be defined. For this purpose, single hantaviral components derived from strains of different pathogenicity are tested in a co-transfection system with the PRR of interest and analysed by an IFN-β promoter-related luciferase readout.

2 Material

2.1 Bacteria

Escherichia coli, XL1-Blue	Stratagene (LaJolla, Canada)
Escherichia coli, One Shot Top10	Invitrogen (Karlsruhe, Germany)

2.2 Cell lines

A549 cells	human epithelial lung cells	ATCC nr.: CCL-185™
A549 ΔRIG-I knockdown	human epithelial lung cells	kindly provided by M. Matthäi, Berlin
A549 control cells	human epithelial lung cells	kindly provided by M. Matthäi, Berlin
293T cells	human epithelial kidney cells	ATCC nr.: CRL-11268™
HEK293 cells	human epithelial kidney cells	ATCC nr.: CRL-1573™
HeLa cells	human cervix carcinoma cells	ATCC nr.: CCL-2
Huh7.5	human hepatoma cell line	(Binder et al., 2007)
Huh7.5 RIG-I wt_GUN	human hepatoma cell line	(Binder et al., 2007)
Huh7.5 RIG-I ca_GUN	human hepatoma cell line	(Binder et al., 2007)
Huh7.5 vector_GUN	human hepatoma cell line	(Binder et al., 2007)
Huh7.5 Mda5_GUN	human hepatoma cell line	kindly provided by M. Binder, Heidelberg
VeroE6 cells	green monkey epithelial kidney cells	ATCC nr.: CRL-1586™

2.3 Plasmids

pcDNA3	Invitrogen (Karlsruhe, Germany)
pcDNA p125-luc (firefly)	(Yoneyama et al., 1996)
pcDNA NAK (TBK) Flag	(Tojima et al., 2000)
pcDNA B/NS1	(Dauber et al., 2004)
pEF-Bos h IKKi Flag	(Shimada et al., 1999)
pEF-Bos-RIG-I Flag	(Yoneyama et al., 2004)
pEF MDA5 myc	(Andrejeva et al., 2004)
pISRE-Luc plasmid (Firefly)	Stratagene (LaJolla, Canada)
pRL-TK-Luc plasmid (Renilla)	Promega (Mannheim, Germany)
pSHAG-magic2	Open Biosystems (Huntsville, USA)
pSHAG-magic2 dRIG	Open Biosystems (Huntsville, USA)
pSCA	Stratagene (LaJolla, Canada)

2.3.1 Hantaviral expression plasmids

The expression plasmids containing hantaviral N or G proteins were kindly provided by Dr. Rainer Ulrich (Berlin/island Riems).

2.3.1.1 G protein expression plasmids

pcDNA DOB saarema G1
pcDNA DOB slovenia G1
pcDNA PUU Kazan G1
pcDNA HTN-GPC

2.3.1.2 N protein expression plasmids

pcDNA DOB slovakia N
pcDNA DOB slovenia N
pcDNA Hantaan fojnica N
pcDNA PUU Vranica N
pcDNA Tula N

2.4 Hantavirus strains

A6 reassortant	Sina Kirsanovs, Berlin
A36 reassortant	Sina Kirsanovs, Berlin
DOBV Sk/Aa	(Klempa et al., 2005)
DOBV Slo/Af	(Avsic-Zupanc et al., 1995)
HTNV (strain 76-118)	Dr. Åke Lundkvist, Stockholm
PHV (type-3571)	Dr. Robert Tesh, Galveston
PUUV	Dr. Åke Lundkvist, Stockholm
TULV (strain Moravia)	Dr. Åke Lundkvist, Stockholm

2.5 VSV

VSV was kindly provided by Prof. Dr. Friedemann Weber (Freiburg).

2.6 Reagents

Aceton	Roth (Karlsruhe, Germany)
Agarose	VWR (Darmstadt, Germany)
APS	Roth (Karlsruhe, Germany)
Avicel	FMC Biopolymer (Philadelphia, USA)
Bacto-Agar	Gibco/ Invitrogen (Karlsruhe, Germany)
BME 10x	Biochrom AG (Berlin, Germany)
BSA	PAA (Pasching, Austria)
Bromphenol blue	Serva (Heidelberg, Germany)
CaCl2	Roth (Karlsruhe, Germany)
Ciprofloxacin	MP Biomedicals (Illkirch, France)
Coomassie blue	Serva (Heidelberg, Germany)
D-MEM	Biochrom AG (Berlin, Germany)

DMSO	Roth (Karlsruhe, Germany)
dNTPs	Bioline (Luckenwalde, Germany)
EDTA	AppliChem (Darmstadt, Germany)
Eisessig	Roth (Karlsruhe, Germany)
Ethanol	Roth (Karlsruhe, Germany)
Ethidiumbromid	Roth (Karlsruhe, Germany)
FCS	Biochrom AG (Berlin, Germany)
Formaldehyd	Merck (Darmstadt, Germany)
Formamid	Merck (Darmstadt, Germany)
Glutamin	Merck (Darmstadt, Germany)
Glycerol	Roth (Karlsruhe, Germany)
Glycin	Roth (Karlsruhe, Germany)
GM-CSF	ImmunoTools (Friesoythe, Germany)
G418-Sulfat Geneticin	PAA (Pasching, Austria)
HBSS	Gibco/Invitrogen (Karlsruhe, Germany)
Hefeextrakt	Roth (Karlsruhe, Germany)
HEPES	Biochrom AG (Berlin, Germany)
HCl	Roth (Karlsruhe, Germany)
H_2SO_4	Merck (Darmstadt, Germany)
Isopropanol	Roth (Karlsruhe, Germany)
Kanamycin	Boehringer-Ingelheim (Ingelheim, Germany)
KCl	Merck (Darmstadt, Germany)
K_2HPO_4	Merck (Darmstadt, Germany)
Lipofectamine 2000	Invitrogen (Karlsruhe, Germany)
MgCl2	J.T. Baker (Griesheim, Germany)
MEM	Biochrom AG (Berlin, Germany)
Mercaptoethanol	Merck (Darmstadt, Germany)
Methanol	Roth (Karlsruhe, Germany)
Milk powder	Sufocin (Zeven, Germany)
MOPS	Merck (Darmstadt, Germany)
N6 primer	Amersham Pharmacia Biotech (Piscataway, USA)
Natriumacetat	Merck (Darmstadt, Germany)
NaCl	Roth (Karlsruhe, Germany)
Na_2HPO_4	Roth (Karlsruhe, Germany)
NaN_3	Roth (Karlsruhe, Germany)
NaOH	Merck (Darmstadt, Germany)
Na-Pyruvat	Biochrom AG (Berlin, Germany)
Non-essential amino acids	Biochrom AG (Berlin, Germany)
Nuclease-free water	Promega (Mannheim, Germany)
OptiMEM	Gibco/Invitrogen (Karlsruhe, Germany)
PBS	PAA (Pasching, Germany)
Penicillin/Streptomycin (10000 U/ml)	Biochrom AG (Berlin, Germany)
PolyI:C	Sigma-Aldrich (Deisendorf, Germany)
Propidiumiodid (95-98%)	Sigma-Aldrich (Deisendorf, Germany)
Protease-Inhibitor-Cocktail	Roche (Mannheim, Germany)

Protector RNase inhibitor	Roche (Mannheim, Germany)
Puromycin	PAA (Pasching, Germany)
Rainbow molecular weight marker RPN 800	Amersham Pharmacia Biotech (Piscataway, USA)
Restore™ Western Blot Stripping Buffer	Pierce (Rockford, USA)
Rnase A	Qiagen (Hilden, Germany)
RNA safe	Fermentas (St. Leon-Rot, Germany)
Rotiphorese-Acrylamid	Roth (Karlsruhe, Germany)
RQ DNase	Promega (Mannheim, Germany)
SDS	Merck (Darmstadt, Germany)
Sodium bicarbonate	Biochrom AG (Berlin, Germany)
TEMED	ICN Biomedicals (Irvine, USA)
Tetrazyclin	Invitrogen (Karlsruhe, Germany)
TNF-α	Roth (Karlsruhe, Germany)
Tris-Aminomethan	Roth (Karlsruhe, Germany)
Tris-HCl	Roth (Karlsruhe, Germany)
Triton X-100	Roche (Mannheim, Germany)
Trypanblau	Serva (Heidelberg, Germany)
Trypsin/EDTA	Invitrogen (Karlsruhe, Germany)
Trypsin (TPCK-treated)	Sigma-Aldrich (Deisendorf, Germany)
Tween 20	Merck (Darmstadt, Germany)
Ultra pure water	PAA (Pasching, Germany)

2.7 Equipment

Autoclave	
Durchreicheautoklav	Getinge (Rastatt, Germany)
Centrifuges	
Biofuge fresco	Heraeus (Kleinostheim, Germany)
Centrifuge 5415D	Eppendorf (Hamburg, Germany)
Megafuge 1.0	Heraeus (Kleinostheim, Germany)
Multifuge H	Heraeus (Kleinostheim, Germany)
Optima LE-80K Ultrazentrifuge	Beckman Coulter (Krefeld, Germany)
Sorvall RC24 Superspeed	DuPont Instruments (Delaware, USA)
Sorvall RC-5B	DuPont Instruments (Delaware, USA)
SpeedVac Univapo 150 H	UniEquip (Martinsried, Germany)
Tischzentrifuge Biofuge pico	Heraeus (Kleinostheim, Germany)
Ultrazentrifuge	Beckton Dickinson (San José, USA)
Counting chamber	
Neubauer improved	Marienfeld (Lauda-Königshofen, Germany)
Cryo container	
CryoContainer Cryo	Nalgene Nunc (Wiesbaden, Germany)
Detection systems	
CCD-Kamera	Bioblock Scientific (Illkirch, France)
DIANA II-CCD	Raytest (Strabenhardt, Germany)
Electrophoresis and blot systems	

Elektrophorese-Kammer Mini Trans-Blot Cell	Bio Rad (München, Germany)
Mini-Protean III	Bio Rad (München, Germany)
Semi-Dry Blot-Kammer	Owi (Porthmouth, Netherlands)
FACS	
FACScalibur	Becton Dickinson (Heidelberg, Germany)
Incubators	
Cellstar	Heraeus (Kleinostheim, Germany)
CO_2 water-jacketed incubator	Nuaire (Plymouth, USA)
CO_2–Inkubator	Heraeus (Kleinostheim, Germany)
Hera Cell 150	Heraeus (Kleinostheim, Germany)
Laminar flows	
Laminarbox Herasafe	Heraeus (Kleinostheim, Germany)
Sterilbank BSB4A	Gelaire (Sydney, Australia)
Luminometer	
Berthold Mithras LB940	Berthold (Bad Wildbach, Germany)
Luminometer LB96V	Berthold (Bad Wildbach, Germany)
Microscopes	
CLSM	Leica Microsystems (Wetzlar, Germany)
Fluoreszenzmikroskop BX60	Olympus (Hamburg, Germany)
Lichtmikroskop Axiovert 40C	Zeiss (Oberkochen, Germany)
Mikroskop Axiovert 25 CFL	Zeiss (Oberkochen, Germany)
Mixer	
Innova 4330	New Brunswick (Nürtingen, Germany)
Polymax 1040	Heidolph (Schwabach, Germany)
Test tube rotator 34528	Snijders Scientific (Tilburg, Netherlands)
Vibrax VXR	IKA (Staufen, Germany)
Vortexer MS1 Minishaker	IKA (Staufen, Germany)
Vortexer Reax 2000	Reax Heidolph (Schwabach, Germany)
PCR cyclers	
LightCycler® 1.5 system	Roche (Mannheim, Germany)
Thermocycler GeneAmp 9700	Applied Biosystems (Foster, Canada)
pH meter	
pH-Meter pH 320	WTW (Weilheim, Germany)
Photometer	
Photometer Ultraspec 3300 pro	Amersham Pharmacia Biotech (Piscataway, USA)
Spektrophotometer Ultraspec 4000	Amersham Pharmacia Biotech (Piscataway, USA)
Power supplies	
Powersupply EPS 300	Amersham Pharmacia Biotech (Piscataway, USA)
Model 200/2.0 Power Supply	Bio Rad (München, Germany)
Pump	
Typ ME2	Vacuubrand (Wertheim, Germany)
Vakuumpumpe	KNF Laboport (New Jersey, USA)
Refrigerator combinations	
Kombi-Kühlschrank Glasline	Liebherr (Ochsenhausen, Germany)
Liebherr Comfort NoFrost	Liebherr (Ochsenhausen, Germany)

Liebherr Premium	Liebherr (Ochsenhausen, Germany)
Scales	
Feinwaage	Sartorius (Göttingen, Germany)
MC1 Laboratory LC 2200P	Sartorius (Göttingen, Germany)
Universalwaage	Sartorius (Göttingen, Germany)
Thermostats	
Blockheater H250	Roth (Karlsruhe, Germany)
BT100	Kleinfeld Labortechnik (Gehrden, Germany)
UBD2	Grant Instruments (Cambridge, UK)
Transilluminator	
BioDoc Analyze	Biometra (Göttingen, Germany)
Water bath	
Lauda A100	Lauda (Königshofen, Germany)
Wasserbad WTE var 3185	Assistent (Sondheim/Rhön, Germany)

2.8 Buffers and solutions

2.8.1 Bacterial media

LB-Medium
1.5% (w/v) Bacto-Agar

After autoclaving and cool-down to 50 °C, 100 µg/µl of canamycine or ampicillin were added and casted into Petri dishes.

2.8.2 DNA and RNA purification

2.8.2.1 DEPC water

0.1% DEPC was ressolved in water, mixed and incubated at RT over night. Sterilisation was carried out by autoclavation.

2.8.2.2 6x DNA sample buffer

0.1% (w/v)	Bromphenol blue
0.1% (w/v)	Xylencyanol
30%	Glycerol
10 mM	EDTA (pH 8.0)

2.8.2.3 1x TAE buffer

40 mM	Tris acetate
1 mM	EDTA
pH 8.5	

2.8.2.4 0.5x TBE buffer

45 mM	Tris
45 mM	Boric acid
1 M	EDTA
pH 8.0	

2.8.2.5 10x FA buffer

200 mM	MOPS
50 mM	Natrium acetate
10 mM	EDTA
pH 7	

2.8.2.6 1x FA buffer

100 ml	10x FA buffer
20 ml	37% Formaldehyde
880 ml	DEPC water

2.8.2.7 5x RNA loading buffer

32 µl	saturated bromphenol solution
80 µl	EDTA (5 mM, pH 8)
720 µl	37% Formaldehyde
2 ml	glycerole
3.084 ml	formamide
4 ml	10x FA buffer

2.8.3 FACS analysis

2.8.3.1 Blocking solution

10%	FCS
0.02%	sodium azide
	PBS

2.8.3.2 Fixation solution

0.37%	formaldehyde
	PBS

2.8.3.3 Washing solution

1%	FCS
0.002%	sodium azide
	PBS

2.8.4 Focus purification assay

2.8.4.1 Avicel (2.4%)

24 g	Avicel
ad 1 l	aqua bidest

2.8.4.2 2x BME

100 ml	10x BME
10 ml	L-Glutamin
40 ml	$NaHCO_3$
350 ml	ultra pure water

2.8.5 Hantavirus titration

2.8.5.1 Agarose overlay

01:01	1% agarose and BME (with 2% streptomycin and penicillin)
10%	FCS
2.5%	HEPES

2.8.5.2 Antibody dilution buffer

0.1%	Tween
5%	FCS
	PBS

2.8.5.3 Avicel Overlay

01:01	1% agarose and BME (with 2% streptomycin and penicillin)
5%	FCS
2.5%	HEPES
	streptomycin/penicillin

2.8.5.4 Virus dilution buffer

25 ml	HBSS
500 µl	HEPES
500 µl	streptomycin/penicillin
250 µl	FCS

2.8.5.5 Washing buffer

0.15%	Tween
	PBS

2.8.6 Immunofluorescence

2.8.6.1 Fixation solution

30%	methanol
10%	acetic acid

2.8.6.2 Triton lysis buffer

20 mM	Tris-HCl (pH 7.4)
137 mM	NaCl
10%	Glycerol
1%	Triton X-100
2 mM	EDTA
50 mM	Na-ß-Glycerophosphate
20 mM	Na-Pyrophosphate
1 mM	Na_3VO_4
1 mM	Pefablock

2.8.6.3 Mowiol

2.4 g	Mowiol
6 ml	Glycerol
7 ml	dH_2O

- incubate over night

12 ml Tris (0.2 M), pH 8.5

- dissolve at 50-60 °C
- centrifuge for 15 min, 4000 rpm and add 10% (w/v) DABCO
- storage of aliquots at -20 °C

2.8.7 SDS-PAGE and Western blot

2.8.7.1 Ponceau Red

0.1%	Ponceau red
1%	Acetic acid

2.8.7.2 2x SDS sample buffer

1.2 ml	H_2O
8.3 ml	0.5 M Tris-HCl (pH 6.8)
6 ml	10% SDS (w/v)
1.5 ml	Glycerin
9 mg/ml	Bromphenol blue
5%	ß-Mercaptoethanol

2.8.7.3 10x SDS electrophoresis buffer

250 mM	Tris
1.92 M	Glycine
10 g/l	SDS

2.8.7.4 Semidry blotting buffer

48 mM	Tris
39 mM	Glycine
1.3 mM	SDS
20%	Methanol

2.8.7.5 TBST

100 mM	Tris-HCl (pH 8.0)
1.5 M	NaCl
0.5%	Tween 20

2.8.7.6 Western blot lysis buffer

10 mM	Tris-HCl (pH 7.4)
1 mM	EDTA
100 mM	NaCl
1 mM	PMSF
1%	Triton X-100

2.9 Antibodies

2.9.1 Antibodies for immunofluorescence and Western blot

Table 2: Primary antibodies for immunofluorescence and Western blot

Title	Manufacturer	Species	Dilution	
			IF	WB
α-β-Actin	Acris	mouse		1:10000
α-FLAG (M2)	Sigma-Aldrich	mouse	1:600	1:3000
α-HA	Upstate	rabbit		1:1000
α-Hanta N	(Razanskiene et al., 2004)	rabbit		1:500
α-Influenza B/NS1	BioGenes	rabbit	1:300	1:5000
α-MAVS	Axxora	rabbit	1:500	1:1000
α-myc (9E10)	Santa Cruz	mouse	1:100	1:1000
α-RIG-I	Axxora	rabbit	1:500	1:1000
α-Tubulin	Sigma	mouse		1:1000

Table 3: Secondary antibodies for immunofluorescence and Western blot

Title	Manufacturer	Target species	Species	Dilution
Alexafluor 488	Molecular Probes	mouse	goat	1:1000 (IF)
Alexafluor 594	Molecular Probes	rabbit	goat	1:1000 (IF)
HRP	DAKO	mouse	rabbit	1:15 000 (WB)
HRP	DAKO	rabbit	pig	1:15 000 (WB)
HRP	Cell Signalling/NEB	rabbit	goat	1:10 000 (WB)

2.9.2 Antibodies for FACS analysis

Table 4: Antibodies for FACS analysis

Modification	Manufacturer	Target species	Species	Dilution
CD29 purified	Immunotools	human	mouse	1:50
CD61 purified	Immunotools	human	mouse	1:50
IgG1 purified	Immunotools	human	mouse	1:50
PE IgG/IgM	Immunotools	mouse	goat	1:67

2.9.3 Antibodies for focus purification assay

Table 5: Antibodies/sera for focus purification assay

Virus strain	antibody	reference	dilution	incubation time [d]
DOBV Slo	rabbit	(Razanskiene et al., 2004)	1:500	10
DOBV Sk	rabbit	(Razanskiene et al., 2004)	1:500	8
HTNV	rabbit	(Razanskiene et al., 2004)	1:1000	7
PHV	rabbit strain Malacky	(Sibold et al., 1999)	1:1000	8
PUUV	rabbit strain Malacky	(Sibold et al., 1999)	1:1000	8
TULV	rabbit strain Malacky	(Sibold et al., 1999)	1:1000	10
A6	rabbit	(Razanskiene et al., 2004)	1:500	8
A36	rabbit	(Razanskiene et al., 2004)	1:500	8
HRP α Rabbit IgG	goat	Dianova	1:1000	

2.10 Kits

Albumin Standard	Pierce (Rockford, USA)
Antarctic Phosphatase	NEB (Frankfurt, Germany)
BCS Protein Assay Kit	Pierce (Rockford, USA)
BigDye® Terminator 3.1 Kit	Applied Biosystems (Foster, Canada)
Dual-Luciferase® Reporter Assay System	Promega (Mannheim, Germany)
EndoFree Plasmid Maxi Kit	Qiagen (Hilden, Germany)
Erase-a-Base®	Promega (Mannheim, Germany)
Expand High Fidelity PCR System	Roche (Mannheim, Germany)
GeneRuler™ DNA Ladder Mix	Fermentas (St. Leon-Rot, Germany)
LightCycler®Fast Start DNA Master^{PLUS} HybProbe Kit	Roche (Mannheim, Germany)
MagNA Pure LC mRNA isolation Kit I	Roche (Mannheim, Germany)
M-MLV-RT	Invitrogen (Karlsruhe, Germany)
OneStep RT-PCR Kit	Qiagen (Hilden, Germany)
QIAamp MinEluteTM Virus Spin Kit	Qiagen (Hilden, Germany)
QIAamp Viral RNA Mini Kit	Qiagen (Hilden, Germany)
QIAEXII Gel Extraction Kit	Qiagen (Hilden, Germany)
QIAfilter Plasmid Maxi Kit	Qiagen (Hilden, Germany)
Qiagen RNAeasy Mini Kit	Qiagen (Hilden, Germany)
QIAprep® Miniprep Kit	Qiagen (Hilden, Germany)
QIAquik PCR Purification Kit	Qiagen (Hilden, Germany)
Qiagen RNeasy® Kit	Qiagen (Hilden, Germany)
Superscript III Reverse Transcriptase	Invitrogen (Karlsruhe, Germany)
Super Signal West Dura Extended duration substrate	Pierce (Rockford, USA)
T7 Transcription Kit	Fermentas (St. Leon-Rot, Germany)
TRIZOL®	Invitrogen (Karlsruhe, Germany)
Venor®*GeM*-Mykoplasmen Detektions Kit	Minerva Biolabs (Berlin, Germany)

2.11 Software

Adobe Photoshop	7.0 software (Adobe Systems Incorporated, San Jose, CA, USA)
CellQuest Pro®	Becton Dickinson (Heidelberg, Germany)
MacVector	Apple (Cupertino, USA)
LightCycler Software 4.05	Roche (Mannheim, Germany)
Expasy	http://www.expasy.org/
Multalin	http://bioinfo.genopole-toulouse.prd.fr/multalin/multalin.html
NCBI	National Center for Biotechnology Information (NCBI) http://www.ncbi.nlm.nih.gov/
TINA	Raytest (Strabenhardt, Germany)

2.12 Consumables

6-, 12-, 24-well plates	Becton Dickinson (Heidelberg, Germany)
Bulbs	Ratiolab (Dreieich-Buchschlag, Germany)
Cell culture flasks T25	Greiner (Frickenhausen, Germany)
Cell culture flasks T75, T125	Nunc (Wiesbaden, Germany)
Cell culture dishes	Greiner (Frickenhausen, Germany)
Cell scraper	TPP (Trasadingen, Switzerland)
Eppendorf tubes	Eppendorf (Hamburg, Germany)
FACS tubes	VWR (Darmstadt, Germany)
Falcon tubes	TPP (Trasadingen, Switzerland)
Microscope slides	Roth (Karlsruhe, Germany)
Nitrocellulose membranes	Whatman (Dassel, Germany)
Parafilm	Pechiney Plastic Packaging (Chicago, USA)
Petri dishes	TPP (Trasadingen, Switzerland)
Pipet tips	Roth (Karlsruhe, Germany)
Serological pipets	TPP (Trasadingen, Switzerland)

3 Methods

3.1 Molecular biology

3.1.1 Plasmid preparation

Single colonies of plated bacteria were picked and grown overnight in appropriate selection media at 37 °C on a shaker. Plasmid DNA was processed with QIAprep® Miniprep Kit QIAfilter, Plasmid Maxi Kit® or with EndoFree Plasmid Maxi Kit® for transfection according to the manufacturer's instructions. The purified DNA was diluted in an appropriate volume of water.

3.1.2 Transformation

To insert DNA into bacteria, appropriate amounts of plasmid DNA (20-200 ng) were added to competent bacteria and incubated on ice for 30 min. Afterwards, a heat shock was carried out at 42 °C for 30 s and 500 µl pre-warmed SOC-medium was added. After 30 min of incubation at 37 °C on a shaker, the suspension was plated on petri dishes containing LB-Agar with the appropriate antibiotics for selection and incubated at 37 °C overnight.

3.1.3 Preparation of competent E. *coli* XL1 blue

200 ml of LB medium was inoculated with 10 ml of an overnight pre-culture and incubated at 37 °C on a shaker. When an OD_{600} of 0.5 was reached, the suspension was centrifuged (10 min, 4000 rpm) at 37 °C. After resuspending the pellet in 20 ml ice-cold $MgCl_2$ solution (100 mM) and chilling on ice for 1 h, the centrifugation was repeated. The pellet was resuspended in 8 ml ice-cold $CaCl_2$ solution (100 mM) and again chilled on ice for 1 h. After addition of glycerol, the competent bacteria were aliquoted and shock frozen in liquid nitrogen. The aliquots were stored at -80 °C.

3.1.4 Agarose gel electrophoresis

At least 500 ng DNA of the samples were mixed with 6x sample buffer and loaded on agarose gels (1%). The DNA was separated with 90-110 V and 300 mA for 30-60 min. Following

staining in ethidium bromide solution for 15 min, the DNA bands were visualised on a transilluminator.

3.1.5 Determination of DNA and RNA concentration

Dissolved DNA and RNA show an absorption maximum at 260 nm that is used for photometric analyses to determine the sample concentration. For this purpose, the sample was diluted and measured.

A = absorption value

1 OD = 50 µg/ml

DNA concentration [µg/µl] = A_{260} x 50 µg/ml x dilution factor / 1000

1 OD = 40 µg/ml

RNA concentration [µg/µl] = A_{260} x 40 µg/ml x dilution factor / 1000

3.1.6 Sequencing of hantavirus expression plasmids

The nucleotide sequence for the entire ORF of each N expression plasmid was confirmed with the BigDye DNA sequencing kit. The principle of this kit is based on the classical chain-termination method by Sanger. The integrities of the constructs were confirmed by DNA cycle sequencing by using an ABI Prism 3100 genetic analyzer (Applied Biosystems) and evaluated with Sequencing Analyses 3.7 Software.

PCR program:

95 °C	1 min
96 °C	10 s
55 °C	5 s
60 °C	4 min
4 °C	
25 cycles	

PCR master mix for one reaction:

200 ng	plasmid
0.5 µl	T7 primer (20 pM) or Sp6
1 µl	BigDye
1.5 µl	5x buffer
ad 10	Ultra pure water

The histogram data were evaluated with MacVector.

3.1.7 Generation of deletion mutants

To analyse the sections of HTNV N ORF important for activating RIG-I signalling, truncated N protein expression plasmids were generated with the Erase-a-Base®-Kit according to the manufacturer's instructions with support of Pritesh Lalwani. Briefly, plasmids were linearised by digestion with two different restriction enzymes (XbaI and ApaI) that leave a 4-base 3' overhang resistent to exonuclease activity and a 5' overhang or blunt end sensitive to exonuclease activity. The reaction was stopped according to the designated truncation since there are temperature-dependent digestion rates. Samples during exonuclease activity were taken at 0, 1, 2, 3 and 4 minutes after starting the reaction. After ligation, the plasmids were expanded and tested.

3.1.8 *In vitro*-transcription and removal of 5'-triphosphates

In vitro-transcription was carried out with G and N protein expression plasmids after digestion with ApaI according to the manufacturer's instructions (Fermentas). After treatment with DNase, the RNA was purified by Phenol/Chloroform extraction or with Qiagen RNAeasy Mini Kit, washed with ice-cold 75% ethanol and used immediately for experiments. To test the influence of 5'-triphosphates, the transcribed RNAs were digested with phosphatase for 15 min at 37 °C. Therafter, the samples were purified by Phenol/Chloroform extraction as described above.

3.1.9 RNA gel electrophoresis

First, the electrophoresis equipment was washed with 0.5% SDS and DEPC water and desinfected with ethanol. The gel containing 1.2 g agarose, 10 ml 10x FA buffer and 100 ml DEPC water was melted, cooled down to 60 °C in a water bath and mixed with 1.8 ml of 37% formaldehyde solution before casting. The gel was equilibrated for 30 min at 65 V. After addition of loading buffer to the samples, the samples were incubated for 10 min at 65 °C, chilled on ice and run for 1 h at 65 V. Following staining in ethidium bromide solution for 30 min, the RNA bands were visualised on a transilluminator.

3.2 Cell biological methods

3.2.1 Cell culture

VeroE6 cells, African green monkey kidney cells, were maintained in EMEM supplemented with 10% FCS, 100 IU penicillin, 100 µg/ml streptomycin and 4.5 mM L-glutamine. A549 cells, Hela cells, 293T cells, HEK293 cells and Huh7.5 cell lines were grown in DMEM supplemented with 10% FCS, 100 IU penicillin, 100 µg/ml streptomycin and 4.5 mM L-glutamine. For A549 ΔRIG–I and control cells, 2 µg/ml puromycin was added. For transfected Huh7.5 cell lines except for the parental cells, 1 mg/ml G418 was added. Medium and FCS were endotoxin-free as certified by the manufacturer.

To passage confluent monolayers, cells were washed with PBS and treated with Trypsin/EDTA at 37 °C until they detached from the bottom of the flask. Then the cells were resuspended in appropriate medium and transferred into a new cell culture flask, plate or dish.

3.2.2 Freezing cells

To maintain cell stocks, confluent cells (T75 flask) were trypsinised and washed in PBS. After centrifugation (3 min, 800 rpm), they were resuspended in 1 ml FCS with 10% DMSO and maintained in a cell culture freezing box at –80 °C over night before transferring them into liquid nitrogen.

3.2.3 Transfection of cells

Confluent cells were splitted one day before transfection at a ratio of 1:2. DNA and Lipofectamine2000 (2 µl/1 µg DNA) were added to 100 µl Optimem, respectively, mixed and incubated for 5 min at RT. Then the two mixes were combined and incubated for 15 min at RT. Meanwhile, the cells were trypsinised and washed with PBS. After centrifugation for 3 min at 800 rpm, the pellet was resuspended in 10 ml of transfection medium (appropriate medium without antibiotics) and seeded into culture dishes or plates. The transfection mix was added dropwise. After 6 hours of incubation at 37 °C, the transfection medium was replaced by full DMEM.

3.3 Virus treatment

3.3.1 Infection of cells

Appropriate cells were infected with viral stocks for 1 h at 37 °C as indicated. The virus was removed, monolayers were washed with PBS, and cells were maintained in complete media.

3.3.2 Hantavirus expansion

Stocks of all hantavirus strains were propagated on VeroE6 cells grown in 25 cm² cell culture flasks. Vero cells are not able to produce Type I IFN due to chromosomal deletions (Diaz, 1988). The cells were inoculated with virus of MOI 0.1 in a total volume of 5 ml medium and incubated at 37 °C/5% CO_2. After 7 to 10 days (depending on the respective virus strain), the cell culture supernatant was transferred to 75 cm² cell culture flasks containing confluent VeroE6 cells in a total volume of 20 ml medium. After 7 to 9 days, the cell culture supernatant was harvested, centrifuged to remove cell debris, aliquoted and stored at -80 °C. Concentrated viral stocks were prepared by pelleting virus from the supernatant of infected cells (4 h, 130 g, 4 °C). Virus pellets were resuspended in MEM supplemented with 5% FCS and stored at -80 °C. Virus stocks were free of mycoplasma contamination as tested by PCR.

3.3.3 Titration of hantaviruses

Virus titration was carried out as previously described (Heider et al., 2001). In short, VeroE6 cells were seeded into 6-well plates. When nearly confluent, cell medium was discarded and replaced by inoculums of 0.2 ml/well viral stock in ten-fold dilutions. After an incubation time of 1 h at 37 °C in a humidified 5% CO_2 atmosphere, cells were overlaid with 1.2% Avicel 1:1 mixture with BME. The plates were incubated for 7 to 10 days (depending on the virus strain) under conditions as indicated above. Thereafter, the overlay was discarded, cells were washed twice with PBS supplemented with 0.15% Tween and finally fixed for 10 min with 2 ml/well methanol. After the methanol had been removed, the cells were allowed to dry and washed again twice. 1 ml of suitable anti-hantaviral serum was added to each well, diluted in PBS containing 10% FCS, and incubated for 1 h at 37 °C. After washing five times, 1 ml of goat anti rabbit IgG conjugated with horseradish peroxidase diluted 1:1000 in PBS with 10% FCS was added per well, incubated for 1 h at 37 °C, and washed five times. After adding 0.5 ml/well of chemiluminescence substrate diluted 1:1 in water, the plates were evaluated

using a DIANA Chemiluminescence System (Figure 8). Thus, focus forming units (FFUs) could be enumerated for titer determination.

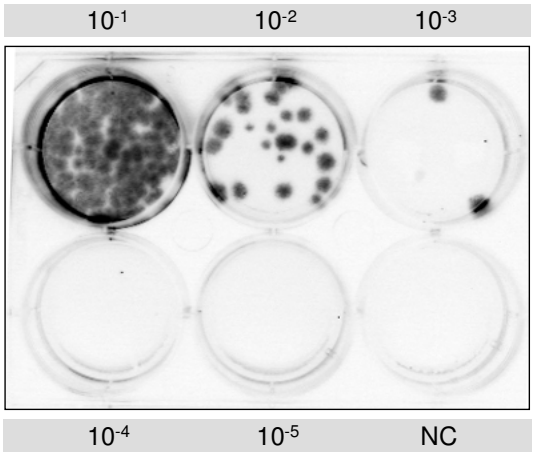

Figure 8. Chemiluminescent detection of hantaviral FFUs: Titration of HTNV in a 6-well plate in ten-fold dilutions

3.3.4 Focus purification assay

To obtain genetically homogeneous virus stocks of high purity, a focus purification was carried out (Rang et al., 2006), an indirect method similar to plaque picking normally used for expansion of CPE-causing viruses. When nearly confluent, VeroE6 cells seeded into 6-well plates were infected with inoculums of 0.2 ml/well viral stock in ten-fold dilutions containing HBSS supplemented with 2% HEPES, 2% FCS, 100 IU/ml penicillin and 100 µg/ml streptomycin. After virus adsorption for one hour at 37 °C in a humidified 5% CO_2 atmosphere, cells were overlaid with 2.5 ml/well of a pre-warmed (42 °C) agarose overlay. The plates were incubated for 7 to 10 days (depending on the virus strain) under conditions as indicated above.
The overlay was then removed carefully and kept at 4 °C while washing the cells with PBS and fixing them with methanol for 10 min. After the methanol had been removed, the cells were allowed to dry and washed again twice. 1 ml of suitable anti-hantaviral serum was added to each well, diluted in PBS containing 10% FCS, and incubated for 1 h at 37 °C.
Following five washing cycles, 1 ml of goat anti rabbit IgG conjugated with horseradish peroxidase diluted 1:1000 in PBS with 10% FCS was added per well, incubated for 1 h at 37 °C, and washed five times. After adding 0.5 ml/well of chemiluminescence substrate diluted 1:1 in water, the foci could be visualised with the DIANA Chemiluminescence System. A mirrored printout of the detected foci with the same size as the original overlay was used to trace

the foci on the agarose overlay and to pick them at the respective position (Figure 9). The picked material was resuspended in 200 µl medium. Thereafter, the purified focus was used for repeated focus purification and virus expansion.

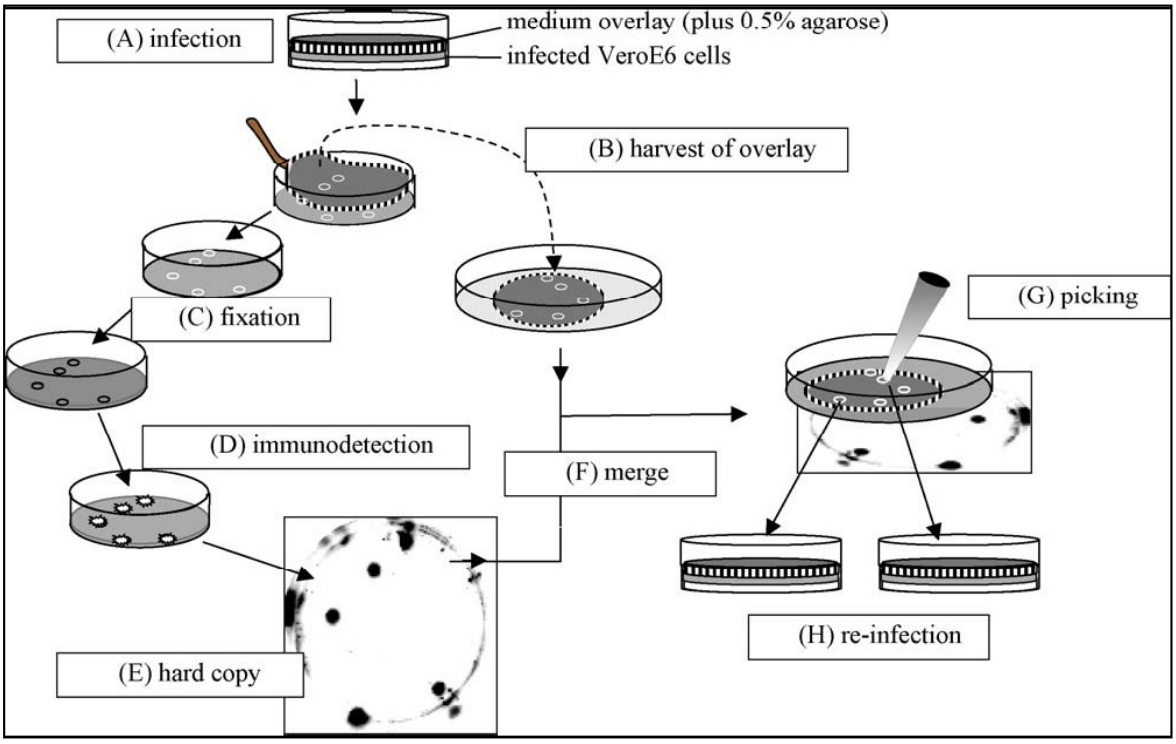

Figure 9. Focus purification procedure (Rang et al., 2006)

3.3.5 Kinetics

3.3.5.1 A549 cells

To examine the physiological importance of RIG-I for hantaviruses, growth kinetics with different hantaviral strains were carried out. A549 wild-type, ΔRIG-I and control cells were generated and kindly provided by Markus Matthäi (Robert Koch-Institute, Berlin). ΔRIG-I and control cells contain the plasmid pSM2c with RIG-I specific and non-target shRNA expression cassettes (Expression Arrest^{TM} human retroviral shRNA^{mir} individual contructs), oligo ID V2HS 199776 and RHS1707, respectively (Open Biosystems).

All three cell lines were seeded into 6-well plates and infected with HTNV, PHV, TULV, DOBV Slo, DOBV Sk (MOI 1) and the reassorted DOBV strains (MOI 0.5). Uninfected cells treated with the same medium used for production of virus stocks were maintained as mock

control. At certain points in time, 200 µl of the supernatant of each well were taken for later titration analyses of virus load.

3.3.5.2 Huh7.5 cells

To test the relevance of RIG-I and MDA5 for hantaviral expansion, growth kinetics with HTNV, DOBV Slo and DOBV Sk were carried out on different Huh.7.5 cell lines. GUN stands for GFP-Ubi-NeoR, the selection cassette of the lentiviral vector. Huh7.5 RIG-wt_GUN contains the wild-type RIG-I sequence whereas Huh7.5 ca-GUN comprises a constitutive active construct of RIG-I. Huh7.5 vector_GUN is the vector control, and the vector of Huh7.5 Mda5_GUN contains the MDA5 ORF. All cell lines were kindly provided by Dr. Marco Binder (Institute of Virology, Heidelberg).
All cell lines were seeded into 6-well plates and infected with HTNV, DOBV Slo and DOBV Sk (MOI 1). Uninfected cells were maintained as mock control. At 0 hours post infection (h p.i.) and 2, 3, 5 and 7 d p.i., 200 µl of the supernatant of each well were taken for subsequent titration analyses of virus load.

3.3.6 Isolation of total viral RNA

Total viral RNA from supernatant of infected VeroE6 cells (HTNV, PHV, TULV (MOI 1) or mock-infected), was isolated with Trizol RNA isolation method 8 d p.i. according to the manufacturer's instructions (Invitrogen).

3.3.7 Expansion of VSV

VeroE6 cells were infected with viral stocks (MOI 0.1) for 1 h at 37 °C as indicated. The virus was removed, monolayers were washed with PBS, and cells were maintained in complete media until virus harvest by collecting the supernatant and freeze/thaw method for remaining cells 2 to 4 d p.i..

3.3.8 Titration of VSV

VeroE6 were cultured in 96-well plates until confluence and inoculated with dilutions of herpesvirus suspensions from 10^{-1} to 10^{-6} in ten-fold increments (8 wells per dilution). The final volume was 100 µl/well. The cells were observed for a cytopathic effect (CPE) daily. Titers were determined by $TCID_{50}$.

3.4 Protein chemistry

3.4.1 Dual luciferase assay

To assess the promotor activity induced by viruses or transfected viral components, dual luciferase assays were carried out. The reporter plasmids contain either a luciferase gene derived from firefly under control of an IFN-ß (pcDNA p125-luc plasmid) or ISRE promotor (pISRE-Luc plasmid) and a constitutive active luciferase gene derived from the jellyfish Renilla (pRL-TK-Luc plasmid). For dual luciferase assays, duplicate 12-wells were transfected with 50 ng IFN-β luciferase reporter p125-luc plasmid and 5 ng of the renilla-derived pRL-TK-Luc plasmid. To assess the activities of viral components in their interplay with particular cellular signalling molecules, cells were co-transfected with the indicated amounts of expression plasmid (viral protein expression plasmids: 1 µg; cellular molecule expression plasmids: 100 ng; RNA: 500 ng). Cells were lysed at 24 h post transfection in 1x passive lysis buffer by incubation at 25 °C (15 min) with gentle agitation. Lysates received from transfected cells were centrifugated (10 min, 12,000 rpm) and then pipetted into white flat-bottom 96-well plates (20 µl).

Dual luciferase assays were performed at least three times in independent experiments and duplicates. Empty vector (pcDNA3) was used as negative control, non-structural protein of influenza B virus (B/NS1) was used as positive control for inhibition. The firefly luciferase activity was normalised with the renilla luciferase activity. Finally, the ratio between each respective RIG-I transfected and untransfected sample was calculated to obtain the fold activation. Efficient transfections were proven by detection of viral antigen, tags or direct detection of molecules by Western blot.

3.4.2 Western blot

The proteins were separated by denaturing SDS-PAGE according to their relative molecular mass during discontinuous gel electrophoresis. Then they were blotted on a membrane and visualised by indirect antibody detection. Cell extracts were prepared by lysing cells in lysis buffer containing protease inhibitor cocktail or taken from luciferase samples resuspended in passive lysis buffer provided within the dual luciferase kit (Promega). The samples were centrifuged for 10 min at 12,000 rpm and 4 °C to remove cell debris. Total protein concentrations were determined according to the Bradford procedure. Samples were then resuspended in

loading buffer containing β-mercaptoethanol and boiled at 95 °C for 5 min for protein denaturation. Proteins in the mass range from 30 to 150 kDa were separated on 10% polyacrylamide gels and run at 25 mA/gel. Following electrophoretic separation, proteins were transferred onto methylcellulose membranes by semidry blotting method at 75 mA/gel.

Table 6: Gel composition for discontinuous SDS-PAGE

	resolving gel 10%	**stacking gel**	
30% Acrylamid/Bis (29:1)	3.3 ml	0.83 ml	
1.5 M Tris-HCl, pH 8.8	2.5 ml	X	
	X	1.25 ml	0.5 M Tris-HCl, pH 6.8
10% SDS	100 µl	50 µl	
10% APS	100 µl	50 µl	
TEMED	6 µl	6 µl	
H_2O	4 ml	2,8 ml	

After verifying the transfer efficiency by staining the membranes with Ponceau red, blots were blocked for 1 h at RT in TBST containing 5% milk powder. Blots were incubated for 1 h till overnight at 4 °C with specific primary antibodies. Thereafter, they were washed three times with TBST, followed by incubation with appropriate secondary antibodies for 1 h at room temperature. After five final washing steps, detection was performed by enhanced chemiluminescence.

3.5 Immunological methods

3.5.1 FACS (fluorescence-activated cell sorting)

To analyse the receptors on the surface of cells which are important for hantavirus attachment and entry, confluent cells were harvested by trypsinisation, centrifuged (4 min, 2,500 rpm) and washed with ice-cold washing solution (PBS, 1% FCS, 0.002% sodium azide). Then they were incubated with the first antibody for 1 h at 4 °C (1 µl in 50 µl blocking solution (PBS, 10% FCS, 0.02% sodium azide)). The washing step was repeated twice before staining the cells with PE-coupled secondary antibody for 1 h at 4 °C. After two additional washing steps, the cells were resuspended in fixation solution (PBS with 0.37% formaldehyde). The measurement was carried out with FACScalibur; for evaluation of obtained results, CellQuest Pro® was used.

3.5.2 Immunofluorescence

To observe the localisation of cellular and viral proteins, an immunofluorescence analysis was carried out. For this purpose, $1x10^6$ Hela cells were transfected with 2.5 µg RIG-I expression plasmid and, if necessary, other expression plasmids (hantaviral N proteins) in 35 mm dishes (4 cover slips). 24 hours post transfection, the cells were washed twice with PBS, fixed with 2.5% formaldehyde and permeabilised with 0.2% Triton in PBS for 10 min, respectively, then washed with PBS again three times. Cover slips were incubated with 20 µl of primary antibody solution for 1 h at RT. After rinsing the cover slips three times with PBS, secondary antibodies were added and after 1 h rinsed again three times. Then the cover slips were mounted on slides using one drop Mowiol and stored at 4 °C until immunofluorescence analysis.

4 Results

4.1 Effects of RIG-I on hantavirus replication

4.1.1.1 A549 cell lines

4.1.1.2 Tests of A549 wild-type, RIG-I knockdown and control cells on integrin expression and functionality

To elucidate the physiological role of RIG-I for hantaviruses, virus growth in A549 wild-type, A549 RIG-I knockdown (ΔRIG-I) and A549 control cells which express a non-target shRNA, was investigated. Unfortunately, the A549 control cells could not be involved until the third experiment. Therefore, A549 wild-type cells served as control in the first two experiments. For all three experiments, different clones of ΔRIG-I cells were used. All cell lines were kindly provided by Markus Matthäi (Robert Koch-Institute, Berlin). To assess the amounts of RIG-I in the cell lines, Western blot with RIG-I specific antibody was carried out (Figure 10).

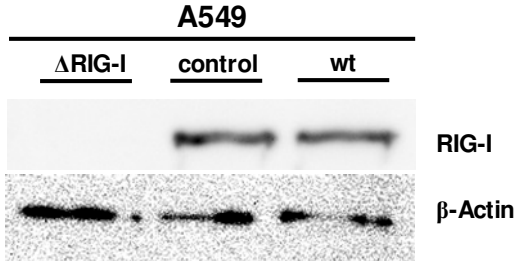

Figure 10. RIG-I expression in A549 wild-type, control and ΔRIG-I cells: Western blot of A549 wild-type, control and ΔRIG-I cells. Lysates were prepared from T25 flasks with confluent cells in early passages treated with type I IFN (500 U/ml).

As expected, RIG-I was not detectable in the ΔRIG-I cells, whereas a strong expression could be shown in the wild-type as well in the control cells. In addition, it has to be mentioned that the growth of the ΔRIG-I and the control cells was impaired in comparison to the wild-type cells.

Furthermore, the levels of β3 (CD61) and β1 (CD29) integrins on the surface of the tested cells were analysed by FACS to exclude differences in hantaviral growth due to different amounts of integrins since these molecules are important for the entry of pathogenic and non-pathogenic hantaviruses, like for example HTNV and PHV, respectively (Figure 11).

(Gavrilovskaya et al., 1999; Gavrilovskaya et al., 1998). Interestingly, the expression of CD61 was not detectable on the surface of any cell line. CD29, however, was strongly expressed on all cell lines. Nevertheless, there are several hints that other receptors are also involved in hantavirus attachment and entry (Krautkramer and Zeier, 2008; Kim et al., 2002; Choi et al., 2008).

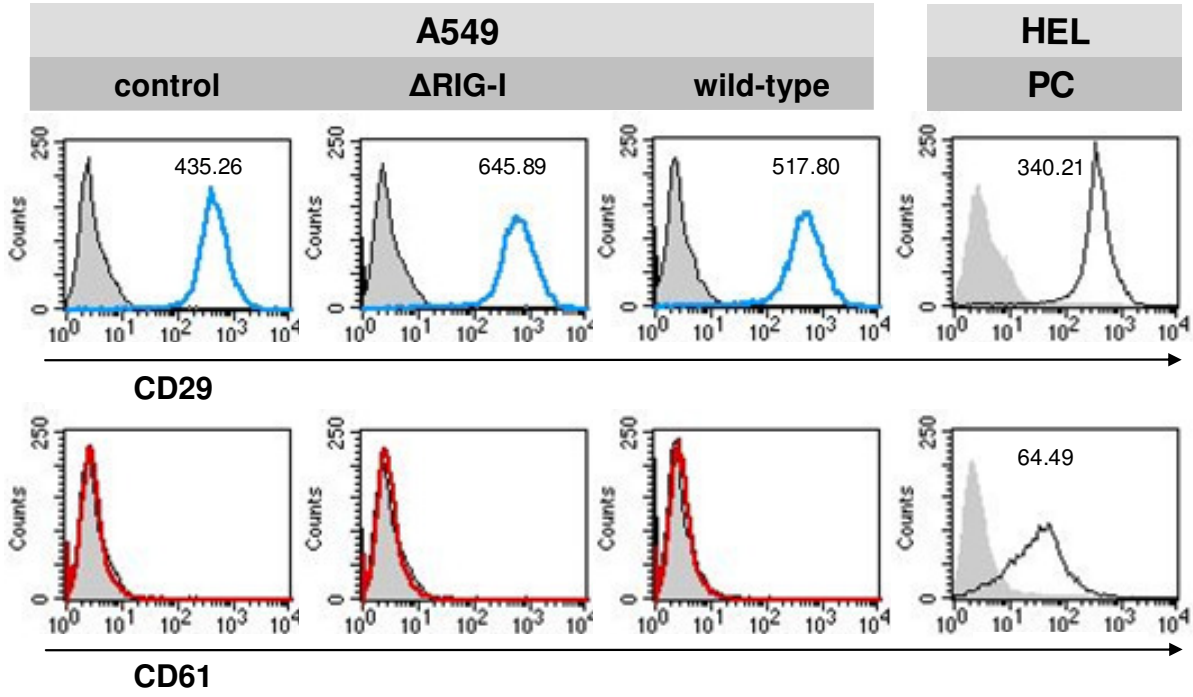

Figure 11. Density of CD29 and CD61 on the surface of A549 wild-type, control and ΔRIG-I cells: Surface expression of CD29 (blue) and CD61 (red) on all three cell lines involved into the growth kinetics was measured by FACS. The mean fluorescence intensities (MFI) is given above shifted peaks. Filled graphs represent isotype controls of respective antibodies. The graph shows the number of cell counts on the Y-axis and the level of emitted fluorescence by labeled cells on the X-Axis. PC means positive control that is represented by unstimulated HEL cells (kindly provided by Nina Lütteke), a human megakaryocyte-like cell line, which expresses both CD29 and CD61 on their surface. These data are representative for the two independent experiments that has been carried out.

As an additional control, VSV growth curves were analysed (Figure 12). As expected, the $TCID_{50}$ values obtained after infection of the ΔRIG-I cells at 1, 3 and 5 d p.i. were up to 1 to 2 log steps higher than those from the other cell lines.

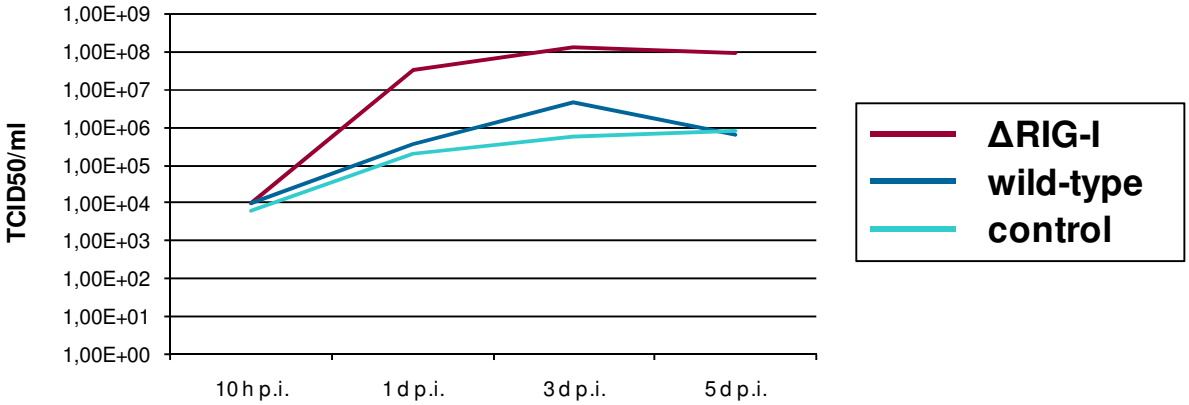

Figure 12. VSV growth curves on A549 cell lines: A549 wild-type, ΔRIG-I and control cells were infected with VSV (MOI 1). Supernatant was collected at different points in time after infection and titrated to assess the amount of virus. The experiments were carried out twice with two different ΔRIG-I cell clones.

For the growth kinetics with hantaviruses, supernatants of infected wild-type and ΔRIG-I cells were harvested at 1, 2, 3, 4, 5, 6, and 7 d p.i. for the first two experiments. For the third experiment, supernatant from all three cell lines (wild-type, ΔRIG-I knockdown and control cells) was collected and analysed after 2, 3, 5 and 7 d p.i.. To assess the production and secretion of progeny of different hantavirus strains in presence and absence of RIG-I, the supernatants taken at different time points as described above were titrated in duplicates.

4.1.1.3 HTNV

In the first experiment HTNV growth curves showed an increasing drift between virus expansion in wild-type and ΔRIG-I cells up to 3 log steps on day 7. In the second experiment, no production of virus, neither in the wild-type nor in the ΔRIG-I cells could be detected. The titer reduction for all viruses in the second and third experiment could be explained by repeated thawing and freezing of the virus supernatants since the titrations had to be carried out several times due to problems with cells prepared for the titrations.

In the third experiment, the HTNV titer peaked at day 3 after infection and then decreased for unknown reasons. In general, HTNV did not replicate well in the wild-type cells, although it has been shown before that A549 cells can be productively infected with HTNV. Additionally, HTNV as one of the more pathogenic strain is more potent to expand in A549 cells than non-pathogenic strains (Figure 14). As expected, the growth behaviour in the control cells was similar to the wild-type A549 cells (Figure 13).

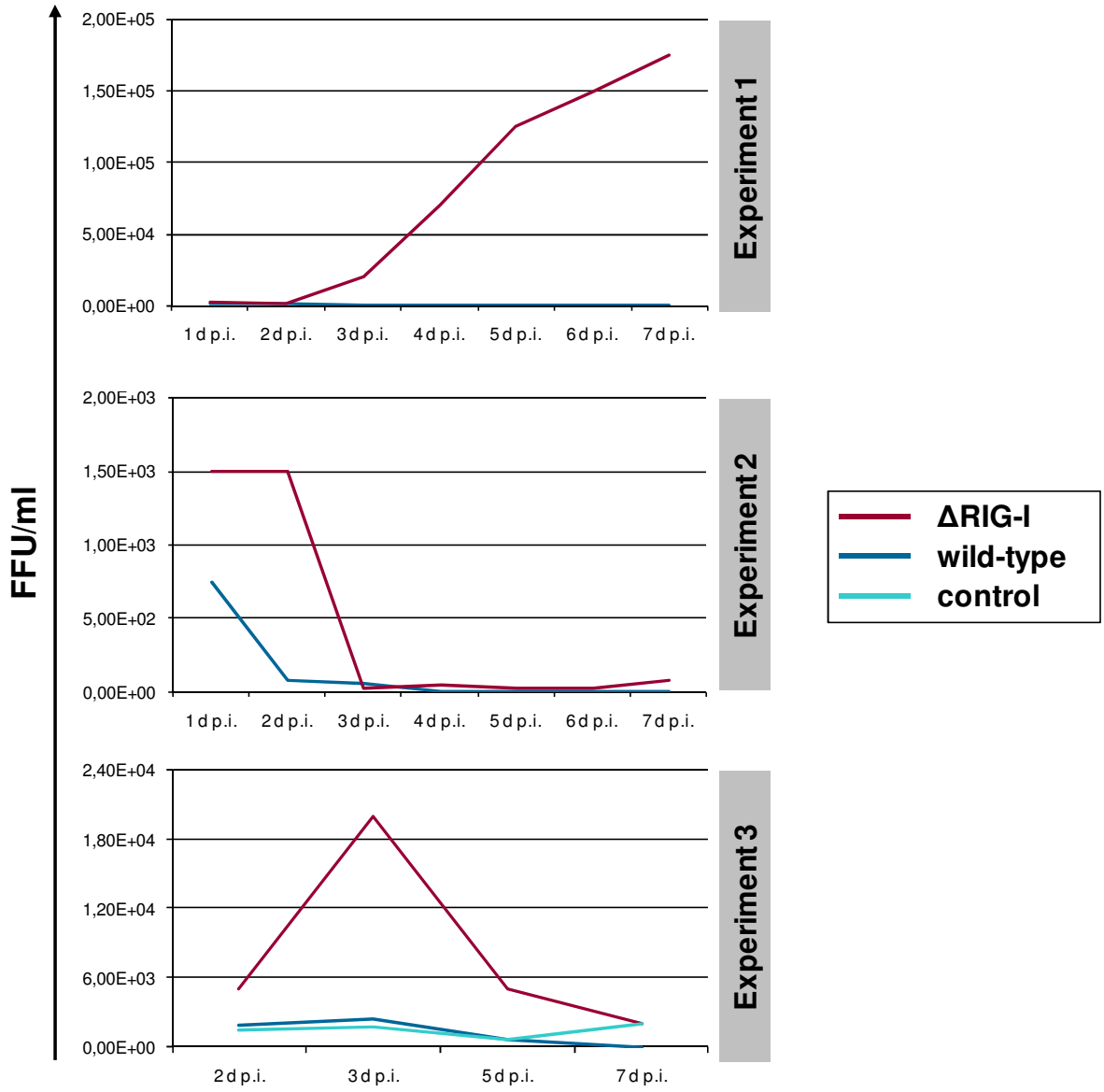

Figure 13. HTNV growth curves on A549 cell lines: A549 wild-type, ΔRIG-I and (for the third experiment) control cells were infected with HTNV (MOI 1). Supernatant was collected at different points in time after infection to determine the virus titers. The experiments were carried out with three different ΔRIG-I cell clones.

4.1.1.4 PHV

In the supernatant of ΔRIG-I cells infected with non-pathogenic PHV, only few foci could be detected, up to 3 log steps at day 6 after infection in comparison to the wild-type cells (Figure 14). PHV did not produce virions in the wild-type cells. This is not surprising, since non-pathogenic hantavirus strains replicate less efficiently than pathogenic ones as a result of, for example, inadequate immune evasion mechanisms. The third experiment could not be evaluated because of technical problems that will be discussed later.

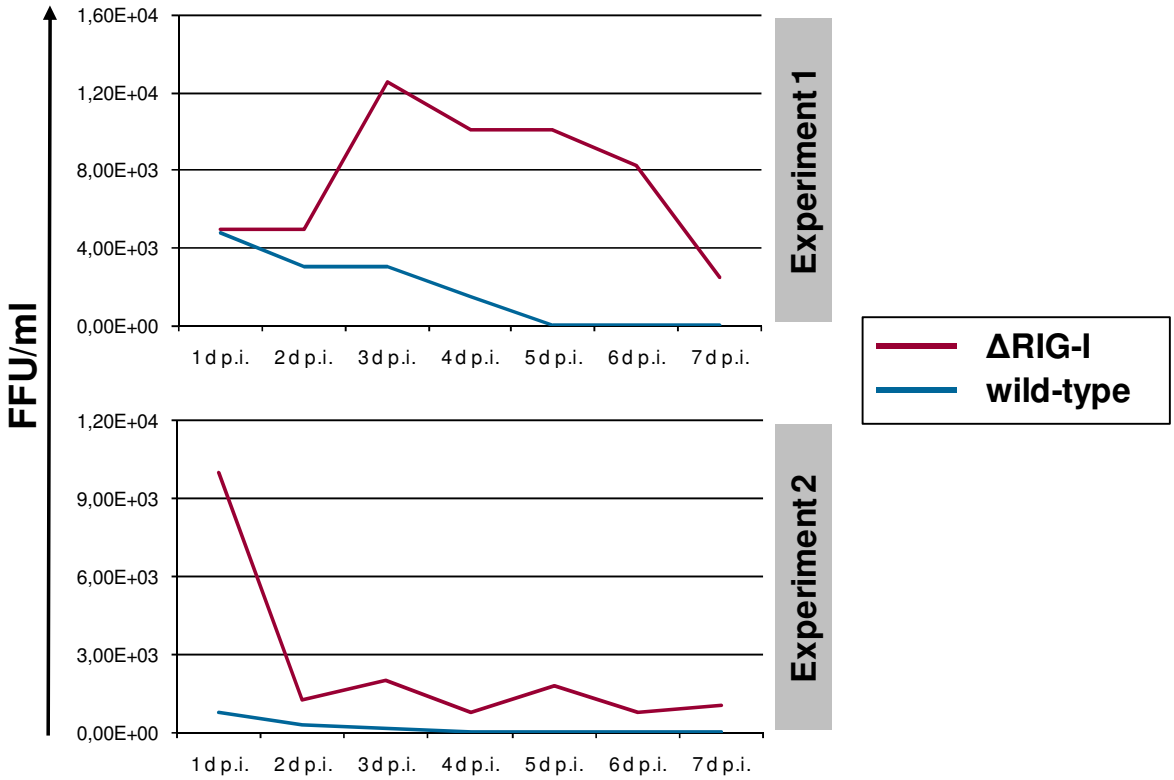

Figure 14. PHV growth curves on A549 cell lines: A549 wild-type and ΔRIG-I cells were infected with PHV (MOI 1). Supernatant was collected at different points in time after infection and titrated. The experiments were carried out with three different ΔRIG-I cell clones. The third experiment could not be evaluated due to technical problems (data not shown).

4.1.1.5 TULV

The kinetics with TULV, which is regarded as non-pathogenic, could only be carried out once due to insufficient virus titers of the expanded stocks. Virus levels reached their maximum of $5x10^4$ FFU/ml at day 7 after infection in the absence of RIG-I whereas in the control as well as in the wild-type cells, almost no replication was detected (Figure 15). TULV is known to replicate slowly in cell culture compared to other hantavirus strains. Therefore, the late increase in progeny virions is not surprising.

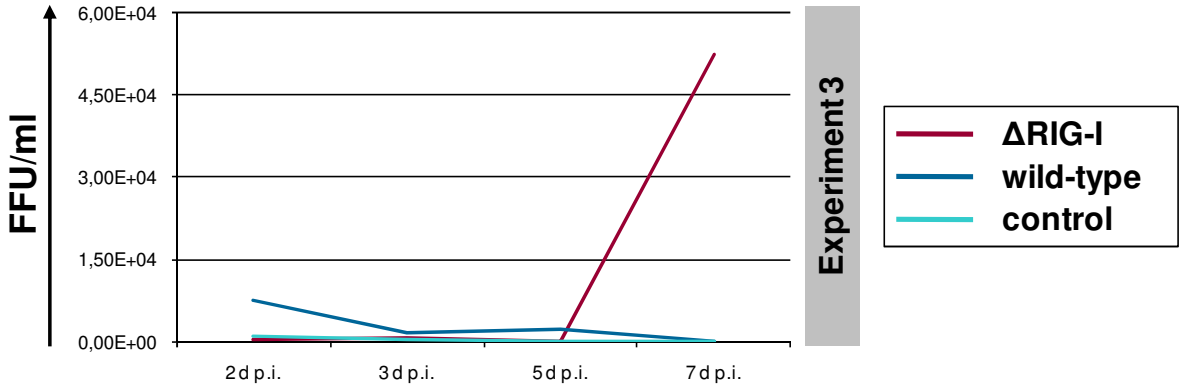

Figure 15. TULV growth curve on A549 cell lines: A549 wild-type, ΔRIG-I and control cells were infected with TULV (MOI 1). Supernatant was collected at different points in time after infection and titrated.

4.1.1.6 DOBV Slo

DOBV Slo, the most pathogenic strain among the Dobrava strains, was the only virus tested that showed high replication efficiency in both ΔRIG-I as well as in the wild-type cell line. The virus load in the supernatant of ΔRIG-I cells was higher than of the wild-type cells, reaching its maximum at day 5 after infection ($2.25x10^5$ FFU/ml) for the first experiment (Figure 16). Productive infection of the ΔRIG-I cell line, however, could only be proven for the first experiment. In the second experiment, few virus progeny was detectable in any supernatant of the infected cells, comparable to the respective experiment with HTNV. Probably, similar technical problems can be assumed for these results. In the third experiment, the FFU of DOBV Slo peaked at day 3 after infection with $7x10^4$ FFU/ml in the wild-type cells but declining rapidly towards the initial values.

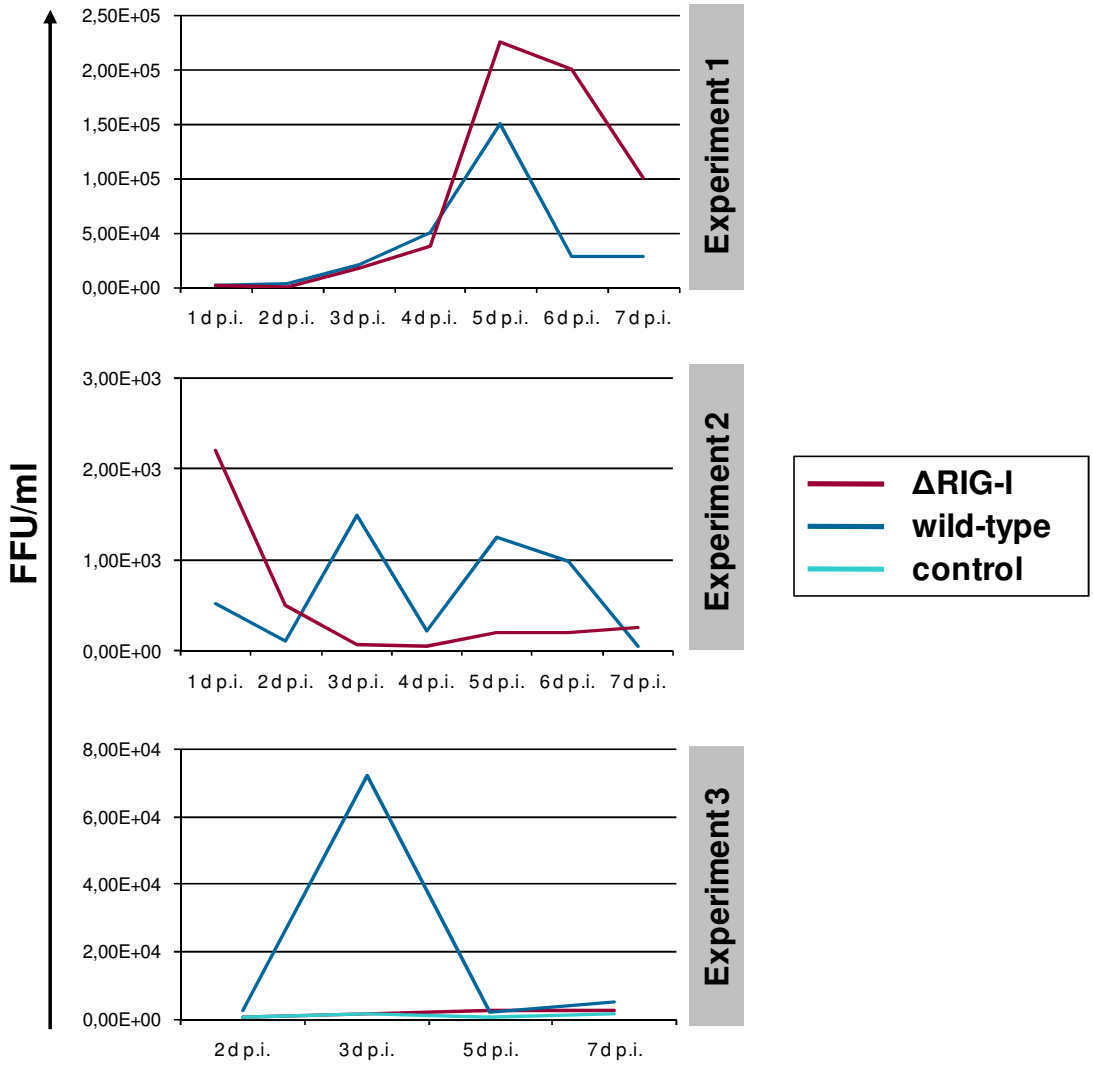

Figure 16. DOBV Slo growth curves on A549 cell lines: A549 wild-type and ΔRIG-I cells were infected with DOBV Slo (MOI 1). Supernatant was collected at different points in time after infection and virus titers were determined. The experiments were carried out with three different ΔRIG-I cell clones.

4.1.1.7 DOBV Sk

For DOBV Sk, ΔRIG-I cells showed production of virus progeny in all three experiments, whereas in the first two experiments, the titers tended towards zero for supernatant from infected wild-type cells (Figure 17). In the third experiment, slight virus replication could also be detected in the wild-type cells. Differences were observed in the time-dependent pattern of detected virions. In the first experiment, the titer peaked at day 5 after infection with $2x10^5$ FFU/ml and reached the maximum at day 7 after infection with $4.5x10^5$ FFU/ml, whereas the virus levels in both following experiments reached their highest values at day 3 after infection

and then declined. However, control cells in the third experiment produced even higher virus counts than the ΔRIG-I cells at day 3 after infection. This value could probably be interpreted as outlier.

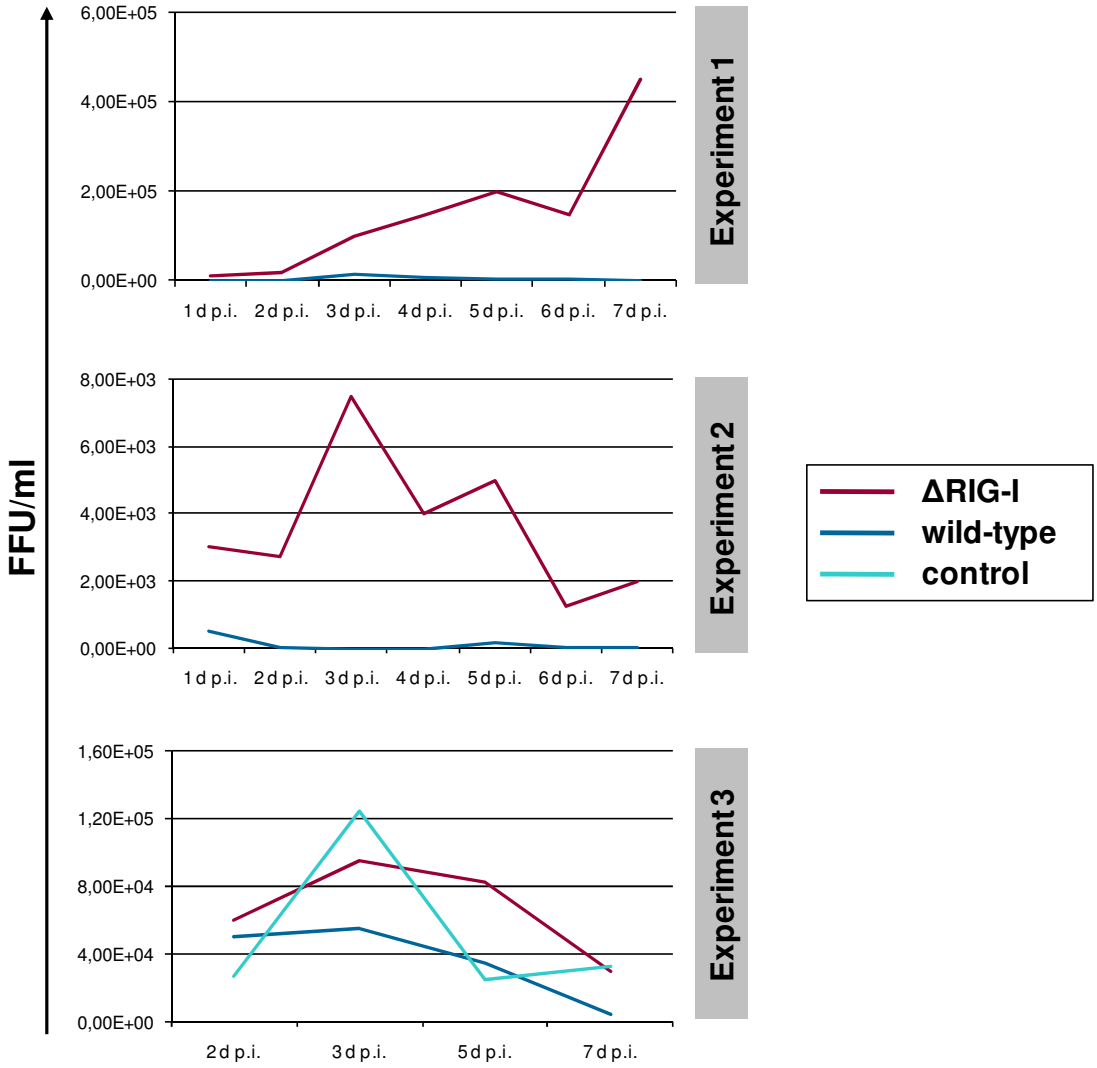

Figure 17. DOBV Sk growth curves on A549 cell lines: A549 wild-type and ΔRIG-I cells were infected with DOBV Sk (MOI 1). Supernatant was collected at different points in time after infection and titrated. The experiments were carried out with three different ΔRIG-I cell clones.

4.1.1.8 DOBV reassortants

To assess the relevance of different segment settings for viral interactions with RIG-I signalling, reassorted virus strains generated by Sina Kirsanovs were involved in the growth studies. Briefly, the DOBV mutants A6 and A36 were generated by artificial reassortment processes between DOBV Slo and DOBV Sk. A6 contains the S and L segment from DOBV Sk whereas

the M segment is derived from DOBV Slo. The segment layout of the reassortant A36 is the reverse of A6 (Figure 18).

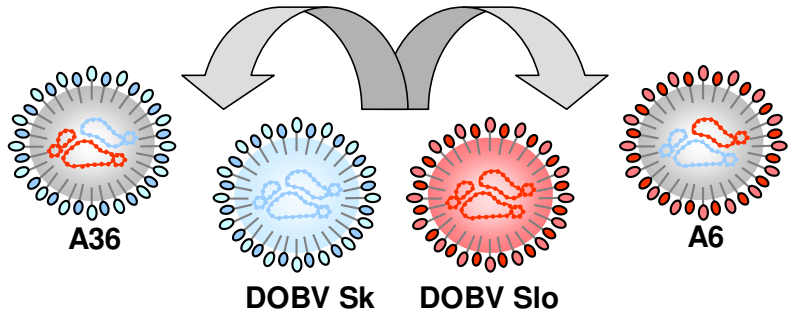

Figure 18. Reassortment scenarios of A6 and A36 with parental strains DOBV Slo and DOBV Sk

The kinetics could only be carried out twice with the reassorted strains due to low titers of virus stocks. Both strains do not replicate as well as their parental strains in VeroE6 which are used for virus expansion. Therefore, they could only be involved in the first and the third experiment (Figure 19).

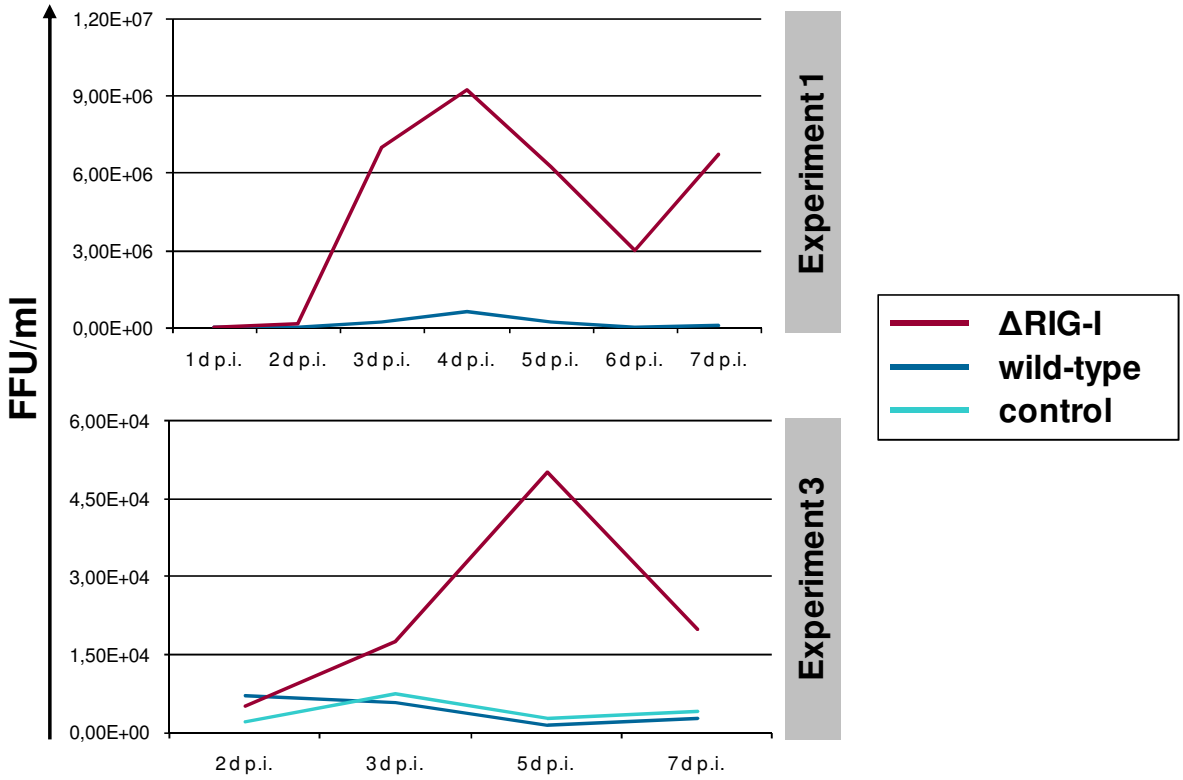

Figure 19. A6 growth curves on A549 cell lines: A549 wild-type, ΔRIG-I and control cells were infected with the reassortant A6 (MOI 0.5). Supernatant was collected at different points in time after infection and titrated. The experiments were carried out with two different ΔRIG-I cell clones.

Interestingly, A6 showed a different growth ratio in ΔRIG-I and wild-type cells similar to the respective experiment with DOBV Sk (approximately one log difference) as both virus strains did not replicate well in the wild-type cell line (Figure 17, Figure 19). In comparison to DOBV Sk, A6 replication started earlier and resulted in higher numbers of virus progeny with a maximum of $9x10^6$ FFU/ml at day 4 after infection compared to the maximum of DOBV Sk with $4.5x10^5$ FFU/ml at day 7 after infection. In the third experiment, A6 also replicated in the ΔRIG-I cells, but scarcely in wild-type and control cells.

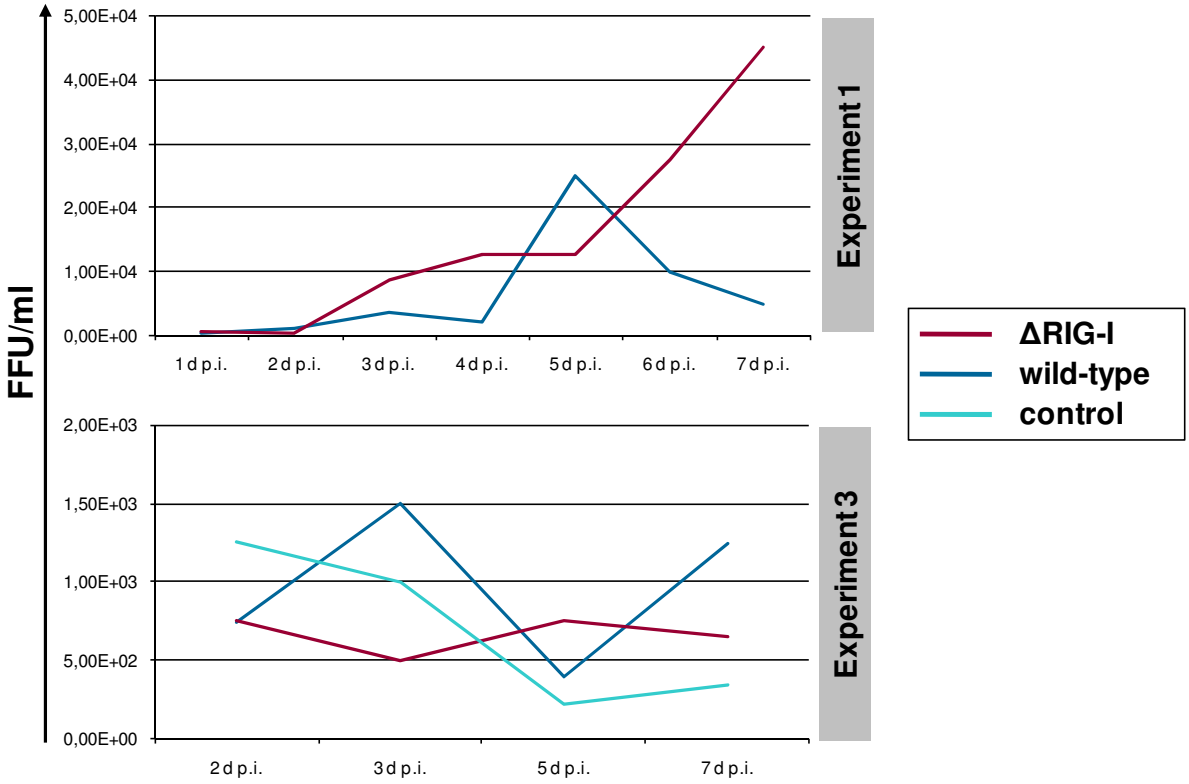

Figure 20. A36 growth curves on A549 cell lines: A549 wild-type, ΔRIG-I and control cells were infected with the reassortant A36 (MOI 0.5). Supernatant was collected at different points in time after infection and titrated. The experiments were carried out with two different ΔRIG-I cell clones.

A36 was able to replicate in wild-type as well as in ΔRIG-I cells, similar to DOBV Slo (Figure 16, Figure 20), with more efficient replication in the ΔRIG-I cells. In the other experiment (experiment 3), almost no replication could be detected. In general, all experiments revealed differences in the growth pattern of pathogenic as well as non-pathogenic hantavirus strains in wild-type and control cells as compared to ΔRIG-I cells.

4.1.2 Huh7.5 cell lines

To investigate the physiological importance of RIG-I for hantavirus replication in an additional cell line, virus growth in different Huh7.5 cell lines was assessed. Huh7.5 cells are not able to express functional RIG-I due to a point mutation in the RIG-I gene (Bartenschlager and Pietschmann, 2005; Blight et al., 2002).

Huh7.5 wild-type cells, Huh7.5 cells stably transfected with a lentiviral vector expressing functional RIG-I, constitutive active RIG-I or MDA5 were infected with HTNV, DOBV Slo and DOBV Sk. Huh7.5 cells transfected with the empty vector were treated in the same way. Supernatants were harvested at distinct points in time. All cell lines were kindly provided by Marco Binder (Institute of Virology, Heidelberg). Since the experiment has been carried out only once, the results have to be regarded as preliminary data.

4.1.2.1 HTNV

HTNV growth reached its maximum in Huh7.5 wild-type cells at day 5 p.i. with a titer of 7.26×10^6 FFU/ml whereas in Huh7.5 vector control, the virus titer peaked at day 3 p.i. with 4.2×10^6 FFU/ml (Figure 21), both immediately declining. All RIG-I- and as well as MDA5-expressing cells exhibited a strongly reduced virus growth.

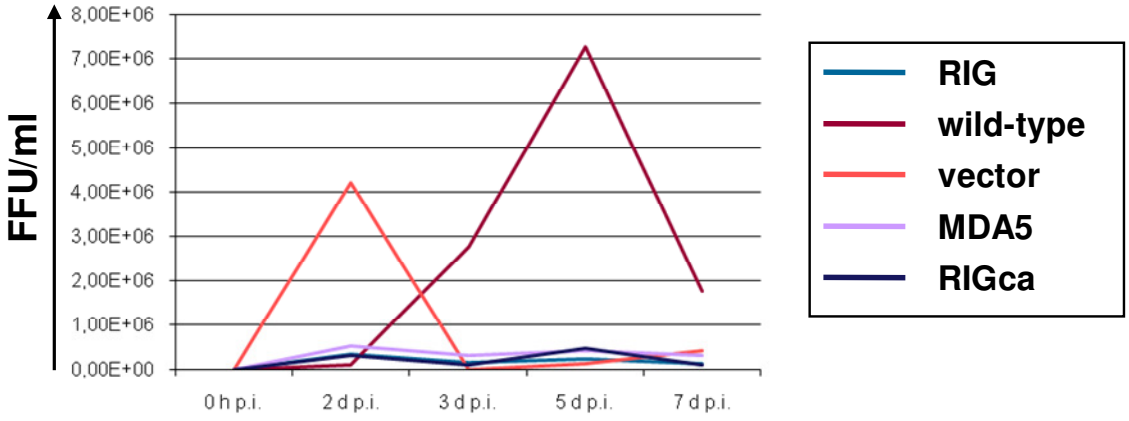

Figure 21. HTNV growth curves on Huh7.5 cell lines: Huh7.5 cells containing lentiviral vectors expressing RIG-I, constitutive active RIG-I (RIGca) or MDA5 and Huh7.5 wild-type (wt) cells were infected with HTNV (MOI 1). Supernatant was collected at different points in time after infection and titrated.

4.1.2.2 DOBV Slo

For DOBV Slo, increasing titers over time could be shown in all cell lines except for RIG-I-expressing Huh7.5 (Figure 22). In general, DOBV Slo proliferated best in Huh7.5 wild-type cells. The amount of FFU found in the supernatants of the other cell lines remained similarly low although the titers of virus from the Huh7.5 vector control were comparatively higher. Surprisingly, the FFU value for the supernatant of MDA5-expressing cells at day 7 p.i. exceeded all other values at the same day.

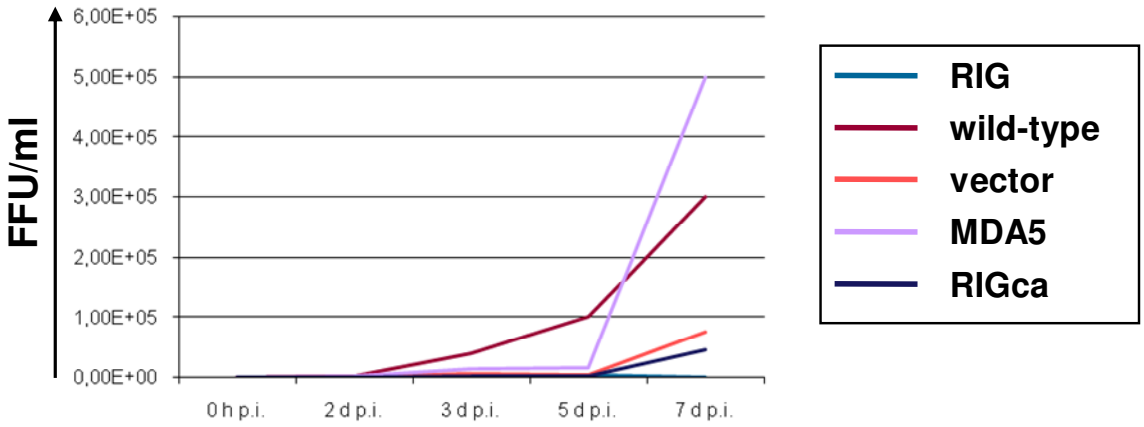

Figure 22. DOBV Slo growth curves on Huh7.5 cell lines: Huh7.5 cells containing lentiviral vectors expressing RIG-I, constitutive active RIG-I (RIGca) or MDA5 and Huh7.5 wild-type (wt) cells were infected with DOBV Slo (MOI 1). Supernatant was collected at different points in time after infection and titrated.

4.1.2.3 DOBV Sk

As already shown for DOBV Slo, the DOBV Sk titers from supernatants of all cell lines increased over time (Figure 23) except for the constitutive active RIG-I-expressing cell line. At day 7 p.i., the supernatant from cells expressing RIG-I showed the highest virus load, even higher than the supernatant taken from cell lines lacking RIG-I. The vector control titers remained at the level of the respective titers derived from RIG-I-expressing cell lines.

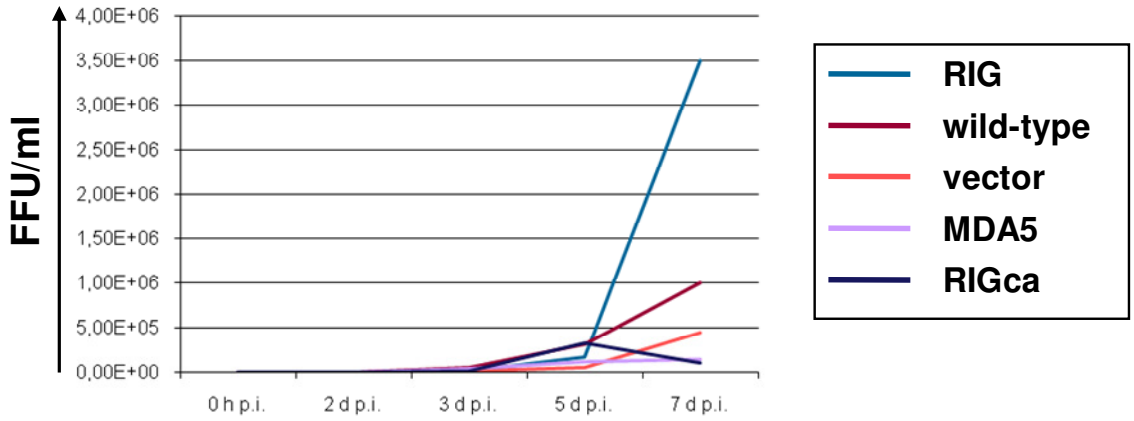

Figure 23. DOBV Sk growth curves on Huh7.5 cell lines: Huh7.5 cells containing lentiviral vectors expressing RIG-I, constitutive active RIG-I (RIGca) or MDA5 and Huh7.5 wild-type (wt) cells were infected with DOBV Sk (MOI 1). Supernatant was collected at different points in time after infection and titrated.

4.2 Impact of single hantaviral components on PRR signalling

4.2.1 Interaction of viral genomic RNA with cytoplasmic PRRs

Nucleic acids belong to the main structures recognised by PRRs leading to a type I IFN response which is known to be of relevance for innate immunity after hantaviral infection. Hantaviruses provide RNA in the form of their genome and during their life cycle as m-, v- and cRNA. To determine whether they act as PAMP for either RIG-I or MDA5, viral genomic RNAs prepared from the supernatant of VeroE6 cells infected with different hantavirus strains were investigated. They were co-transfected into 293T cells with luciferase reporters (constitutive active luciferase reporter and IFN-β promotor-controlled luciferase reporter) and PRRs in definite amounts. As negative controls, pcDNA3 without N ORF (NC) and supernatant prepared from uninfected cells (NC (cell)) were used (Figure 24).

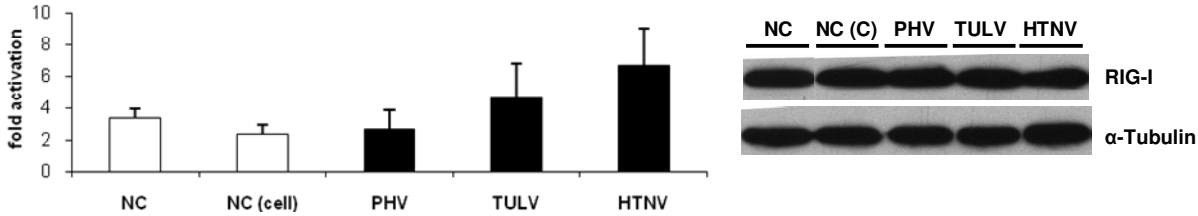

Figure 24. Influence of hantaviral genomic RNAs on IFN-β promotor activation through RIG-I: Total RNA from the supernatant of infected or uninfected (NC (cell)) VeroE6 cells (MOI 1) was isolated with Trizol RNA isolation method 8 d p.i. and transfected into 293T cells together with IFN-β-activated luciferase reporter plasmid (firefly), luciferase reporter plasmid (renilla) and RIG-I expression plasmid. As transfection control, an additional sample was transfected with empty expression plasmid (NC). 24 hours after transfection, dual luciferase assay was carried out. Standard deviations are based on the mean values of three independent experiments with transfections performed in duplicates. Appropriate expression of transfected RIG-I and consistent protein load were verified by Western blot.

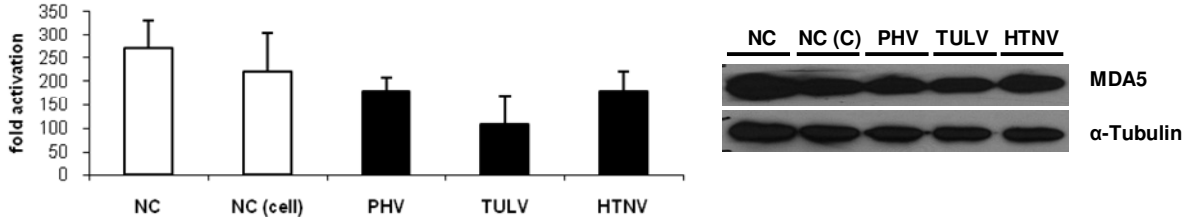

Figure 25. Effect of hantaviral genomic RNAs on IFN-β promotor activation through MDA5: Preparation of RNA, transfection, dual luciferase assay and Western blot were carried out as described in Figure 24. Instead of RIG-I-expressing plasmid, MDA5 expression plasmid was co-transfected into the cells.

Only genomic RNAs of HTNV (6.6-fold) and TULV (4.6-fold) virions had a slight, but not significant effect on IFN-β promotor activation through RIG-I (Figure 24), whereas none of the tested viral RNAs triggered the signalling pathway through MDA5 (Figure 25).

4.2.2 Induction or inhibition of RIG-I or MDA5 signalling by hantaviral G expressing plasmids

Other investigations have already shown inhibitory effects of hantaviral G1 on RIG-I signalling (Alff et al., 2006; Alff et al., 2008). Based on these findings, several G1 and G protein expression plasmids derived from different hantavirus strains were tested in dual luciferase assays as described above. Furthermore, a strong inhibitor of RIG-I signalling, the Influenza B/NS1 protein, was used as a positive control for inhibition, expecting similar inhibitory capacity for the tested G proteins.

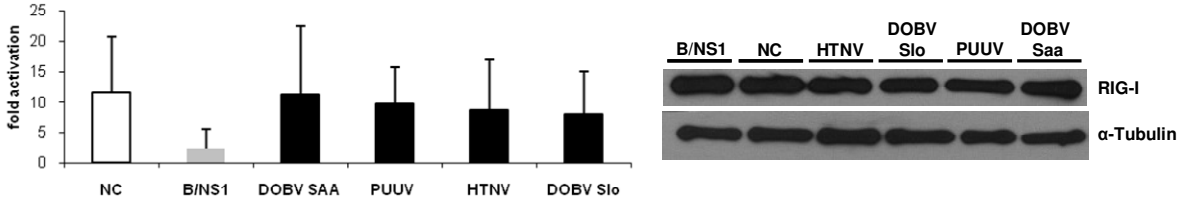

Figure 26. Influence of hantaviral G proteins on IFN-β promotor activation through RIG-I: 293T cells were transfected with hantaviral G protein expression plasmids, empty plasmid (NC) or B/NS1 expression plasmid and IFN-β-activated luciferase reporter plasmid (firefly), luciferase reporter plasmid (renilla) and RIG-I expression plasmid. 24 hours after transfection, dual luciferase assay was carried out. Standard deviations are based on the mean values of three independent experiments with transfections performed in duplicates. Appropriate expression of transfected RIG-I and consistent protein load were verified by Western blot.

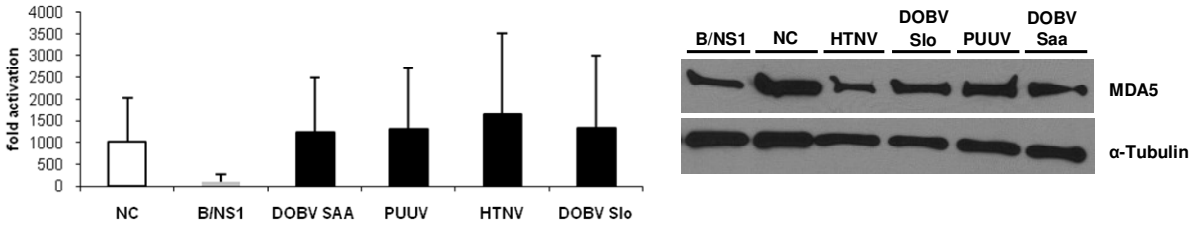

Figure 27. Effect of hantaviral G proteins on IFN-β promotor activation through MDA5: Transfection, dual luciferase assay and Western blot were carried out as described in Figure 26. Instead of RIG-I-expressing plasmid, MDA5 expression plasmid was co-transfected into the cells.

In contrast to B/NS1, in our system the investigated G expression plasmids had neither a stimulatory nor an inhibitory effect on IFN-β promotor activation through RIG-I (Figure 26) or MDA5 (Figure 27).

4.2.3 RIG-I pathway triggering by expression of hantaviral nucleocapsid ORFs

To examine whether N expression from different hantaviruses affects signalling by cytoplasmic sensor molecules, the influence of N ORF expressing plasmids was studied in dual luciferase assays.

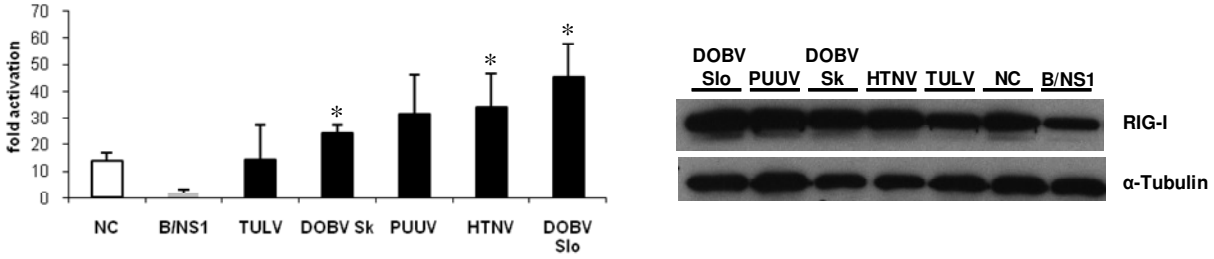

Figure 28. Induction of IFN-β promotor activity through RIG-I by hantaviral N expression plasmids: 293T cells were transfected with hantaviral N protein expression plasmids, empty plasmid (NC) or B/NS1 expression plasmid together with IFN-β-activated luciferase reporter plasmid (firefly), luciferase reporter plasmid (renilla) and RIG-I expression plasmid. 24 hours after transfection, dual luciferase assay was carried out. Standard deviations are based on the mean values of three independent experiments with transfections performed in duplicates. The probability of significance concerning the fold activation of negative control was determined by Student's t-test (* = $p \leq 0.05$). Appropriate expression of transfected RIG-I and consistent protein load were verified by Western blot.

Surprisingly, expression of N ORFs derived from pathogenic hantaviruses showed a significant deviation from the negative control. HTNV and DOBV Slo, both strains with comparatively high virulence and lethality of infected patients, for example, showed significant promotor activations of 34- and 45-fold, respectively, whereas TULV which is normally not implicated in cases of illness, stayed in the range of the negative control (12-fold) (Figure 28). In contrast, slight, but not significant activation linked to MDA5 could be detected after expression of DOBV Slo N protein, whereas all other samples had no impact in relation to this PRR. TULV even declined below the level of negative control down to inhibition control level (Figure 29).

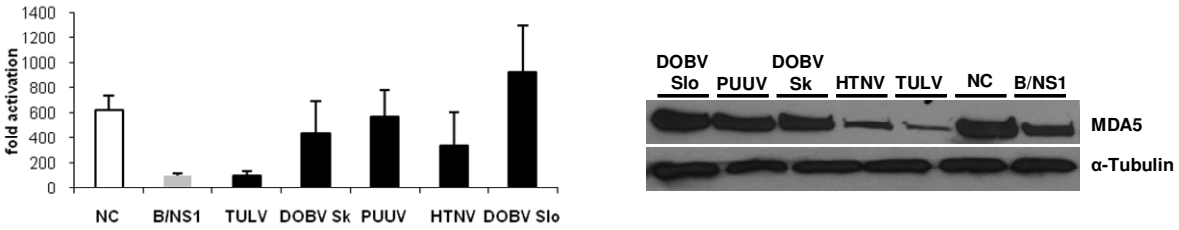

Figure 29. Influence of hantaviral N expression plasmids on IFN-β promotor activation through MDA5: Transfection, dual luciferase assay and Western blot were carried out as described in Figure 28. Instead of RIG-I expressing plasmid, a MDA5 expression plasmid was co-transfected into the cells.

4.2.4 Activation of RIG-I by RNAs encoding hantaviral nucleocapsids

Since the hitherto known PRRs localised cytoplasmically recognise RNA patterns, it was examined how the N proteins nevertheless were able to trigger IFN promotor activation through RIG-I. To prove the hypothesis that the N mRNA is the real activator of RIG-I signalling all N protein and – for the sake of completeness – G protein expression plasmids were transcribed *in vitro* and exposed to RIG-I in dual luciferase assays (Figure 31, Figure 32). The integrity of generated RNA was tested in a RNA gel (Figure 30). Only N protein expression plasmid-derived RNAs activated the reporter system, tending to result in similar patterns like the assayed N proteins, again correlating with pathogenicity of the original virus.

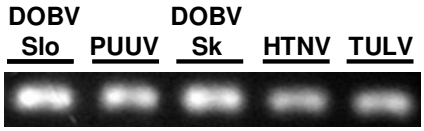

Figure 30. RNA gel of *in vitro*-transcribed N ORFs

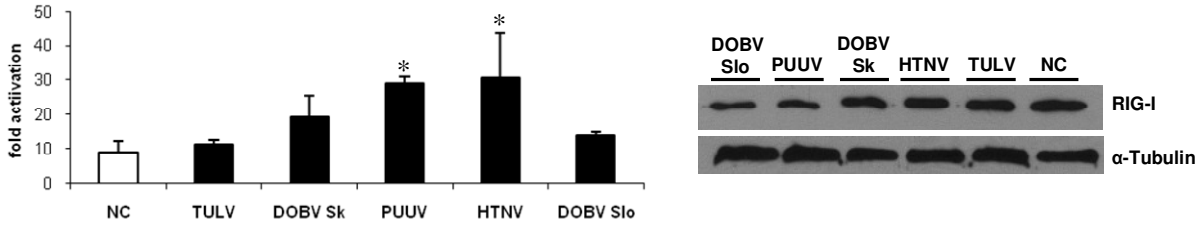

Figure 31. Triggering of IFN-β promotor activity by *in vitro*-transcribed nucleocapsid RNAs through RIG-I: RNAs from *in vitro*-transcribed N protein expression plasmids or empty plasmid (NC) were transfected into 293T cells together with IFN-β-activated luciferase reporter plasmid (firefly), luciferase reporter plasmid (renilla) and RIG-I. 24 hours after transfection, dual luciferase assay was carried out. Standard deviations refer to the mean values of three independent experiments with transfections performed in duplicates. The probability of significance concerning the fold activation of negative control was determined by Student's t-test (* = $p \leq 0.05$). Appropriate expression of transfected RIG-I and consistent protein load were verified by Western blot.

Nevertheless, one exception could be observed: DOBV Slo only showed a slight activation similar to TULV, although revealing the highest activation level in the previous experimental setting.

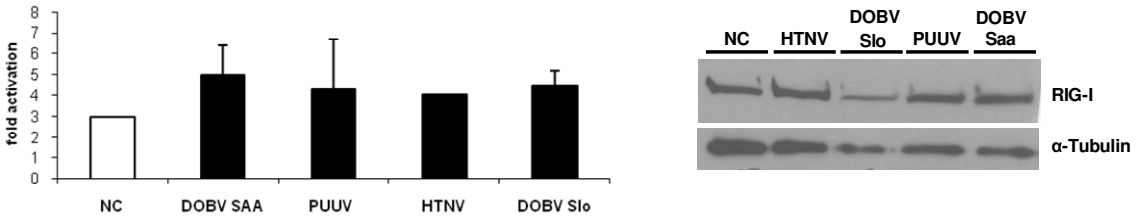

Figure 32. Influence of *in vitro*-transcribed G RNAs on IFN-β promotor activation through RIG-I: Transfection, dual luciferase assay and Western blot were carried out as described in Figure 31. Instead of *in vitro*-transcripts of the N ORFs, *in vitro*-trancribed G RNAs were transfected into the cells. Standard deviations are mean values of two independent experiments with transfections performed in duplicates.

The G protein-derived RNA, however, induced RIG-I signalling only marginally (Figure 32), as already shown for the respective expression plasmids.

4.2.5 Importance of 5'-triphosphates and inner-sequential structures of *in vitro*-transcribed N ORFs on induction of RIG-I signalling

RIG-I is preferentially activated by single-stranded RNA with 5'-triphosphates that are also generated during *in vitro*-transcription. However, RIG-I is also is able to bind to other RNA types depending on length, nucleoside motifs and secondary structures (Kato et al., 2006; Kato et al., 2008; Saito et al., 2008). Since the gradual differences in strain-dependent luciferase activation could not be explained only by considering the 5'-triphosphates, the importance of the 5'-triphosphates for the observed RIG-I signalling was examined. Therefore, the transcribed RNAs were digested with alkaline shrimp phosphatase to remove the phosphate endings and again co-transfected and analysed in the dual luciferase system (Figure 33).

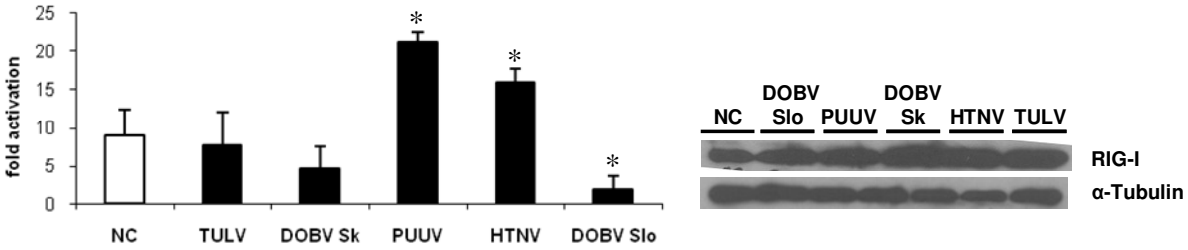

Figure 33. Importance of 5'-triphosphates at nucleocapsid RNAs on IFN-β promotor activation through RIG-I: *In vitro*-transcribed, phosphatase-treated N RNAs or empty plasmid (NC) were transfected into 293T cells together with IFN-β-activated luciferase reporter plasmid (firefly), luciferase reporter plasmid (renilla) and RIG-I. 24 hours after transfection, dual luciferase assay was carried out. Standard deviations are based on the mean values of three independent experiments with transfections performed in duplicates. The probability of significance concerning the fold activation of negative control was determined by Student's t-test (* = $p \leq 0.05$). Appropriate expression of transfected RIG-I and consistent protein load were approved by Western blot.

Again, differences of the activation pattern could be observed despite of lacking 5'-triphosphates. However, the activation level was in each case lower than in the previous experimental setting, and the signalling strength of HTNV (16-fold) and DOBV Slo (2-fold) decreased and declined even under the level of PUUV (21-fold).

4.2.6 Altered levels of RIG-I activation by 3' truncated N ORF mutants

In general, there are no obvious sequence homologies of the tested N expression plasmids to allow for a conclusion concerning a stimulatory or inhibitory motif. However, to assess the questions whether and which parts of the N protein itself or its RNA are responsible for induction of RIG-I signalling, deletion mutants of HTNV N protein expression plasmid were generated in cooperation with Pritesh Lalwani using the exonuclease approach. Three candidate plasmids with truncations of different length at their 3' ends were tested in a DNA gel, Western blot and dual luciferase assay (Figure 34).

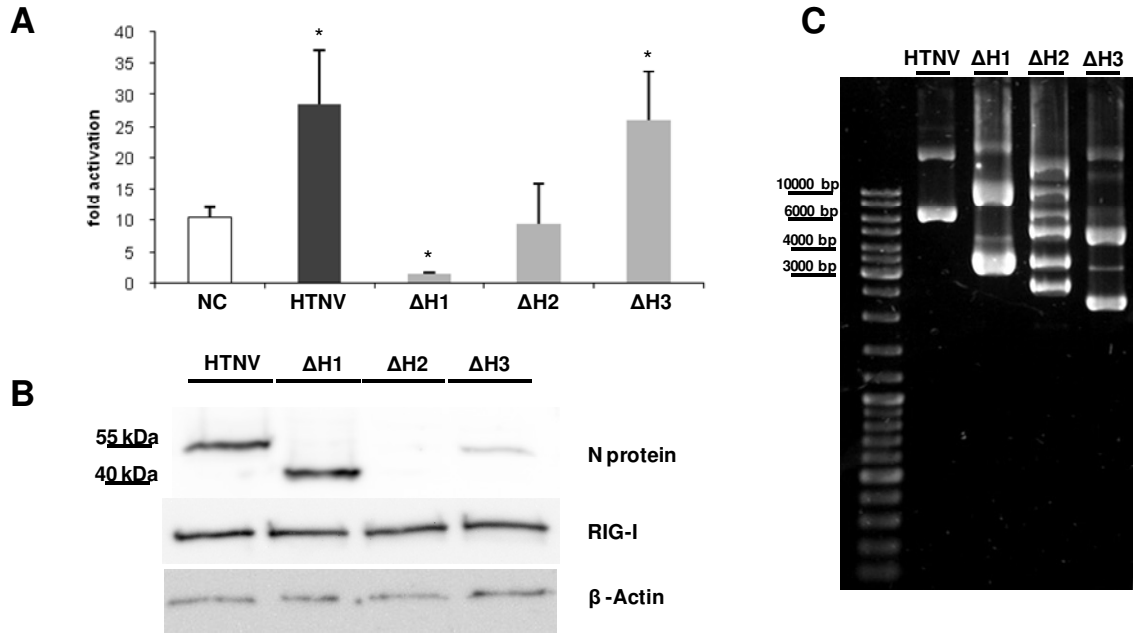

Figure 34. Impact of 3' deletion in HTNV N ORF on IFN-β promotor activation through RIG-I: HTNV N expression plasmid and expression plasmids with 3' truncated ORFs as well as empty plasmid (NC) were transfected into 293T cells together with IFN-β-activated luciferase reporter plasmid (firefly), luciferase reporter plasmid (renilla) and RIG-I. 24 hours after transfection, dual luciferase assay has been carried out. Standard deviations are based on the mean values of three independent experiments with transfections performed in duplicates. The probability of significance concerning the fold activation of negative control was determined by Student's t-test (* = $p \leq 0.05$). Appropriate expression of transfected RIG-I, N proteins and consistent protein load were approved by Western blot (B). Furthermore, the undigested plasmids were visualised in a DNA gel (C).

The deletion mutant ΔH1 with the longest truncation showed a strongly reduced activation of RIG-I signalling in comparison to the untruncated N protein and remained even below the level of the negative control. In contrast, the deletion mutant ΔH3 with a short truncation induced levels of luciferase activity similar to the untruncated protein of HTNV despite of its weak espression. Although ΔH2 showed a strange band-pattern in the DNA gel and no expression in the Western blot, it was carried through the experiments as additional control and stayed on NC level.

4.2.7 Analyses of downstream activation of RIG-I signalling pathway by hantaviral N ORF expression

To examine further components involved in signalling downstream of RIG-I and MDA5, the pathway was analysed with all hantaviral N expression plasmids in relation to TBK1 and IKKi. The experimental settings were the same as described in the previous sub-chapters, the only difference was the exchange of RIG-I as overexpressed molecule with TBK1 (Figure 35) or IKKi (Figure 36).

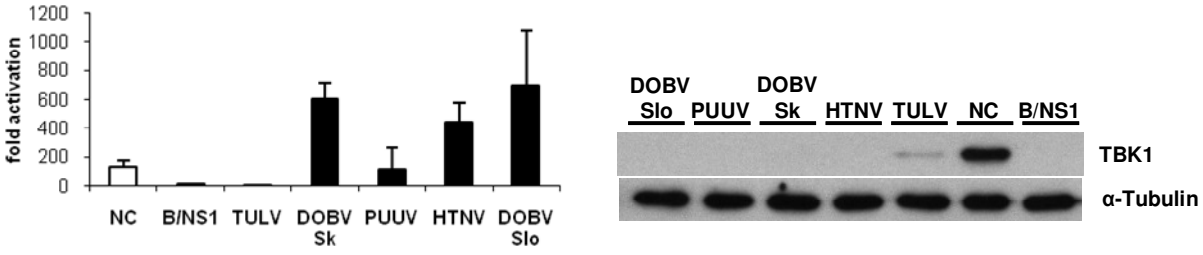

Figure 35. Influence of hantaviral N expression plasmids on IFN-β promotor activation through TBK1: 293T cells were transfected with hantaviral N protein expression plasmids, empty plasmid (NC) or B/NS1 expression plasmid together with IFN-β-activated luciferase reporter plasmid (firefly), luciferase reporter plasmid (renilla) and TBK1 expression plasmid. 24 hours after transfection, dual luciferase assay was carried out. Standard deviations are based on the mean values of two independent experiments with transfections performed in duplicates. Appropriate expression of transfected TBK1 and consistent protein load were verified by Western blot.

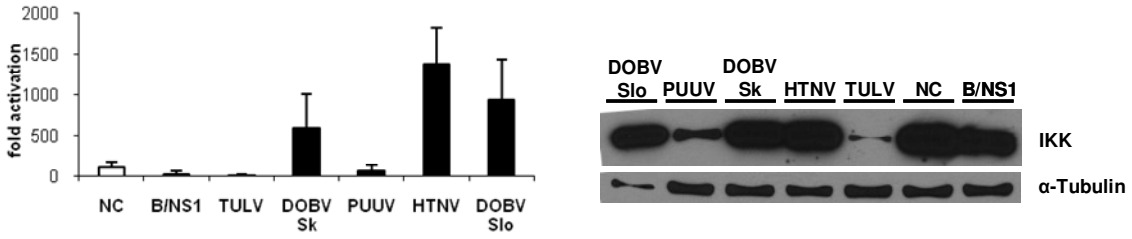

Figure 36. Effect of hantaviral N expression plasmids on IFN-β promotor activation through IKKi: 293T cells were transfected with hantaviral N protein expression plasmids, empty plasmid (NC), B/NS1 expression plasmid, IFN-β-activated luciferase reporter plasmid (firefly), luciferase reporter plasmid (renilla) and IKKi expression plasmid. 24 hours after transfection, dual luciferase assay was carried out. Standard deviations are based on the mean values of three independent experiments with transfections performed in duplicates. Appropriate expression of transfected IKKi and consistent protein load were verified by Western blot.

Although background activation levels were higher compared to the previous experiments, the gradually increasing activation depending on pathogenicity of the respective strain resembled those of the previous experiments by trend, with exception of PUUV that remained on or below the level of the negative control (110-fold for TBK1 (Figure 35) and 70-fold for IKKi (Figure 36)). TULV (1-fold for TBK1 and 11.6-fold for IKKi) even declined below the of B/NS1 activation level (8.5-fold for TBK1 and 29.3–fold for IKKi) (Figure 36). For TBK1, DOBV Slo again showed the highest activation with nearly 692.5-fold (Figure 35). For IKKi, HTNV headed the activation level with 1378.7-fold, whereas DOBV Slo only reached 946.6-fold activation (Figure 36).

To test the protein expression of the transfected plasmids, Western blots were carried out for each experiment. However, in all experiments, each transfected hantaviral expression plasmid seemed to interfere strongly with TBK1 expression for unknown reasons (Figure 35, Western blot). Interestingly, IKKi expression tested in Western blots was impaired by PUUV and TULV N, respectively (Figure 36, Western blot).

4.2.8 Influences of hantaviral N expression on IFN feedback loop through RIG-I

Virus-induced IFN expression is enhanced by a positive feedback loop through the JAK-STAT signalling pathway resulting in transcriptional activation of ISREs. To assess the downstream activation levels induced through RIG-I, all N expression plasmids were co-transfected with an ISRE-controlled luciferase reporter, transfection control and RIG-I expression plasmid (Figure 37).

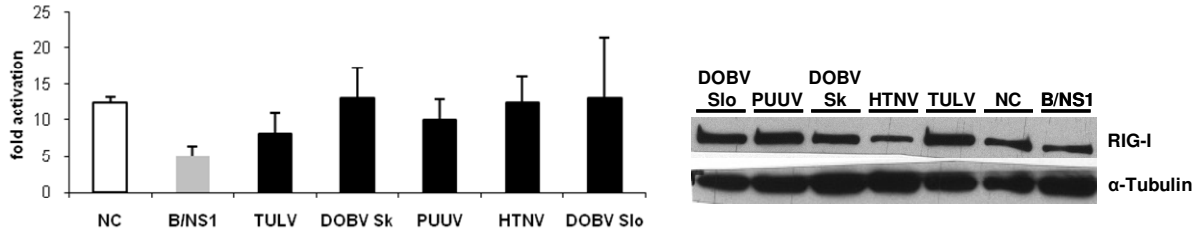

Figure 37. Influence of hantaviral N expression plasmids on ISRE-promotor activation through RIG-I: 293T cells were transfected with hantaviral N protein expression plasmids, empty plasmid (NC) or B/NS1 expression plasmid together with ISRE-activated luciferase reporter plasmid (firefly), luciferase reporter plasmid (renilla) and RIG-I expression plasmid. 24 hours after transfection, dual luciferase assay was carried out. Standard deviations are based on the mean values of two independent experiments with transfections performed in duplicates. Appropriate expression of transfected RIG-I and consistent protein load were verified by Western blot.

Interestingly, ISRE activation through RIG-I signalling by N expression was not detectable. The activation levels of all tested N expression plasmids remained in range of the negative control, those of TULV and PUUV even declined below.

4.3 Influence on RIG-I localisation by HTNV N expression plasmid

N ORF expression leads to IFN-β promotor activation and the putative activating agent is the N ORF-derived RNA according to the results of this study. However, it cannot be excluded that the N proteins also play a role for a way of RIG-I signalling which is unkown yet. To examine possible sterical interactions between RIG-I and the hantaviral N proteins as well as their spacial distribution, HeLa cells were transfected with RIG-I and N protein expression plasmids. One day after transfection, the cells were stained with antibodies specifically binding to RIG-I and hantaviral N protein and prepared for confocal microscopy. As controls, uninfected cells were co-transfected with RIG-I and empty expression plasmid. Additionally, they were stained with antibody against ubiquitious MAVS instead of N protein.

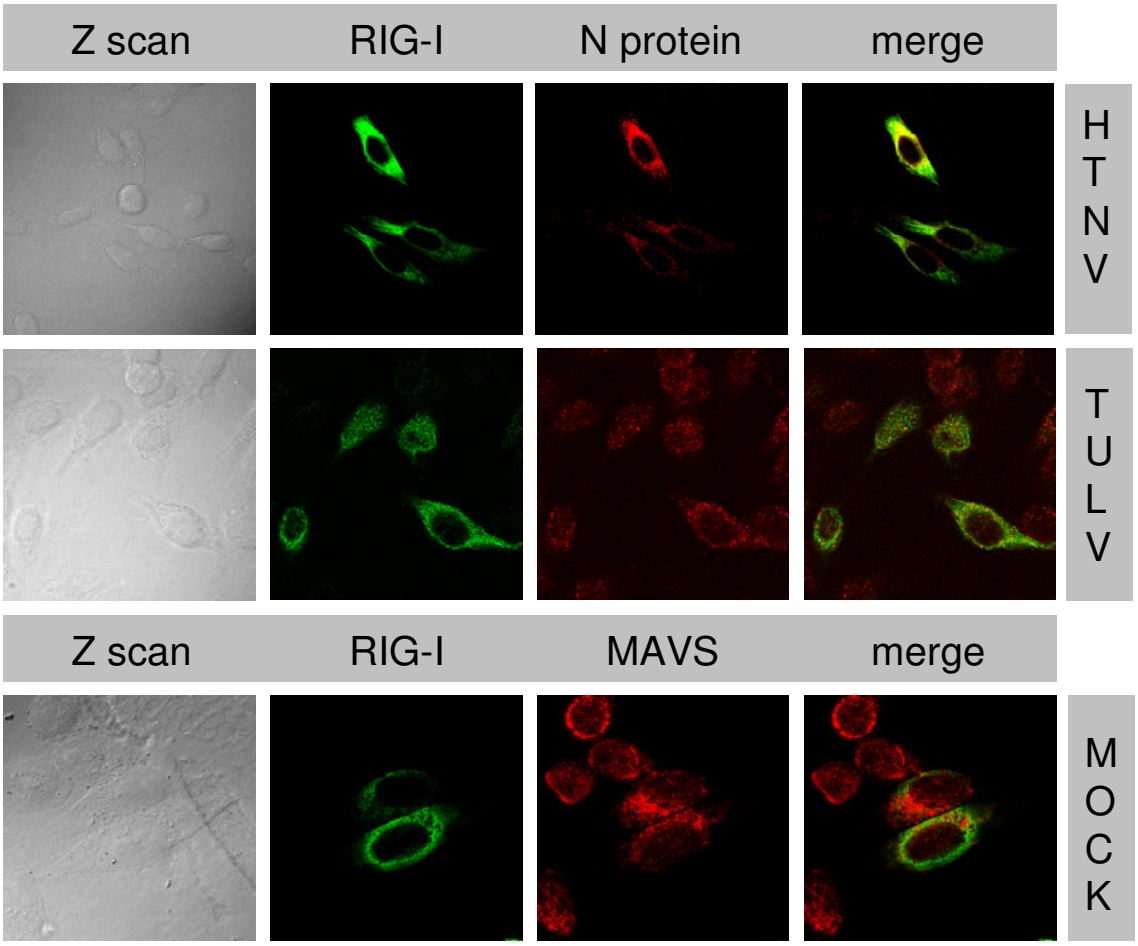

Figure 38. Altered localisation of RIG-I in presence of hantaviral N proteins: HeLa cells were co-transfected with RIG-I and N protein expression plasmids (HTNV, TULV) or empty vector as mock control. 24 hours after transfection, the cells were harvested and stained against RIG-I (green) and hantaviral N protein (red) or against MAVS (red) for the control cells and analysed with confocal immunofluorescence microscopy.

In all samples, cytoplasmic localisation of RIG-I and hantaviral N protein could be detected. For cells expressing HTNV N protein, RIG-I seemed to be distributed homogeneously whereas in TULV N protein containing as well as in the control cells, RIG-I was localised more granularly in the cytoplasm. Co-localisation of N protein with RIG-I could not be observed (Figure 38).

5 Discussion

5.1 Physiological role of RIG-I for restriction of hantavirus replication

In this thesis, the interplay between hantaviruses and cytoplasmically localised PRRs was analysed. Although type I IFN undoubtedly plays an important role for cellular defence towards hantaviruses (Kraus et al., 2004; Pensiero et al., 1992), the details of hantavirus-related type I IFN induction still remain unclear. Since hantaviruses replicate in the cellular cytoplasm thereby revealing putative PAMPs, cytoplasmic PRRs seem to be likely molecules for hantavirus detection. Moreover, an evasion mechanism mediated by the cytoplasmic tail of hantavirus G1 protein targeting the RIG-I signalling pathway was revealed recently (Alff et al., 2006; Alff et al., 2008; Spiropoulou et al., 2007).

RIG-I and MDA5 stand at the beginning of a cascade that involves several transcription factors merging in expression of IFN. They are more widespread PRRs than for example TLRs that are mainly expressed by macrophages and DCs (Kadowaki et al., 2001). For many RNA viruses, their involvement as sensor molecules has already been shown.

To assess their relevance for hantaviruses, the growth of pathogenic (Figure 13, Figure 16) and non-pathogenic (Figure 14, Figure 15) strains in A549 cells lacking RIG-I expression as compared to the respective wild-type cell line was examined. In addition to original *Murinae*- and *Arvicolinae*-associated virus strains, reassorted virus strains generated from DOBV Slo and DOBV Sk as parental strains (unpublished data of Sina Kirsanovs) were involved in the growth studies (Figure 19, Figure 20). The experiment was carried out three times, under utilisation of three different knockdown clones. For the third experimental setting, a cell line containing the lentiviral vector with a control shRNA instead of RIG-I-directed shRNA was added as additional control. The validity of the experimental system was verified by carrying out growth kinetics with VSV, a virus for which RIG-I is known to be the relevant PRR. As expected, VSV replicated better in the ΔRIG-I cells whereas the growth was limited in wild-type as well as in the control cell line (Figure 12). Therefore, off-target effects by the vector can probably be excluded for our read-out since VSV growth behaviour was similar in wild-type and control cells. In addition, clonal variability of the ΔRIG-I cell clones is not very likely as only slight variations for VSV titers were observed (Figure 12).

For hantaviruses, the comparability of the three single experiments is hampered for several reasons. Firstly, different clones of the ΔRIG-I cells were employed although no distinctive

features could be noticed in growth kinetics with VSV or FACS analyses of surface molecules. Secondly, the cells provided by the cell culture lab for titration of the supernatant of infected cells were of varying quality. In the first experiment, logistical problems did not occur so that the data could be evaluated after the first titrations and the supernatants had not to be frozen and thawn repeatedly.

In general, the control cells involved in the third experiment showed similar curves for virus progeny as the wild-type cell line except for DOBV Sk where one value even exceeded the respective value of the ΔRIG-I cells after infection, which most likely can be taken as an outlier (Figure 17). Interestingly, the reassortant A6 containing the M segment of DOBV Slo and the S and L segments of DOBV Sk replicated best in the ΔRIG-I cells compared to all other viruses. In addition, A6 showed growth differences in ΔRIG-I and wild-type cells similar to DOBV Sk, approximately 1 to 2 logs (Figure 17, Figure 19, first experiments, respectively). A36 and DOBV Slo, in turn, which both were able to replicate in ΔRIG-I as well as in wild-type cells, also showed similar growth differences up to only a half log (Figure 16, Figure 20, first experiment, respectively). This hints at a special relevance of the S and/or the L segment for viral expansion.

To exclude growth differences based on differential integrin expression on the cell lines, the density of CD29 and CD61, regarded as important for the entry of non-pathogenic and pathogenic hantaviruses, respectively (Gavrilovskaya et al., 1998; Gavrilovskaya et al., 1999; Gavrilovskaya et al., 2002), were measured by FACS analyses (Figure 11). Surprisingly, the quantification of integrins revealed that CD61 was not present at all on the cell surface of ΔRIG-I, wild-type as well as of control cells. This was also observed by other groups (Hamada et al., 2001). In contrast, CD29 could be detected on the surfaces of all three cell lines. Nevertheless, productive infection with pathogenic HTNV was observed. These results hint at other receptor molecules involved in hantavirus entry (Krautkramer and Zeier, 2008; Choi et al., 2008). In general, despite of high differences in virulence, pathogenic and non-pathogenic hantaviruses could better replicate in the ΔRIG-I cells than in the A549 wild-type cell line.

To confirm the observed effects, a similar kinetic was carried out in another cell line, Huh7.5 cells that contains a point mutation in the RIG-I gene (Bartenschlager and Pietschmann, 2005; Blight et al., 2002). For gain-of-function experiments, the same cell line complemented with a RIG-I and a constitutive active RIG-I expressing lentiviral vector or with empty vector and MDA5 was infected with HTNV, DOBV Slo and DOBV Sk. Preliminary data show that all

three hantavirus strains proliferate better in cells lacking RIG-I (Figure 21, Figure 22, Figure 23). The value for cells infected with DOBV Sk at day 7 p.i. is taken as an outlier. Highest titers were found in Huh7.5 wild-type cells, slightly reduced titers in supernatants derived from the infected Huh7.5 vector control cells. This suggests that the lentiviral vector influences hantavirus entry and/or replication to some extent. Virus growth in RIG-I and constitutive RIG-I expressing cells was generally low except for cells infected with DOBV Sk RIG as described above. Hence, in this experimental setting, it does not seem to be important for virus proliferation whether RIG-I is constitutively active or initially has to be activated by infection. The role of MDA5 is not clear yet, since for HTNV and DOBV Sk, the titers remained on the level of RIG-I expressing cells whereas for DOBV Slo MDA5, the value of FFU/ml even exceeded all other titers at 7 d p.i..

In general, there was no clear correlation between virus growth and pathogenicity of the corresponding hantavirus strain as we did not find significantly higher replication of pathogenic hantaviruses compared to the non-pathogenic strains in the respective cell line. Most of the investigated hantavirus strains grew better in cells with impaired RIG-I expression in comparison to control cells. Therefore, we can conclude that RIG-I seems to play a role as sensor molecule for pathogenic as well as for non-pathogenic hantaviruses in cell culture. However, the mechanism and possible influences by other PRRs are not understood yet due to delicate balances between viral defence mechanisms and the cellular detection system initiating an antiviral response.

5.2 Interaction of hantaviral components with RIG-I and MDA5

To define potential hantaviral PAMPs, all available components of several hantaviruses differing in pathogenicity, epidemiology and reservoir hosts, were examined. Their ability of triggering or blocking innate immune response through cytoplasmic PRRs was investigated. It had been assumed that RIG-I and MDA5 are activated mainly by interaction with 5'-triphosphate single-stranded RNA and double-stranded RNA, respectively. However, the possibility of a certain redundancy in recognition of different RNA patterns cannot be excluded (Imaizumi et al., 2005; Yoneyama et al., 2004). For example, RIG-I could also be activated by dsRNA dependent on its length, and a polyuridine motif in the non-coding region of HCV was found to play a role for RIG-I induction (Saito et al., 2008). In addition, involvement of both

RIG-I und MDA5 in recognition of West nile virus (WNV) (Fredericksen et al., 2008) and of dsDNA was observed (Cheng et al., 2007).

5.2.1 Relevance of genomic RNA as ligand of RIG-I

Viruses with a negatively orientated RNA genome do not necessarily form detectable double-stranded RNA structures. Furthermore, neither hantaviral genomes nor the viral mRNAs normally contain free 5'-triphosphates at their end. The genome is structured as a panhandle bound by the viral N protein, thus preventing detection by RIG-I by masking the RNA (Mir and Panganiban, 2006). Therefore, it is not surprising that only weak or no activation of RIG-I signalling by hantaviral genomic RNAs could be detected (Figure 24), as also observed by Habjan et al. (Habjan et al., 2008).

Although vRNA did not activate the IFN-β promotor through MDA5 either (Figure 25), the relative fold activations were much higher than for respective RIG-I samples. This could be explained by the fact that MDA5 does not possess a C-terminal repressor domain like RIG-I therefore inducing high background activity (Pichlmair et al., 2006; Saito et al., 2007).

5.2.2 Role of hantaviral glycoproteins in the interplay between hantaviruses and cytoplasmic sensor molecules

The hantaviral G proteins examined in our experimental setting neither triggered nor inhibited signalling through MDA5 or RIG-I (Figure 26, Figure 27). In comparison to another inhibitor, the Influenza B/NS1 protein (Opitz et al., 2007; Dauber et al., 2004), blocking properties of the hantaviral G proteins could hardly be detected. However, it has to be mentioned that no challenge for proving or excluding specific inhibition as carried out by other groups was included into our experimental setting. In contrast to our findings, it has been shown by Alff *et al.* that G1 protein tails derived from pathogenic hantavirus strains inhibit RIG-signalling after transfection of a constitutive active RIG-I deletion mutant, whereas the G1 protein from non-pathogenic PHV was not able to suppress the signalling cascade (Alff et al., 2006; Alff et al., 2008).

Activation of PRR signalling by G proteins could not be observed either. Interestingly, even the *in vitro*-generated G ORF RNA did not result in IFN-β induction through RIG-I (Figure 32), although it contains 5'-triphosphates. Possibly, the RNA derived from G encoding ORF has structural or sequential properties that abrogate the impact of 5'-triphosphates on detec-

tion by RIG-I. If hantaviral G proteins provide PAMPs, then the respective PRRs are probably localised on the surface of the host cell or in the endosomes like for example TLRs which could be activated during attachment and entry processes.

5.2.3 Induction of RIG-I signalling by hantaviral N ORF expressing plasmids

5.2.3.1 Activation of RIG-I signal transduction by expression of hantaviral N ORFs

For many viruses, the interplay between PRRs or downstream molecules and a viral protein has been discovered. For example, an interaction of RIG-I and NS1 of Influenza viruses was recently described (Dauber et al., 2006; Pichlmair et al., 2006). For hantaviruses, similar coherences could be assumed as well. A potential candidate for interactions with PRRs is the hantaviral N protein. It plays an important role during the life cycle of hantaviruses, functioning as an RNA chaperon and recognising the viral genomic panhandle (Alminaite et al., 2006; Mir and Panganiban, 2006). It potentially binds to other RNA structures, thus protecting or sequestering target structures that stimulate cytoplasmic sensors, thereby establishing a dynamic equilibrium between induction and inhibition of innate signalling. Furthermore, it is the most considerable target to initiate innate immune response since it is the first viral gene to be transcribed. RNA derived from the S segment as for example shown for SNV can be detected 4 to 6 h p.i. when the hantavirus-related innate response is induced (Hutchinson et al., 1998; Schmaljohn and Hjelle, 1997; Hutchinson et al., 1996). In addition, it is the most conserved structural protein of hantaviruses and the main target of cellular and humoral immune response (Kaukinen et al., 2005). Therefore, the N protein or the corresponding RNA could play a pivotal role in interaction with PRRs.

In fact, different effects on RIG-I signalling could be observed, depending on the origin of the N ORF (Figure 28). RIG-I-mediated activation levels of the IFN promotor increased with the degree of pathogenicity of the hantavirus strain from which the N protein was derived. The highest activation was induced by the DOBV Slo N protein expression plasmid. In contrast, only slight but not significant activation could be detected after expression of DOBV Slo N protein in combination with MDA5, while the other N protein expression plasmids induced no activation or rather diminished IFN-β promotor activity as seen for TULV N (Figure 29).

5.2.3.2 Determination of the hantaviral component stimulating RIG-I

To assess whether the N protein itself or its RNA is the inducing component, the expression plasmids were *in vitro*-transcribed and examined in the same experimental setting (Figure 31). Although the fold activations were slightly lower than in the previous described experiments, the same induction pattern could be observed, except for DOBV Slo N RNA. The integrity of the transcripts has been tested in an RNA gel ensuring that the DOBV Slo N RNA was not degraded (Figure 30). A possible explanation could be altered secondary structures of the *in vitro*-transcribed RNA that affect the influence on RIG-I signalling, for example by hiding stimulatory motifs or exposing inhibitory sequences. In contrast, *in vivo* appropriate binding of cellular RNA chaperons to DOBV Slo N RNA could allow for the formation of additional RIG-I stimulatory structures. Nevertheless, it cannot be entirely excluded that the N protein itself also interacts with RIG-I signalling.

Usually, hantaviral mRNA is capped and tailed by cap snatching mechanism. Accordingly, possible 5'-triphosphate ends should only be available in a short time frame for recognition by PRRs (Elliott et al., 1991). Since *in vitro*-transcribed RNA also possess triphosphates at their 5' ends that are known as ligands of RIG-I (Hornung et al., 2006), in a subsequent experimental setting, the transcripts were digested to remove the triphosphates to assess their influence on signalling (Figure 33). Activation levels decreased for all digested samples, and the pattern also was altered, but still, differences in activation levels could be shown. This observation leads to the assumption that certain motifs – maybe in addition to 5'-triphosphates – within the RNA and/or the protein derived from the S segment are responsible for activation or even inhibition of RIG-I signalling (Figure 31**,** Figure 33).

Unfortunately, there was no possibility to verify the amount of 5'-triphosphates for a better evaluation of their relevance for signalling induction, but there should not be large differences between the samples since all plasmids were treated identically. Furthermore, for example JEV mRNA is known to be 5' capped and no triphosphates are exposed at the 5' end. However, it is still detected by RIG-I (Chang et al., 2006; Kato et al., 2006). It has been suggested before that RIG-I-mediated RNA recognition is not only dependent on 5'-triphosphates (Cui et al., 2008). Motifs inducing or interfering with RIG-I signalling are also liable for viruses, as already shown for the 3'-untranslated region of HCV (Saito et al., 2008).

5.2.3.3 Definition of a potential RIG-I stimulating motif within the hantaviral N ORF

To define a potential motif within the N ORF, random deletion mutants of the HTNV N ORF with truncated 3' ends were generated. The candidates were tested for appropriate expression and for IFN-β promotor activation through RIG-I signalling (Figure 34). Interestingly, the N ORF mutant ΔH1 did not activate the reporter system at all and declined even below negative control level, although expression could be proven in Western blot. ΔH2 behaved almost like the negative control and was not detectable in Western blot, whereas the third mutant ΔH3 lacking only a short 3' end of the ORF reached nearly the IFN-β promotor activation level of the full-length plasmid. However, it was expressed much weaker than HTNV N or ΔH1 N. Since the deleted sequence is not yet characterised, it is difficult to define the distinct sequence or structure which is possibly responsible for activation of RIG-I signalling.

5.2.3.4 *In silico* analyses of N ORFs

For theoretical predictions, sequences of all N ORFs involved in our experiments were subjected to a similarity test in comparison to either DOBV Slo or HTNV N ORF (Figure 39) which showed the highest activation levels in our experimental setting. Basically, we hoped to see conserved domains for the pathogenic hantavirus strains and/or for the non-pathogenic ones. Although homologies could be observed, they do not necessarily correlate with the RIG-I signalling activation levels. For example, DOBV Slo and DOBV Sk, differing in the strength of IFN induction resemble each other strongly. On the other hand, the relations of *Murinae*- and *Arvicolinae*-associated hantavirus strains are very obvious in the distance plots.
Therefore, we cannot explain different activation patterns by conserved motifs in the primary RNA sequence, and it can be expected that more complex motifs are possibly involved in signalling induction like for example secondary structures and charges depending on the length of the nucleotides. A better knowledge of the binding and activating capacities of RIG-I may help to draw conclusions about potential ligands.

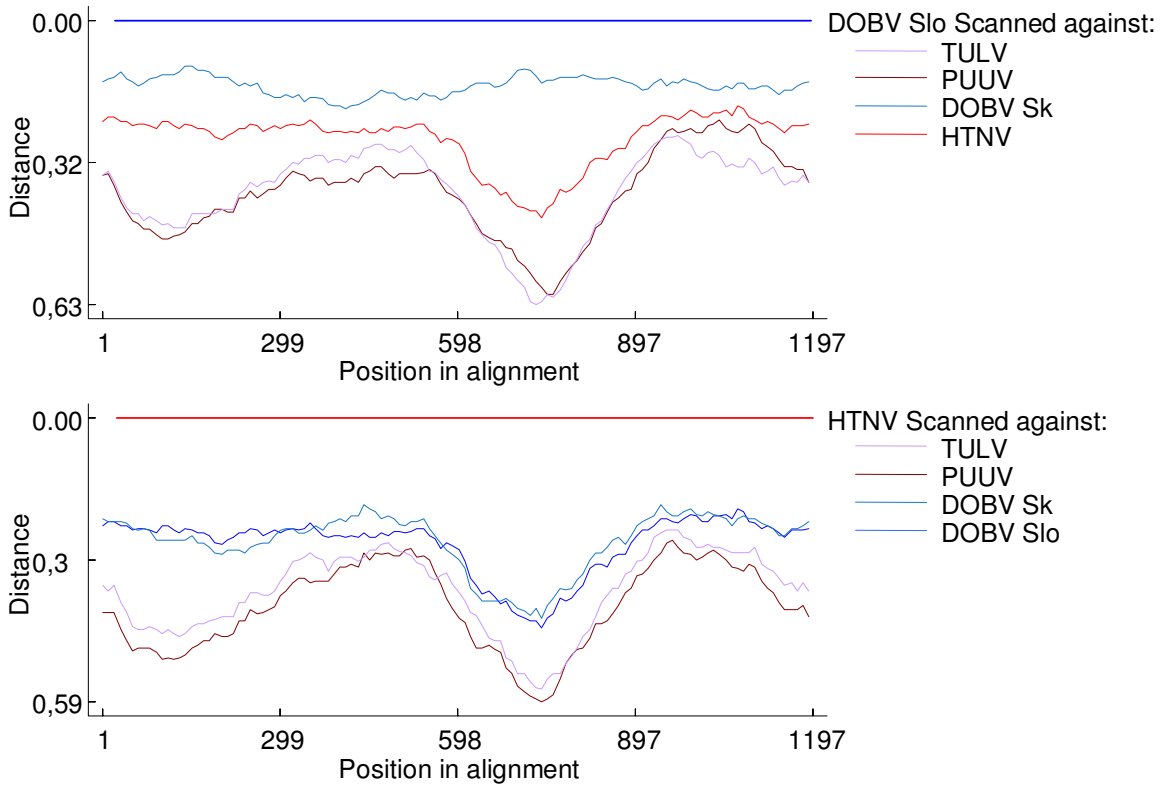

Figure 39. Distance plots of N ORFs against DOBV Slo and HTNV

5.2.3.5 Significance of RIG-I for hantaviruses

We propose that the observed different patterns of RIG-I activation are related to inhibitory or stimulatory motifs on the hantaviral RNA molecules as mentioned above. The exact nature of these motifs still has to be elucidated, but the activation patterns of phosphatase-treated transcripts and of the deletion mutants suggest that not only the 5' ends regulate RIG-I and support the motif hypothesis (Figure 33). Furthermore, viruses that are detected by RIG-I do not all possess triphosphates at their 5' ends or present them only during a very short time frame. Although pathogens are characterised by their high diversity, all of them have nucleic acids in common (Kato et al., 2006), independent of their modifications. Thus, many cellular detection systems make use of the viral genomes during entry or of their products generated by replication and expression processes of the viruses. For example, endosomally located TLR3 recognises dsRNA independently from its sequence (Alexopoulou et al., 2001; Matsumoto et al., 2003). Therefore, virus genomes are mostly protected by viral proteins to prevent detection. In contrast, mRNA is often uncovered to be accessible for translation complexes. It may be

possible that for activation of RIG-I, the 5'-triphosphates of viral RNAs are sufficient and necessary whereas for others, intrinsic motifs play an important role. It is also imaginable that these motifs show accumulative effects, whether stimulating or inhibiting. Furthermore, there are first hints that for longer RNAs, the 5'-triphosphate is less important for detection by RIG-I, and structures within the sequence play a crucial role.

The relevance of RIG-I for hantaviruses could also be shown on the functional level. However, it was not possible to investigate the particular relevance of N ORFs within the context of virus infections because up to now a system for reverse genetics is not available for hantaviruses. Furthermore, cellular mechanisms responsible for hantavirus detection and subsequent triggering of antiviral immune response have not been completely defined either. Therefore, the impact of N ORF expression on hantavirus-related immune response cannot be evaluated yet. Possibly, non-pathogenic hantaviruses trigger innate immunity early as shown by different groups (Alff et al., 2006; Kraus et al., 2004; Spiropoulou et al., 2007) because of lacking evasion mechanisms whereas pathogenic strains interfere with the immune system more aggressively thereby getting the opportunity to replicate more efficiently. In addition, different or additional PRRs may be responsible for the recognition of pathogenic and non-pathogenic hantaviruses, merging in the same signalling cascades to achieve synergistic effects for virus clearance in simultaneous or successive manners whereas single PRRs show only comparatively weak signalling induction.

5.3 Hantavirus-associated modulation of signalling downstream of PRRs

After investigating the relations between hantaviral components and innate immune response by overexpression of PRRs, the effect on molecules downstream of RIG-I and MDA5 like TBK1 and IKKi has been examined. However, the activation levels induced by the tested N expression plasmids changed and were not congruent to the RIG-I-related pattern. For overexpression of both TBK1 and IKKi, TULV declined to inhibition control level whereas PUUV activation decreased to the negative control level. Expression plasmids containing N ORFs from the two DOBV strains showed similar fold activations. Surprisingly, TBK1 was strongly downregulated on protein level in presence of all N protein expression plasmids. It is not clear yet whether this finding is due to reduced TBK1 expression which would be surprising considering the high amounts of transfected TBK1 expression plasmid. Alternatively, antibody detection of TBK1 could be impaired by hantaviral nucleocapsid expression (Figure 35).

For IKKi, TULV and PUUV N expression plasmids reduced IKKi expression for unknown reasons. The weak fold inductions by both plasmids could be explained by the downregulation of IKKi (Figure 36). No induction of the ISRE-coupled luciferase reporter could be observed, although the feedback mediated by IFN secretion should enhance the IFN-β expression (Figure 37). A possible explanation could be a yet unknown viral evasion mechanism that interferes with signalling elements of the feedback loop. Alternatively, a merge of different innate signalling cascades triggered by hantaviruses could be necessary for detectable type I IFN production. Such synergistic effects may lack in our experimental systems.

To assess direct interactions and subsequent changes in the localisation of RIG-I by hantaviral N protein, co-transfections with RIG-I and N protein expression plasmids derived from pathogenic HTNV and non-pathogenic TULV were carried out and analysed by confocal microscopy. Expression of HTNV N protein led to homogeneous distribution of RIG-I. In contrast, co-transfection with TULV N protein resulted in a similar RIG-I localisation as the control. Thus, HTNV N protein seems to influence the distribution of RIG-I (Figure 38). More detailed investigations are necessary to demonstrate a potential interaction, for example by immunoprecipitation, and to define the mechanism and subsequent consequences for virus and cell.

5.4 Importance of innate mechanisms upstream from PRRs

Other mechanisms that may be involved in activation of RIG-I signalling by hantaviruses also have to be considered. So far, only the PRRs and the molecules downstream have been discussed, but upstream molecules and the control of PRR expression could also play a role.

RNA processing mechanisms could be of importance for PRR signalling since RNAs of different lengths and modifications are potential ligands (Kato et al., 2008). Longer RNA may also be less stable, therefore, cellular and viral proteins are possibly involved in forming secondary RNA structures, providing or hiding potential PAMPs. For viruses, it has been shown that MDA5 only recognises EMCV, whereas RIG-I detects RNA viruses with longer genomes. In general, the precise viral PAMPs are mostly undefined yet for the cytoplasmically located PRRs. RIG-I is able to bind double-stranded as well as single-stranded RNA, nucleotide overhangs and 5' end modifications seem to play a role with varying importance depending on the RNA length. Recently, a viral motif has been found (Saito et al., 2008), but it is difficult to assess the activation potentials of the different PAMPs. Furthermore, it is not yet

clear whether PAMPs synergise in the signalling through one or more PRRs. Once more detailed information about these relations becomes available, RNA processing mechanisms located upstream of RIG-I and MDA5 and the influence of chaperons will be of special interest.

5.5 Conclusion and outlook

The identification of hantaviral nucleocapsid expression as a trigger of RIG-I signalling is a further step to a better understanding of hantavirus-related innate immunity. In detail, IFN-β promoter activation increases depending on the virulence of the hantavirus strain from which the expressed N ORF is derived. More precisely, the N ORF RNA seems to be the component responsible for the activation of RIG-I.

The pathogenicity-dependent activation pattern can be explained by inhibitory or stimulatory motifs within the N RNA. Our results give first hints on the nature of such motifs that are possibly located at the 3' end of the N ORF and will be proven by gain- and loss-of-function experiments. Furthermore, still unknown PRRs (Paladino et al., 2006) could be involved in the detection of hantaviruses as N ORF expressing plasmids or mRNA derived from non-pathogenic hantaviruses did neither trigger RIG-I nor MDA5 signalling pathways.

However, it has to be analysed as well whether the low IFN-β promotor activation by some expressed N ORFs is the result of missing activation by stimulatory motifs or of active inhibition by inhibitory structures and the N protein itself. Similarly, the G ORF expression did not lead to an activation or an inhibition of RIG-I or MDA5 signalling. Even *in vitro*-transcribed G ORFs, containing 5'-triphosphates, did not trigger IFN promotor signalling, possibly due to the reduced importance of 5'-triphosphates for the recognition of longer RNAs by RIG-I.

Therefore, the discovery of other PRRs involved in hantavirus detection and their degree of redundancy would be quite interesting. Induction of innate immunity leads to differential activation of signal transduction pathways depending on the triggered PRR. Hence, adaptive immune response may vary in strength and efficiency. Our growth kinetics revealed that replication of non-pathogenic strains was also affected in RIG-I expressing cells compared to cells in which RIG-I expression is impaired. To explain these findings, the functions of all hantaviral components and their interplay during infection have to be investigated in more depth. Reverse genetic systems and appropriate animal models could be of great advantage for such studies. In general, partial redundancy of PRRs responsible for hantavirus detection would not be surprising for the induction of an important antiviral defence system like the type I IFN

response and for the benefit of synergistic effects. However, the delicate regulation mechanisms of the type I IFN system do not simplify respective investigations. The role of IFN is ambiguously critical for the host since it has to operate fast to contribute successfully to virus clearance, but a prolonged expression can also lead to autoimmune reactions (Le Bon et al., 2003; Ronnblom et al., 2006; Taniguchi and Takaoka, 2001).

In addition, RIG-I and MDA5 signal transduction may not "only" be involved in IFN induction, but also other pathways. For example, their adaptor molecule MAVS seems to be involved in regulation of apoptosis and of surface molecules (Kumar et al., 2006).

Furthermore, differences in PRR distribution and function do not only occur in different cell types of the same organism, but also in comparable cell types of different species. This fact is of special interest for the comparison of hantavirus-related immune response in reservoir hosts and humans: hantaviral infection remains apathogenic in rodents and persists, whereas in humans, the virus is cleared under (partially severe) courses of disease (Botten et al., 2000). All these analyses may contribute to an understanding of differences in immune responses and divergent cytokine expression patterns caused by hantaviruses differing in virulence towards humans. Thus, they could build a basis for a better understanding of the differences in severity of clinical symptoms and furthermore elucidate the asymptomatic persistence in reservoir hosts. Finally, these findings could help to develop improved treatments after hantaviral infection or prophylactic means like vaccines.

References

Akira, S. and Takeda, K. (2004). Toll-like receptor signalling. Nat. Rev. Immunol. *4,* 499-511.

Alexopoulou, L., Holt, A.C., Medzhitov, R., and Flavell, R.A. (2001). Recognition of double-stranded RNA and activation of NF-kappaB by Toll-like receptor 3. Nature *413,* 732-738.

Alfadhli, A., Love, Z., Arvidson, B., Seeds, J., Willey, J., and Barklis, E. (2001). Hantavirus nucleocapsid protein oligomerization. J. Virol. *75,* 2019-2023.

Alff, P.J., Gavrilovskaya, I.N., Gorbunova, E., Endriss, K., Chong, Y., Geimonen, E., Sen, N., Reich, N.C., and Mackow, E.R. (2006). The pathogenic NY-1 hantavirus G1 cytoplasmic tail inhibits RIG-I- and TBK-1-directed interferon responses. J. Virol. *80,* 9676-9686.

Alff, P.J., Sen, N., Gorbunova, E., Gavrilovskaya, I.N., and Mackow, E.R. (2008). The NY-1 hantavirus Gn cytoplasmic tail coprecipitates TRAF3 and inhibits cellular interferon responses by disrupting TBK1-TRAF3 complex formation. J. Virol. *82,* 9115-9122.

Alminaite, A., Halttunen, V., Kumar, V., Vaheri, A., Holm, L., and Plyusnin, A. (2006). Oligomerization of hantavirus nucleocapsid protein: analysis of the N-terminal coiled-coil domain. J. Virol. *80,* 9073-9081.

Andrejeva, J., Childs, K.S., Young, D.F., Carlos, T.S., Stock, N., Goodbourn, S., and Randall, R.E. (2004). The V proteins of paramyxoviruses bind the IFN-inducible RNA helicase, mda-5, and inhibit its activation of the IFN-beta promoter. Proc. Natl. Acad. Sci. U. S. A *101,* 17264-17269.

Arikawa, J., Takashima, I., and Hashimoto, N. (1985). Cell fusion by haemorrhagic fever with renal syndrome (HFRS) viruses and its application for titration of virus infectivity and neutralizing antibody. Arch. Virol. *86,* 303-313.

Avsic-Zupanc, T., Toney, A., Anderson, K., Chu, Y.K., and Schmaljohn, C. (1995). Genetic and antigenic properties of Dobrava virus: a unique member of the Hantavirus genus, family Bunyaviridae. J. Gen. Virol. *76 (Pt 11),* 2801-2808.

Balachandran, S. and Barber, G.N. (2004). Defective translational control facilitates vesicular stomatitis virus oncolysis. Cancer Cell *5,* 51-65.

Bartenschlager, R. and Pietschmann, T. (2005). Efficient hepatitis C virus cell culture system: what a difference the host cell makes. Proc. Natl. Acad. Sci. U. S. A *102,* 9739-9740.

Binder, M., Kochs, G., Bartenschlager, R., and Lohmann, V. (2007). Hepatitis C virus escape from the interferon regulatory factor 3 pathway by a passive and active evasion strategy. Hepatology *46,* 1365-1374.

Blight, K.J., McKeating, J.A., and Rice, C.M. (2002). Highly permissive cell lines for subgenomic and genomic hepatitis C virus RNA replication. J. Virol. *76,* 13001-13014.

Botten, J., Mirowsky, K., Kusewitt, D., Bharadwaj, M., Yee, J., Ricci, R., Feddersen, R.M., and Hjelle, B. (2000). Experimental infection model for Sin Nombre hantavirus in the deer mouse (Peromyscus maniculatus). Proc. Natl. Acad. Sci. U. S. A *97,* 10578-10583.

Bowen, M.D., Kariwa, H., Rollin, P.E., Peters, C.J., and Nichol, S.T. (1995). Genetic characterization of a human isolate of Puumala hantavirus from France. Virus Res. *38,* 279-289.

Carey, D.E., Reuben, R., Panicker, K.N., Shope, R.E., and Myers, R.M. (1971). Thottapalayam virus: a presumptive arbovirus isolated from a shrew in India. Indian J. Med. Res. *59,* 1758-1760.

Chang, T.H., Liao, C.L., and Lin, Y.L. (2006). Flavivirus induces interferon-beta gene expression through a pathway involving RIG-I-dependent IRF-3 and PI3K-dependent NF-kappaB activation. Microbes. Infect. *8,* 157-171.

Chapman, L.E., Ellis, B.A., Koster, F.T., Sotir, M., Ksiazek, T.G., Mertz, G.J., Rollin, P.E., Baum, K.F., Pavia, A.T., Christenson, J.C., Rubin, P.J., Jolson, H.M., Behrman, R.E., Khan, A.S., Bell, L.J., Simpson, G.L., Hawk, J., Holman, R.C., and Peters, C.J. (2002). Discriminators between hantavirus-infected and -uninfected persons enrolled in a trial of intravenous ribavirin for presumptive hantavirus pulmonary syndrome. Clin. Infect. Dis. *34,* 293-304.

Chapman, L.E., Mertz, G.J., Peters, C.J., Jolson, H.M., Khan, A.S., Ksiazek, T.G., Koster, F.T., Baum, K.F., Rollin, P.E., Pavia, A.T., Holman, R.C., Christenson, J.C., Rubin, P.J., Behrman, R.E., Bell, L.J., Simpson, G.L., and Sadek, R.F. (1999). Intravenous ribavirin for hantavirus pulmonary syndrome: safety and tolerance during 1 year of open-label experience. Ribavirin Study Group. Antivir. Ther. *4,* 211-219.

Cheng, G., Zhong, J., Chung, J., and Chisari, F.V. (2007). Double-stranded DNA and double-stranded RNA induce a common antiviral signaling pathway in human cells. Proc. Natl. Acad. Sci. U. S. A *104,* 9035-9040.

Choi, Y., Kwon, Y.C., Kim, S.I., Park, J.M., Lee, K.H., and Ahn, B.Y. (2008). A hantavirus causing hemorrhagic fever with renal syndrome requires gC1qR/p32 for efficient cell binding and infection. Virology *381,* 178-183.

Chu, W.M., Ostertag, D., Li, Z.W., Chang, L., Chen, Y., Hu, Y., Williams, B., Perrault, J., and Karin, M. (1999). JNK2 and IKKbeta are required for activating the innate response to viral infection. Immunity *11,* 721-731.

Clement, J.P. (2003). Hantavirus. Antiviral Res. *57,* 121-127.

Cosgriff, T.M. and Lewis, R.M. (1991). Mechanisms of disease in hemorrhagic fever with renal syndrome. Kidney Int. Suppl *35,* S72-S79.

Cui, S., Eisenacher, K., Kirchhofer, A., Brzozka, K., Lammens, A., Lammens, K., Fujita, T., Conzelmann, K.K., Krug, A., and Hopfner, K.P. (2008). The C-terminal regulatory domain is the RNA 5'-triphosphate sensor of RIG-I. Mol. Cell *29,* 169-179.

Dauber, B., Heins, G., and Wolff, T. (2004). The influenza B virus nonstructural NS1 protein is essential for efficient viral growth and antagonizes beta interferon induction. J. Virol. *78,* 1865-1872.

Dauber, B., Schneider, J., and Wolff, T. (2006). Double-stranded RNA binding of influenza B virus nonstructural NS1 protein inhibits protein kinase R but is not essential to antagonize production of alpha/beta interferon. J. Virol. *80,* 11667-11677.

Du, W. and Maniatis, T. (1992). An ATF/CREB binding site is required for virus induction of the human interferon beta gene [corrected]. Proc. Natl. Acad. Sci. U. S. A *89,* 2150-2154.

Dunn, E.F., Pritlove, D.C., Jin, H., and Elliott, R.M. (1995). Transcription of a recombinant bunyavirus RNA template by transiently expressed bunyavirus proteins. Virology *211,* 133-143.

Easterbrook, J.D., Zink, M.C., and Klein, S.L. (2007). Regulatory T cells enhance persistence of the zoonotic pathogen Seoul virus in its reservoir host. Proc. Natl. Acad. Sci. U. S. A *104,* 15502-15507.

Elliott, R.M. (1990). Molecular biology of the Bunyaviridae. J. Gen. Virol. *71 (Pt 3),* 501-522.

Elliott, R.M., Schmaljohn, C.S., and Collett, M.S. (1991). Bunyaviridae genome structure and gene expression. Curr. Top. Microbiol. Immunol. *169,* 91-141.

Ellis, D.S., Shirodaria, P.V., Fleming, E., and Simpson, D.I. (1988). Morphology and development of Rift Valley fever virus in Vero cell cultures. J. Med. Virol. *24,* 161-174.

Fredericksen, B.L., Keller, B.C., Fornek, J., Katze, M.G., and Gale, M., Jr. (2008). Establishment and maintenance of the innate antiviral response to West Nile Virus involves both RIG-I and MDA5 signaling through IPS-1. J. Virol. *82,* 609-616.

Frese, M., Kochs, G., Feldmann, H., Hertkorn, C., and Haller, O. (1996). Inhibition of bunyaviruses, phleboviruses, and hantaviruses by human MxA protein. J. Virol. *70,* 915-923.

Garcin, D., Lezzi, M., Dobbs, M., Elliott, R.M., Schmaljohn, C., Kang, C.Y., and Kolakofsky, D. (1995). The 5' ends of Hantaan virus (Bunyaviridae) RNAs suggest a prime-and-realign mechanism for the initiation of RNA synthesis. J. Virol. *69,* 5754-5762.

Gavrilovskaya, I.N., Brown, E.J., Ginsberg, M.H., and Mackow, E.R. (1999). Cellular entry of hantaviruses which cause hemorrhagic fever with renal syndrome is mediated by beta3 integrins. J. Virol. *73,* 3951-3959.

Gavrilovskaya, I.N., Gorbunova, E.E., Mackow, N.A., and Mackow, E.R. (2008). Hantaviruses direct endothelial cell permeability by sensitizing cells to the vascular permeability factor VEGF, while angiopoietin 1 and sphingosine 1-phosphate inhibit hantavirus-directed permeability. J. Virol. *82,* 5797-5806.

Gavrilovskaya, I.N., Peresleni, T., Geimonen, E., and Mackow, E.R. (2002). Pathogenic hantaviruses selectively inhibit beta3 integrin directed endothelial cell migration. Arch. Virol. *147,* 1913-1931.

Gavrilovskaya, I.N., Shepley, M., Shaw, R., Ginsberg, M.H., and Mackow, E.R. (1998). beta3 Integrins mediate the cellular entry of hantaviruses that cause respiratory failure. Proc. Natl. Acad. Sci. U. S. A *95,* 7074-7079.

Geimonen, E., Fernandez, I., Gavrilovskaya, I.N., and Mackow, E.R. (2003). Tyrosine residues direct the ubiquitination and degradation of the NY-1 hantavirus G1 cytoplasmic tail. J. Virol. *77,* 10760-10868.

Geimonen, E., Neff, S., Raymond, T., Kocer, S.S., Gavrilovskaya, I.N., and Mackow, E.R. (2002). Pathogenic and nonpathogenic hantaviruses differentially regulate endothelial cell responses. Proc. Natl. Acad. Sci. U. S. A *99,* 13837-13842.

Gitlin, L., Barchet, W., Gilfillan, S., Cella, M., Beutler, B., Flavell, R.A., Diamond, M.S., and Colonna, M. (2006). Essential role of mda-5 in type I IFN responses to polyriboinosinic:polyribocytidylic acid and encephalomyocarditis picornavirus. Proc. Natl. Acad. Sci. U. S. A *103,* 8459-8464.

Goldsmith, C.S., Elliott, L.H., Peters, C.J., and Zaki, S.R. (1995). Ultrastructural characteristics of Sin Nombre virus, causative agent of hantavirus pulmonary syndrome. Arch. Virol. *140,* 2107-2122.

Gonzalez, J.P., McCormick, J.B., Baudon, D., Gautun, J.P., Meunier, D.Y., Dournon, E., and Georges, A.J. (1984). Serological evidence for Hantaan-related virus in Africa. Lancet *2,* 1036-1037.

Gott, P., Stohwasser, R., Schnitzler, P., Darai, G., and Bautz, E.K. (1993). RNA binding of recombinant nucleocapsid proteins of hantaviruses. Virology *194,* 332-337.

Gott, P., Zoller, L., Darai, G., and Bautz, E.K. (1997). A major antigenic domain of hantaviruses is located on the aminoproximal site of the viral nucleocapsid protein. Virus Genes *14,* 31-40.

Green, W., Feddersen, R., Yousef, O., Behr, M., Smith, K., Nestler, J., Jenison, S., Yamada, T., and Hjelle, B. (1998). Tissue distribution of hantavirus antigen in naturally infected humans and deer mice. J. Infect. Dis. *177,* 1696-1700.

Groen, J., Dalrymple, J., Fisher-Hoch, S., Jordans, J.G., Clement, J.P., and Osterhaus, A.D. (1992). Serum antibodies to structural proteins of Hantavirus arise at different times after infection. J. Med. Virol. *37*, 283-287.

Habjan, M., Andersson, I., Klingstrom, J., Schumann, M., Martin, A., Zimmermann, P., Wagner, V., Pichlmair, A., Schneider, U., Muhlberger, E., Mirazimi, A., and Weber, F. (2008). Processing of genome 5' termini as a strategy of negative-strand RNA viruses to avoid RIG-I-dependent interferon induction. PLoS. ONE. *3,* e2032.

Hamada, J., Omatsu, T., Okada, F., Furuuchi, K., Okubo, Y., Takahashi, Y., Tada, M., Miyazaki, Y.J., Taniguchi, Y., Shirato, H., Miyasaka, K., and Moriuchi, T. (2001). Overexpression of homeobox gene HOXD3 induces coordinate expression of metastasis-related genes in human lung cancer cells. Int. J. Cancer *93,* 516-525.

Hart, C.A. and Bennett, M. (1999). Hantavirus infections: epidemiology and pathogenesis. Microbes. Infect. *1,* 1229-1237.

Heider, H., Ziaja, B., Priemer, C., Lundkvist, A., Neyts, J., Kruger, D.H., and Ulrich, R. (2001). A chemiluminescence detection method of hantaviral antigens in neutralisation assays and inhibitor studies. J. Virol. Methods *96,* 17-23.

Hjelle, B. and Yates, T. (2001). Modeling hantavirus maintenance and transmission in rodent communities. Curr. Top. Microbiol. Immunol. *256,* 77-90.

Hobman, T.C. (1993). Targeting of viral glycoproteins to the Golgi complex. Trends Microbiol. *1,* 124-130.

Hornung, V., Ellegast, J., Kim, S., Brzozka, K., Jung, A., Kato, H., Poeck, H., Akira, S., Conzelmann, K.K., Schlee, M., Endres, S., and Hartmann, G. (2006). 5'-Triphosphate RNA is the ligand for RIG-I. Science *314,* 994-997.

Huggins, J.W., Hsiang, C.M., Cosgriff, T.M., Guang, M.Y., Smith, J.I., Wu, Z.O., LeDuc, J.W., Zheng, Z.M., Meegan, J.M., Wang, Q.N. (1991). Prospective, double-blind, concurrent, placebo-controlled clinical trial of intravenous ribavirin therapy of hemorrhagic fever with renal syndrome. J. Infect. Dis. *164,* 1119-1127.

Huggins, J.W., Kim, G.R., Brand, O.M., and McKee, K.T., Jr. (1986). Ribavirin therapy for Hantaan virus infection in suckling mice. J. Infect. Dis. *153,* 489-497.

Hutchinson, K.L., Peters, C.J., and Nichol, S.T. (1996). Sin Nombre virus mRNA synthesis. Virology *224,* 139-149.

Hutchinson, K.L., Rollin, P.E., and Peters, C.J. (1998). Pathogenesis of a North American hantavirus, Black Creek Canal virus, in experimentally infected Sigmodon hispidus. Am. J. Trop. Med. Hyg. *59,* 58-65.

Imaizumi, T., Hatakeyama, M., Yamashita, K., Ishikawa, A., Yoshida, H., Satoh, K., Taima, K., Mori, F., and Wakabayashi, K. (2005). Double-stranded RNA induces the synthesis of retinoic acid-inducible gene-I in vascular endothelial cells. Endothelium *12,* 133-137.

Jaaskelainen, K.M., Kaukinen, P., Minskaya, E.S., Plyusnina, A., Vapalahti, O., Elliott, R.M., Weber, F., Vaheri, A., and Plyusnin, A. (2007). Tula and Puumala hantavirus NSs ORFs are functional and the products inhibit activation of the interferon-beta promoter. J. Med. Virol. *79,* 1527-1536.

Janeway, C.A., Jr. and Medzhitov, R. (2002). Innate immune recognition. Annu. Rev. Immunol. *20,* 197-216.

Jantti, J., Hilden, P., Ronka, H., Makiranta, V., Keranen, S., and Kuismanen, E. (1997). Immunocytochemical analysis of Uukuniemi virus budding compartments: role of the intermediate compartment and the Golgi stack in virus maturation. J. Virol. *71,* 1162-1172.

Jin, M., Park, J., Lee, S., Park, B., Shin, J., Song, K.J., Ahn, T.I., Hwang, S.Y., Ahn, B.Y., and Ahn, K. (2002). Hantaan virus enters cells by clathrin-dependent receptor-mediated endocytosis. Virology *294,* 60-69.

Jones, K.E., Patel, N.G., Levy, M.A., Storeygard, A., Balk, D., Gittleman, J.L., and Daszak, P. (2008). Global trends in emerging infectious diseases. Nature *451,* 990-993.

Jonsson, C.B. and Schmaljohn, C.S. (2001). Replication of hantaviruses. Curr. Top. Microbiol. Immunol. *256,* 15-32.

Kadowaki, N., Ho, S., Antonenko, S., Malefyt, R.W., Kastelein, R.A., Bazan, F., and Liu, Y.J. (2001). Subsets of human dendritic cell precursors express different toll-like receptors and respond to different microbial antigens. J. Exp. Med. *194,* 863-869.

Kanerva, M., Melen, K., Vaheri, A., and Julkunen, I. (1996). Inhibition of puumala and tula hantaviruses in Vero cells by MxA protein. Virology *224,* 55-62.

Kanerva, M., Mustonen, J., and Vaheri, A. (1998). Pathogenesis of puumala and other hantavirus infections. Rev. Med. Virol. *8,* 67-86.

Kariko, K., Buckstein, M., Ni, H., and Weissman, D. (2005). Suppression of RNA recognition by Toll-like receptors: the impact of nucleoside modification and the evolutionary origin of RNA. Immunity *23,* 165-175.

Kato, H., Sato, S., Yoneyama, M., Yamamoto, M., Uematsu, S., Matsui, K., Tsujimura, T., Takeda, K., Fujita, T., Takeuchi, O., and Akira, S. (2005). Cell type-specific involvement of RIG-I in antiviral response. Immunity. *23,* 19-28.

Kato, H., Takeuchi, O., Mikamo-Satoh, E., Hirai, R., Kawai, T., Matsushita, K., Hiiragi, A., Dermody, T.S., Fujita, T., and Akira, S. (2008). Length-dependent recognition of double-stranded ribonucleic acids by retinoic acid-inducible gene-I and melanoma differentiation-associated gene 5. J. Exp. Med. *205,* 1601-1610.

Kato, H., Takeuchi, O., Sato, S., Yoneyama, M., Yamamoto, M., Matsui, K., Uematsu, S., Jung, A., Kawai, T., Ishii, K.J., Yamaguchi, O., Otsu, K., Tsujimura, T., Koh, C.S., Reis e Sousa, Matsuura, Y., Fujita, T., and Akira, S. (2006). Differential roles of MDA5 and RIG-I helicases in the recognition of RNA viruses. Nature *441,* 101-105.

Kaukinen, P., Koistinen, V., Vapalahti, O., Vaheri, A., and Plyusnin, A. (2001). Interaction between molecules of hantavirus nucleocapsid protein. J. Gen. Virol. *82,* 1845-1853.

Kaukinen, P., Sillanpaa, M., Kotenko, S., Lin, R., Hiscott, J., Melen, K., and Julkunen, I. (2006). Hepatitis C virus NS2 and NS3/4A proteins are potent inhibitors of host cell cytokine/chemokine gene expression. Virol. J. *3,* 66.

Kaukinen, P., Vaheri, A., and Plyusnin, A. (2003). Non-covalent interaction between nucleocapsid protein of Tula hantavirus and small ubiquitin-related modifier-1, SUMO-1. Virus Res. *92,* 37-45.

Kaukinen, P., Vaheri, A., and Plyusnin, A. (2005). Hantavirus nucleocapsid protein: a multi-functional molecule with both housekeeping and ambassadorial duties. Arch. Virol. *150,* 1693-1713.

Kawai, T., Takahashi, K., Sato, S., Coban, C., Kumar, H., Kato, H., Ishii, K.J., Takeuchi, O., and Akira, S. (2005). IPS-1, an adaptor triggering RIG-I- and Mda5-mediated type I interferon induction. Nat. Immunol. *6,* 981-988.

Khaiboullina, S.F. and St Jeor, S.C. (2002). Hantavirus immunology. Viral Immunol. *15,* 609-625.

Khan, A.S. and Young, J.C. (2001). Hantavirus pulmonary syndrome: at the crossroads. Curr. Opin. Infect. Dis. *14,* 205-209.

Kim, T.Y., Choi, Y., Cheong, H.S., and Choe, J. (2002). Identification of a cell surface 30 kDa protein as a candidate receptor for Hantaan virus. J. Gen. Virol. *83,* 767-773.

Kitamura, T., Morita, C., Komatsu, T., Sugiyama, K., Arikawa, J., Shiga, S., Takeda, H., Akao, Y., Imaizumi, K., Oya, A., Hashimoto, N., and Urasawa, S. (1983). Isolation of virus causing hemorrhagic fever with renal syndrome (HFRS) through a cell culture system. Jpn. J. Med. Sci. Biol. *36,* 17-25.

Klempa, B., Meisel, H., Rath, S., Bartel ,J., Ulrich, R., and Kruger, D.H. (2003). Occurrence of renal and pulmonary syndrome in a region of northeast Germany where Tula hanta-virus circulates. J. Clin. Microbiol. *41,* 4894-4897.

Klempa, B., Stanko, M., Labuda, M., Ulrich, R., Meisel, H., and Kruger, D.H. (2005). Central European Dobrava Hantavirus isolate from a striped field mouse (Apodemus agrarius). J. Clin. Microbiol. *43,* 2756-2763.

Klempa, B., Tkachenko, E.A., Dzagurova, T.K., Yunicheva, Y.V., Morozov, V.G., Okulova, N.M., Slyusareva, G.P., Smirnov, A., and Kruger, D.H. (2008). Hemorrhagic fever with renal syndrome caused by 2 lineages of Dobrava hantavirus, Russia. Emerg. Infect. Dis. *14,* 617-625.

Komuro, A. and Horvath, C.M. (2006). RNA- and virus-independent inhibition of antiviral signaling by RNA helicase LGP2. J. Virol. *80,* 12332-12342.

Kraus, A.A., Raftery, M.J., Giese, T., Ulrich, R., Zawatzky, R., Hippenstiel, S., Suttorp, N., Kruger, D.H., and Schonrich, G. (2004). Differential antiviral response of endothelial cells after infection with pathogenic and nonpathogenic hantaviruses. J. Virol. *78,* 6143-6150.

Krautkramer, E. and Zeier, M. (2008). Hantavirus causing hemorrhagic fever with renal syndrome enters from the apical surface and requires decay-accelerating factor (DAF/CD55). J. Virol. *82,* 4257-4264.

Kruger, D.H., Ulrich, R., and Lundkvist, A.A. (2001). Hantavirus infections and their prevention. Microbes. Infect. *3,* 1129-1144.

Kuismanen, E., Saraste, J., and Pettersson, R.F. (1985). Effect of monensin on the assembly of Uukuniemi virus in the Golgi complex. J. Virol. *55,* 813-822.

Kumar, H., Kawai, T., Kato, H., Sato, S., Takahashi, K., Coban, C., Yamamoto, M., Uematsu, S., Ishii, K.J., Takeuchi, O., and Akira, S. (2006). Essential role of IPS-1 in innate immune responses against RNA viruses. J. Exp. Med. *203,* 1795-1803.

Le Bon, A., Etchart, N., Rossmann, C., Ashton, M., Hou, S., Gewert, D., Borrow, P., and Tough, D.F. (2003). Cross-priming of CD8+ T cells stimulated by virus-induced type I interferon. Nat. Immunol. *4,* 1009-1015.

Le Bon, A., Schiavoni, G., D'Agostino, G., Gresser, I., Belardelli, F., and Tough, D.F. (2001). Type i interferons potently enhance humoral immunity and can promote isotype switching by stimulating dendritic cells in vivo. Immunity. *14,* 461-470.

Lee, B.H., Yoshimatsu, K., Maeda, A., Ochiai, K., Morimatsu, M., Araki, K., Ogino, M., Morikawa, S., and Arikawa, J. (2003). Association of the nucleocapsid protein of the Seoul and Hantaan hantaviruses with small ubiquitin-like modifier-1-related molecules. Virus Res. *98,* 83-91.

Lee, H.W. (1982). Hemorrhagic fever with renal syndrome (HFRS). Scand. J. Infect. Dis. Suppl *36,* 82-85.

Lee, H.W. and Cho, H.J. (1981). Electron microscope appearance of Hantaan virus, the causative agent of Korean haemorrhagic fever. Lancet *1,* 1070-1072.

Lee, H.W., Lee, P.W., and Johnson, K.M. (2004). Isolation of the etiologic agent of Korean hemorrhagic fever. 1978. J. Infect. Dis. *190,* 1711-1721.

Li, D., Schmaljohn, A.L., Anderson, K., and Schmaljohn, C.S. (1995). Complete nucleotide sequences of the M and S segments of two hantavirus isolates from California: evidence for reassortment in nature among viruses related to hantavirus pulmonary syndrome. Virology *206,* 973-983.

Li, X.D., Makela, T.P., Guo, D., Soliymani, R., Koistinen, V., Vapalahti, O., Vaheri, A., and Lankinen, H. (2002). Hantavirus nucleocapsid protein interacts with the Fas-mediated apoptosis enhancer Daxx. J. Gen. Virol. *83,* 759-766.

Li, Z. W., Chu, W., Hu, Y., Delhase, M., Deerinck, T., Ellisman, M., Johnson, R., and Karin, M. (1999). The IKKbeta subunit of IkappaB kinase (IKK) is essential for nuclear factor kappaB activation and prevention of apoptosis. J. Exp. Med. *189,* 1839-1845.

Lin, R., Heylbroeck, C., Pitha, P.M., and Hiscott, J. (1998). Virus-dependent phosphorylation of the IRF-3 transcription factor regulates nuclear translocation, transactivation potential, and proteasome-mediated degradation. Mol. Cell Biol. *18,* 2986-2996.

Linderholm, M., Ahlm, C., Settergren, B., Waage, A., and Tarnvik, A. (1996). Elevated plasma levels of tumor necrosis factor (TNF)-alpha, soluble TNF receptors, interleukin (IL)-6, and IL-10 in patients with hemorrhagic fever with renal syndrome. J. Infect. Dis. *173,* 38-43.

Lober, C., Anheier, B., Lindow, S., Klenk, H.D., and Feldmann, H. (2001). The Hantaan virus glycoprotein precursor is cleaved at the conserved pentapeptide WAASA. Virology *289,* 224-229.

Loo, Y.M., Fornek, J., Crochet, N., Bajwa, G., Perwitasari, O., Martinez-Sobrido, L., Akira, S., Gill, M.A., Garcia-Sastre, A., Katze, M.G., and Gale, M., Jr. (2008). Distinct RIG-I and MDA5 signaling by RNA viruses in innate immunity. J. Virol. *82,* 335-345.

Lundkvist, A., Bjorsten, S., Niklasson, B., and Ahlborg, N. (1995). Mapping of B-cell determinants in the nucleocapsid protein of Puumala virus: definition of epitopes specific for acute immunoglobulin G recognition in humans. Clin. Diagn. Lab Immunol. *2,* 82-86.

Lundkvist, A., Horling, J., and Niklasson, B. (1993). The humoral response to Puumala virus infection (nephropathia epidemica) investigated by viral protein specific immunoassays. Arch. Virol. *130,* 121-130.

Maes, P., Clement, J., Gavrilovskaya, I., and Van Ranst, M. (2004). Hantaviruses: immunology, treatment, and prevention. Viral Immunol. *17,* 481-497.

Makela, S., Mustonen, J., Ala-Houhala, I., Hurme, M., Koivisto, A.M., Vaheri, A., and Pasternack, A. (2004). Urinary excretion of interleukin-6 correlates with proteinuria in acute Puumala hantavirus-induced nephritis. Am. J. Kidney Dis. *43,* 809-816.

Maniatis, T., Falvo, J.V., Kim, T.H., Kim, T.K., Lin, C.H., Parekh, B.S., and Wathelet, M.G. (1998). Structure and function of the interferon-beta enhanceosome. Cold Spring Harb. Symp. Quant. Biol. *63,* 609-620.

Martin, M.L., Lindsey-Regnery, H., Sasso, D.R., McCormick, J.B., and Palmer, E. (1985). Distinction between Bunyaviridae genera by surface structure and comparison with Hantaan virus using negative stain electron microscopy. Arch. Virol. *86,* 17-28.

Matsumoto, M., Funami, K., Tanabe, M., Oshiumi, H., Shingai, M., Seto, Y., Yamamoto, A., and Seya, T. (2003). Subcellular localization of Toll-like receptor 3 in human dendritic cells. J. Immunol. *171,* 3154-3162.

McCaughey, C. and Hart, C.A. (2000). Hantaviruses. J. Med. Microbiol. *49,* 587-599.

Meylan, E., Curran, J., Hofmann, K., Moradpour, D., Binder, M., Bartenschlager, R., and Tschopp, J. (2005). Cardif is an adaptor protein in the RIG-I antiviral pathway and is targeted by hepatitis C virus. Nature *437,* 1167-1172.

Mir, M.A. and Panganiban, A.T. (2006). The bunyavirus nucleocapsid protein is an RNA chaperone: possible roles in viral RNA panhandle formation and genome replication. RNA. *12,* 272-282.

Montoya, M., Schiavoni, G., Mattei, F., Gresser, I., Belardelli, F., Borrow, P., and Tough, D.F. (2002). Type I interferons produced by dendritic cells promote their phenotypic and functional activation. Blood *99,* 3263-3271.

Nagai, T., Tanishita, O., Takahashi, Y., Yamanouchi, T., Domae, K., Kondo, K., Dantas, J.R., Jr., Takahashi, M., and Yamanishi, K. (1985). Isolation of haemorrhagic fever with renal syndrome virus from leukocytes of rats and virus replication in cultures of rat and human macrophages. J. Gen. Virol. *66 (Pt 6),* 1271-1278.

Nam, J.H., Hwang, K.A., Yu, C.H., Kang, T.H., Shin, J.Y., Choi, W.Y., Kim, I.B., Joo, Y.R., Cho, H.W., and Park, K.Y. (2003). Expression of interferon inducible genes following Hantaan virus infection as a mechanism of resistance in A549 cells. Virus Genes *26,* 31-38.

Obijeski, J.F., Bishop, D.H., Murphy, F.A., and Palmer, E.L. (1976). Structural proteins of La Crosse virus. J. Virol. *19,* 985-997.

Oelschlegel, R., Kruger, D.H., and Rang, A. (2007). MxA-independent inhibition of Hantaan virus replication induced by type I and type II interferon in vitro. Virus Res. *127,* 100-105.

Okuno, Y., Yamanishi, K., Takahashi, Y., Tanishita, O., Nagai, T., Dantas, J.R., Jr., Okamoto, Y., Tadano, M., and Takahashi, M. (1986). Haemagglutination-inhibition test for haemorrhagic fever with renal syndrome using virus antigen prepared from infected tissue culture fluid. J. Gen. Virol. *67 (Pt 1),* 149-156.

Opitz, B., Rejaibi, A., Dauber, B., Eckhard, J., Vinzing, M., Schmeck, B., Hippenstiel, S., Suttorp, N., and Wolff, T. (2007). IFNbeta induction by influenza A virus is mediated by RIG-I which is regulated by the viral NS1 protein. Cell Microbiol. *9,* 930-938.

Padula, P.J., Edelstein, A., Miguel, S.D., Lopez, N.M., Rossi, C.M., and Rabinovich, R.D. (1998). Hantavirus pulmonary syndrome outbreak in Argentina: molecular evidence for person-to-person transmission of Andes virus. Virology *241,* 323-330.

Paladino, P., Cummings, D.T., Noyce, R.S., and Mossman, K.L. (2006). The IFN-independent response to virus particle entry provides a first line of antiviral defense that is independent of TLRs and retinoic acid-inducible gene I. J. Immunol. *177,* 8008-8016.

Pardigon, N., Vialat, P., Girard, M., and Bouloy, M. (1982). Panhandles and hairpin structures at the termini of germiston virus RNAs (Bunyavirus). Virology *122,* 191-197.

Pensiero, M.N., Sharefkin, J.B., Dieffenbach, C.W., and Hay, J. (1992). Hantaan virus infection of human endothelial cells. J. Virol. *66,* 5929-5936.

Peters, C.J. and Khan, A.S. (2002). Hantavirus pulmonary syndrome: the new American hemorrhagic fever. Clin. Infect. Dis. *34,* 1224-1231.

Pichlmair, A., Schulz, O., Tan, C.P., Naslund, T.I., Liljestrom, P., Weber, F., and Reis e Sousa (2006). RIG-I-mediated antiviral responses to single-stranded RNA bearing 5'-phosphates. Science *314,* 997-1001.

Plyusnin, A. (2002). Genetics of hantaviruses: implications to taxonomy. Arch. Virol. *147,* 665-682.

Plyusnin, A., Cheng, Y., Lehvaslaiho, H., and Vaheri, A. (1996). Quasispecies in wild-type tula hantavirus populations. J. Virol. *70,* 9060-9063.

Plyusnin, A. and Morzunov, S.P. (2001). Virus evolution and genetic diversity of hantaviruses and their rodent hosts. Curr. Top. Microbiol. Immunol. *256,* 47-75.

Raftery, M.J., Kraus, A.A., Ulrich, R., Kruger, D.H., and Schonrich, G. (2002). Hantavirus infection of dendritic cells. J. Virol. *76,* 10724-10733.

Ramsden, C., Melo, F.L., Figueiredo, L.M., Holmes, E.C., and Zanotto, P.M. (2008). High rates of molecular evolution in hantaviruses. Mol. Biol. Evol. *25,* 1488-1492.

Rang, A., Heider, H., Ulrich, R., and Kruger, D.H. (2006). A novel method for cloning of non-cytolytic viruses. J. Virol. Methods *135,* 26-31.

Ravkov, E.V., Nichol, S.T., and Compans, R.W. (1997). Polarized entry and release in epithelial cells of Black Creek Canal virus, a New World hantavirus. J. Virol. *71,* 1147-1154.

Ravkov, E.V., Nichol, S.T., Peters, C.J., and Compans, R.W. (1998). Role of actin microfilaments in Black Creek Canal virus morphogenesis. J. Virol. *72,* 2865-2870.

Razanskiene, A., Schmidt, J., Geldmacher, A., Ritzi, A., Niedrig, M., Lundkvist, A., Kruger, D.H., Meisel, H., Sasnauskas, K., and Ulrich, R. (2004). High yields of stable and highly pure nucleocapsid proteins of different hantaviruses can be generated in the yeast Saccharomyces cerevisiae. J. Biotechnol. *111,* 319-333.

Rizvanov, A.A., Khaiboullina, S.F., and St Jeor, S. (2004). Development of reassortant viruses between pathogenic hantavirus strains. Virology *327,* 225-232.

Roberts, R.M., Liu, L., Guo, Q., Leaman, D., and Bixby, J. (1998). The evolution of the type I interferons. J. Interferon Cytokine Res. *18,* 805-816.

Rodriguez, L.L., Owens, J.H., Peters, C.J., and Nichol, S.T. (1998). Genetic reassortment among viruses causing hantavirus pulmonary syndrome. Virology *242,* 99-106.

Ronnblom, L., Eloranta, M.L., and Alm, G.V. (2006). The type I interferon system in systemic lupus erythematosus. Arthritis Rheum. *54,* 408-420.

Rusnak, J.M., Byrne, W.R., Chung, K.N., Gibbs, P.H., Kim, T.T., Boudreau, E.F., Cosgriff, T., Pittman, P., Kim, K.Y., Erlichman, M.S., Rezvani, D.F., and Huggins, J.W. (2008). Experience with intravenous ribavirin in the treatment of hemorrhagic fever with renal syndrome in Korea. Antiviral Res.

Ruusala, A., Persson, R., Schmaljohn, C.S., and Pettersson, R.F. (1992). Coexpression of the membrane glycoproteins G1 and G2 of Hantaan virus is required for targeting to the Golgi complex. Virology *186,* 53-64.

Rwambo, P.M., Shaw, M.K., Rurangirwa, F.R., and DeMartini, J.C. (1996). Ultrastructural studies on the replication and morphogenesis of Nairobi sheep disease virus, a Nairovirus. Arch. Virol. *141,* 1479-1492.

Saito, T. and Gale, M., Jr. (2008a). Differential recognition of double-stranded RNA by RIG-I-like receptors in antiviral immunity. J. Exp. Med. *205,* 1523-1527.

Saito, T. and Gale, M., Jr. (2008b). Regulation of innate immunity against hepatitis C virus infection. Hepatol. Res. *38,* 115-122.

Saito, T., Hirai, R., Loo, Y.M., Owen, D., Johnson, C.L., Sinha, S.C., Akira, S., Fujita, T., and Gale, M., Jr. (2007). Regulation of innate antiviral defenses through a shared repressor domain in RIG-I and LGP2. Proc. Natl. Acad. Sci. U. S. A *104,* 582-587.

Saito, T., Owen, D.M., Jiang, F., Marcotrigiano, J., and Gale, M. (2008). Innate immunity induced by composition-dependent RIG-I recognition of hepatitis C virus RNA. Nature.

Samanta, M., Iwakiri, D., Kanda, T., Imaizumi, T., and Takada, K. (2006). EB virus-encoded RNAs are recognized by RIG-I and activate signaling to induce type I IFN. EMBO J. *25,* 4207-4214.

Samuel, C.E. (2001). Antiviral actions of interferons. Clin. Microbiol. Rev. *14,* 778-809, table.

Sato, M., Tanaka, N., Hata, N., Oda, E., and Taniguchi, T. (1998). Involvement of the IRF family transcription factor IRF-3 in virus-induced activation of the IFN-beta gene. FEBS Lett. *425,* 112-116.

Schmaljohn, C. and Hjelle, B. (1997). Hantaviruses: a global disease problem. Emerg. Infect. Dis. *3,* 95-104.

Schonrich, G., Rang, A., Lutteke, N., Raftery, M.J., Charbonnel, N., and Ulrich, R.G. (2008). Hantavirus-induced immunity in rodent reservoirs and humans. Immunol. Rev. *225,* 163-189.

Schountz, T., Prescott, J., Cogswell, A.C., Oko, L., Mirowsky-Garcia, K., Galvez, A.P., and Hjelle, B. (2007). Regulatory T cell-like responses in deer mice persistently infected with Sin Nombre virus. Proc. Natl. Acad. Sci. U. S. A *104,* 15496-15501.

Seth, R.B., Sun, L., and Chen, Z.J. (2006). Antiviral innate immunity pathways. Cell Res. *16,* 141-147.

Seth, R.B., Sun, L., Ea, C.K., and Chen, Z.J. (2005). Identification and characterization of MAVS, a mitochondrial antiviral signaling protein that activates NF-kappaB and IRF 3. Cell *122,* 669-682.

Shi, X. and Elliott, R.M. (2002). Golgi localization of Hantaan virus glycoproteins requires coexpression of G1 and G2. Virology *300,* 31-38.

Shimada, T., Kawai, T., Takeda, K., Matsumoto, M., Inoue, J., Tatsumi, Y., Kanamaru, A., and Akira, S. (1999). IKK-i, a novel lipopolysaccharide-inducible kinase that is related to IkappaB kinases. Int. Immunol. *11,* 1357-1362.

Sibold, C., Meisel, H., Lundkvist, A., Schulz, A., Cifire, F., Ulrich, R., Kozuch, O., Labuda, M., and Kruger, D.H. (1999). Short report: simultaneous occurrence of Dobrava, Puumala, and Tula Hantaviruses in Slovakia. Am. J. Trop. Med. Hyg. *61,* 409-411.

Smadel, J.E. (1953). Epidemic hemorrhagic fever. Am. J. Public Health Nations. Health *43,* 1327-1330.

Song, J.W., Gu, S.H., Bennett, S.N., Arai, S., Puorger, M., Hilbe, M., and Yanagihara, R. (2007). Seewis virus, a genetically distinct hantavirus in the Eurasian common shrew (Sorex araneus). Virol. J. *4,* 114.

Spiropoulou, C.F., Albarino, C.G., Ksiazek, T.G., and Rollin, P.E. (2007). Andes and Prospect Hill hantaviruses differ in early induction of interferon although both can downregulate interferon signaling. J. Virol. *81,* 2769-2776.

Sundstrom, J.B., McMullan, L.K., Spiropoulou, C.F., Hooper, W.C., Ansari, A.A., Peters, C.J., and Rollin, P.E. (2001). Hantavirus infection induces the expression of RANTES and IP-10 without causing increased permeability in human lung microvascular endothelial cells. J. Virol. *75,* 6070-6085.

Taniguchi, T. and Takaoka, A. (2001). A weak signal for strong responses: interferon-alpha/beta revisited. Nat. Rev. Mol. Cell Biol. *2,* 378-386.

Temonen, M., Lankinen, H., Vapalahti, O., Ronni, T., Julkunen, I., and Vaheri, A. (1995). Effect of interferon-alpha and cell differentiation on Puumala virus infection in human monocyte/macrophages. Virology *206,* 8-15.

Tkachenko, E.A. and Lee, H.W. (1991). Etiology and epidemiology of hemorrhagic fever with renal syndrome. Kidney Int. Suppl *35,* S54-S61.

Tojima, Y., Fujimoto, A., Delhase, M., Chen, Y., Hatakeyama, S., Nakayama, K., Kaneko, Y., Nimura, Y., Motoyama, N., Ikeda, K., Karin, M., and Nakanishi, M. (2000). NAK is an IkappaB kinase-activating kinase. Nature *404,* 778-782.

Tsai, T.F. (1987). Hemorrhagic fever with renal syndrome: mode of transmission to humans. Lab Anim Sci. *37,* 428-430.

Van Epps, H.L., Schmaljohn, C.S., and Ennis, F.A. (1999). Human memory cytotoxic T-lymphocyte (CTL) responses to Hantaan virus infection: identification of virus-specific and cross-reactive CD8(+) CTL epitopes on nucleocapsid protein. J. Virol. *73,* 5301-5308.

Van Epps, H.L., Terajima, M., Mustonen, J., Arstila, T.P., Corey, E.A., Vaheri, A., and Ennis, F.A. (2002). Long-lived memory T lymphocyte responses after hantavirus infection. J. Exp. Med. *196,* 579-588.

Vapalahti, O., Kallio-Kokko, H., Narvanen, A., Julkunen, I., Lundkvist, A., Plyusnin, A., Lehvaslaiho, H., Brummer-Korvenkontio, M., Vaheri, A., and Lankinen, H. (1995). Human B-cell epitopes of Puumala virus nucleocapsid protein, the major antigen in early serological response. J. Med. Virol. *46,* 293-303.

Vapalahti, O., Mustonen, J., Lundkvist, A., Henttonen, H., Plyusnin, A., and Vaheri, A. (2003). Hantavirus infections in Europe. Lancet Infect. Dis. *3,* 653-661.

Venkataraman, T., Valdes, M., Elsby, R., Kakuta, S., Caceres, G., Saijo, S., Iwakura, Y., and Barber, G.N. (2007). Loss of DExD/H box RNA helicase LGP2 manifests disparate antiviral responses. J. Immunol. *178,* 6444-6455.

Weaver, B.K., Kumar, K.P., and Reich, N.C. (1998). Interferon regulatory factor 3 and CREB-binding protein/p300 are subunits of double-stranded RNA-activated transcription factor DRAF1. Mol. Cell Biol. *18,* 1359-1368.

Weber, F., Wagner, V., Rasmussen, S.B., Hartmann, R., and Paludan, S.R. (2006). Double-stranded RNA is produced by positive-strand RNA viruses and DNA viruses but not in detectable amounts by negative-strand RNA viruses. J. Virol. *80,* 5059-5064.

Wells, R.M., Young, J., Williams, R.J., Armstrong, L.R., Busico, K., Khan, A.S., Ksiazek, T.G., Rollin, P.E., Zaki, S.R., Nichol, S.T., and Peters, C.J. (1997). Hantavirus transmission in the United States. Emerg. Infect. Dis. *3,* 361-365.

White, J.D., Shirey, F.G., French, G.R., Huggins, J.W., Brand, O.M., and Lee, H.W. (1982). Hantaan virus, aetiological agent of Korean haemorrhagic fever, has Bunyaviridae-like morphology. Lancet *1,* 768-771.

Williams, B.R. (2002). Type I interferons (IFN) are essential mediators of innate and specific immunity against viruses. Viral Immunol. *15,* 1-2.

Xu, L.G., Wang, Y.Y., Han, K.J., Li, L.Y., Zhai, Z., and Shu, H.B. (2005). VISA is an adapter protein required for virus-triggered IFN-beta signaling. Mol. Cell *19,* 727-740.

Yanagihara, R., Amyx, H.L., and Gajdusek, D.C. (1985). Experimental infection with Puumala virus, the etiologic agent of nephropathia epidemica, in bank voles (Clethrionomys glareolus). J. Virol. *55,* 34-38.

Yanagihara, R. and Silverman, D.J. (1990). Experimental infection of human vascular endothelial cells by pathogenic and nonpathogenic hantaviruses. Arch. Virol. *111,* 281-286.

Yoneyama, M., Kikuchi, M., Matsumoto, K., Imaizumi, T., Miyagishi, M., Taira, K., Foy, E., Loo, Y.M., Gale, M., Jr., Akira, S., Yonehara, S., Kato, A., and Fujita, T. (2005). Shared and unique functions of the DExD/H-box helicases RIG-I, MDA5, and LGP2 in antiviral innate immunity. J. Immunol. *175,* 2851-2858.

Yoneyama, M., Kikuchi, M., Natsukawa, T., Shinobu, N., Imaizumi, T., Miyagishi, M., Taira, K., Akira, S., and Fujita, T. (2004). The RNA helicase RIG-I has an essential function

in double-stranded RNA-induced innate antiviral responses. Nat. Immunol. *5,* 730-737.

Yoneyama, M., Suhara, W., Fukuhara, Y., Fukuda, M., Nishida, E., and Fujita, T. (1998). Direct triggering of the type I interferon system by virus infection: activation of a transcription factor complex containing IRF-3 and CBP/p300. EMBO J. *17,* 1087-1095.

Yoneyama, M., Suhara, W., Fukuhara, Y., Sato, M., Ozato, K., and Fujita, T. (1996). Autocrine amplification of type I interferon gene expression mediated by interferon stimulated gene factor 3 (ISGF3). J. Biochem. *120,* 160-169.

Zaki, S.R., Greer ,P.W., Coffield, L.M., Goldsmith, C.S., Nolte, K.B., Foucar, K., Feddersen, R.M., Zumwalt, R.E., Miller, G.L., Khan, A.S. (1995). Hantavirus pulmonary syndrome. Pathogenesis of an emerging infectious disease. Am. J. Pathol. *146,* 552-579.

Acknowledgements

I would like to express my gratitude to all who gave me the possibility to complete this thesis, first of all Prof. Dr. Detlev H. Krüger, Head of the Institute of Virology, for his support and guidance.

I am especially obliged to Prof. Dr. Günther Schönrich for the supervision of my thesis and his perpetual readiness for discussion and to Dr. Martin Raftery to whom I could always address any question.

I would like to thank all of my colleagues for their great company throughout good and bad times of research, in particular Sina Kirsanovs, Cindy Gutzeit, Nina Lütteke, Angela Kather and Manuel Hitzler.

This work was supported by grants of the DFG, Graduiertenkolleg 1121, and the Charité medical school. Without the cordial commitment of Dr. Martina Sick, coordinator, and Prof. Dr. Richard Lucius, Spokesman of the Graduiertenkolleg 1121, it would have been much more difficult to cope with organisational challenges.

My special gratitude is dedicated to AG Wolff from the Robert Koch-Institute, in particular to PD Dr. Thorsten Wolff, Dr. Bianca Dauber, Jana Schneider and Markus Matthäi, for useful discussions and support.

Last but not least, I am deeply grateful to Bruno Gries who always supported me in all ways, and to my parents, my siblings and my grand-parents for their enduring encouragement and confidence.

Eidesstattliche Erklärung

Hiermit erkläre ich an Eides statt, dass ich die vorliegende Dissertation selbständig und nur unter Verwendung der genannten Hilfen und Hilfsmittel verfasst habe.

Min-Hi Lee